**Universidade Federal do Rio Grande do Sul**

**Instituto de Ciências Básicas da Saúde**

**Departamento de Bioquímica**

**Programa de Pós-Graduação em Ciências Biológicas: Bioquímica**

# EFEITOS DA ADMINISTRAÇÃO SISTÊMICA DE GUANOSINA EM HIPERAMONEMIA AGUDA E CARACTERIZAÇÃO COMPORTAMENTAL, METABÓLICA E ELETROENCEFALOGRÁFICA DE UM MODELO CIRÚRGICO DE ENCEFALOPATIA HEPÁTICA AGUDA EM ROEDORES

**TESE DE DOUTORADO**

**Aluno Giordano Fabricio Cittolin Santos**

**Orientador Professor Diogo Onofre Gomes de Souza**

**Porto Alegre, RS, 2017**

**Início:** 03/2013

**Fim:** 02/2017

Giordano Fabricio Cittolin Santos

# EFEITOS DA ADMINISTRAÇÃO SISTÊMICA DE GUANOSINA EM HIPERAMONEMIA AGUDA E CARACTERIZAÇÃO COMPORTAMENTAL, METABÓLICA E ELETROENCEFALOGRÁFICA DE UM MODELO CIRÚRGICO DE ENCEFALOPATIA HEPÁTICA AGUDA EM ROEDORES

Tese de Doutorado apresentada ao Programa de Pós-Graduação em Ciências Biológicas: Bioquímica, da Universidade Federal do Rio Grande do Sul, como requisito parcial para obtenção de título de Doutor em Bioquímica.

Porto Alegre, Rio Grande do Sul, Brasil

2017

Professor Diogo Onofre Gomes de Souza

Orientador

CIP - Catalogação na Publicação

Cittolin Santos, Giordano Fabricio
EFEITOS DA ADMINISTRAÇÃO SISTÊMICA DE GUANOSINA EM HIPERAMONEMIA AGUDA E CARACTERIZAÇÃO COMPORTAMENTAL, METABÓLICA E ELETROENCEFALOGRÁFICA DE UM MODELO CIRÚRGICO DE ENCEFALOPATIA HEPÁTICA AGUDA EM ROEDORES / Giordano Fabricio Cittolin Santos. -- 2017.
127 f.

Orientador: Diogo Onofre Gomes de Souza.

Tese (Doutorado) -- Universidade Federal do Rio Grande do Sul, Instituto de Ciências Básicas da Saúde, Programa de Pós-Graduação em Ciências Biológicas: Bioquímica, Porto Alegre, BR-RS, 2017.

1. Encefalopatia Hepática. 2. Hiperamonemia. 3. Guanosina. 4. Metabolismo. 5. Neuroproteção. I. Onofre Gomes de Souza, Diogo, orient. II. Título.

Elaborada pelo Sistema de Geração Automática de Ficha Catalográfica da UFRGS com os dados fornecidos pelo(a) autor(a).

## Agradecimentos

Não é inteiramente possível agradecer aos meus pais Marcia e Rubens, por me oferecerem a luz do conhecimento. Por serem meus maiores modelos de bondade e respeito à vida que conheço,

Ao meu tio Otávio, minha avó Eneida e toda minha família, por ajudar a me socorrer da atemporalidade que crio em meus estudos.

A minha amada Daniela, por ter sempre compreendido, pela sua paciência, pela sua dedicação.

Ao Lucas Paniz e Pedro Guazzelli, por serem meus amigos que se tornaram também meus mestres.

Ao Adriano Martimbianco de Assis, por ser meu mestre que se tornou também meu amigo. Por ter se tornado essencial para o desenvolvimento de todas as etapas deste trabalho.

À professora Maria Elisa, por participar de todas as etapas deste trabalho com amizade, dedicação e brilhantismo.

Ao professor Alessandro Osvaldt pelo companheirismo e engajamento, por ter entrado de cabeça nesse projeto com entusiasmo e permitir sua realização.

Aos colegas de laboratório, por enriquecerem essa caminhada, Roberto, Vitor, Yasmine, Mayara, Bruna, Douglas, Eduardo e Kamila, Zimmer, André, Luciana, Aline, Bernardo e tantos outros.

Aos colegas da Faculdade de Medicina e outros amigos que tanto me apoiaram.

Ao Douglas, Giordano e principalmente à Cléia, por sua profissionalidade e leveza, por me salvarem diversas e incontáveis vezes.

A CAPES, CNPQ, e ao Governo Brasileiro, por terem estimulado a pesquisa.

Ao professor Raymond A. Swanson, por me acolher em seu laboratório em San Francisco e ter me ensinado tanto em tão pouco tempo. Por me apoiar em um ano inesquecível, em um lugar que considero minha casa fora de casa.

Ao meu orientador e amigo, professor Diogo. Por ter acreditado em mim desde o início, por me ensinar a fazer o mesmo. Por ser o maior exemplo de paixão à vida e à ciência que conheço. Por ter liderado todas as etapas de nosso trabalho. Por entender que não conseguiria lhe agradecer o suficiente. Por ajudar a moldar quem sou.

A majestosa UFRGS, onde me graduo como Médico e Doutor em Bioquímica, onde conheci as pessoas maravilhosas que mudaram meu mundo.

**Sumário**

**Parte 1**

**Parte 2**



**Parte 3**

**ANEXOS**

# APRESENTAÇÃO

A tese é dividida em 4 partes:

Na parte primeira, é brevemente desenvolvida uma revisão das bases teóricas pré-concebidas sobre temas-chave contidos em minha tese de doutorado, assim como os objetivos;

Na parte segunda, três manuscritos desenvolvidos durante meu doutorado estão apresentados em forma de Artigo Científico. Nessa parte se encontram materiais, métodos e resultados de cada um desses trabalhos.

Na parte terceira, encontram-se as perspectivas do grupo e discussão da tese, que nada mais é que a transcrição do fruto de reuniões do nosso grupo e, sobretudo, do conhecimento do professor Diogo.

Na parte Anexo, encontra-se a gravura proposta para capa da revista Molecular Neurobiology, feita por mim e por meu tio Otávio Santos. Também, conto brevemente minha experiência estudando como aluno de doutorado-sanduíche na *University California of San Francisco* em 2014-2015, na qual participei da publicação de dois manuscritos que também se encontram nessa parte.

# PARTE 1

**“GUANOSINA, UMA NOVA ESPERANÇA”**

## RESUMO

A encefalopatia hepática é uma disfunção cerebral causada por insuficiência hepática que se manifesta através de um amplo espectro de anormalidades neurológicas e psiquiátricas, variando de alterações subclínicas à coma. Sua base fisiopatológica é complexa, envolvendo principalmente o aumento de amônia, glutamato, glutamina, estresse oxidativo e alteração no metabolismo cerebral. O nucleosídeo guanosina apresenta propriedades neuroprotetoras frente à excitotoxicidade glutamatérgica, estresse oxidativo e convulsão, tendo um potencial papel neuroprotetor em encefalopatia hepática e hiperamonemia. Nesta tese, apresentamos dois modelos experimentais. No primeiro, induzimos encefalopatia através da administração de acetato de amônia por via intraperitoneal em ratos. O grupo tratamento recebeu guanosina 20 minutos antes de receber acetato de amônia. Analisamos alterações hepáticas e sistêmicas, letalidade, análises neurológicas (normal, pré-coma, coma e morte) e eletroencefalográficas, níveis liquóricos de glutamato, glutamina, alanina e amônia, marcadores de estresse oxidativo no sistema nervoso central, captação de glutamato cortical, e atividade e imunoconteúdo cortical da enzima glutamina sintetase. A guanosina drasticamente reduziu a taxa de letalidade (50%) e duração de coma (30%). Outros desfechos foram melhora no traçado eletroencefalográfico, normalização de níveis liquóricos de glutamato, normalização na captação de glutamato e manutenção dos níveis normais de estresse oxidativo no sistema nervoso central. No segundo modelo, induzimos encefalopatia hepática em ratos através de hepatectomia subtotal (92%). Tivemos como objetivos aprofundar o conhecimento nos mecanismos da encefalopatia hepática e consequentes alterações no metabolismo cerebral. Avaliamos letalidade cirúrgica, alterações hepáticas e sistêmicas, atividade comportamental em teste de campo aberto, análise eletroencefalográfica, níveis liquóricos de aminoácidos, imunoconteúdo de transportadores glutamatérgicos, marcadores de estresse oxidativo, atividade das enzimas do ciclo dos ácidos tricarboxílicos e oxidação de glutamato, além de glutamina e glicose no sistema nervoso central. A cirurgia de hepatectomia subtotal provocou profundas alterações na análise eletroencefalográficas e no perfil comportamental dos animais, que apresentaram diminuição da locomoção. Também, houve alterações no metabolismo cerebral e em marcadores de estresse oxidativo compatíveis com aumento de proteólise cerebral (aumento de glutamina, glutamato e aminoácidos de cadeia ramificada), aumento de glicólise, aumento na oxidação cerebral de glutamato e diminuição na oxidação de glicose e lactato. Com dois modelos complementares, correlacionamos alterações neuroquímicas, metabólicas, eletroencefalográficas e comportamentais, aprofundando-nos na fisiopatologia da EH. Esta tese traz novas evidências para a utilização do nucleosídeo guanosina em tratamento de hiperamonemia e encefalopatia hepática.

## ABSTRACT

Hepatic encephalopathy is a brain dysfunction caused by liver failure that manifests itself through a broad spectrum of neurological and psychiatric abnormalities, ranging from subclinical symptoms to coma. Its pathophysiological basis is complex, involving mainly the increase of ammonia, glutamate, glutamine, oxidative stress and alteration in cerebral metabolism. The nucleoside guanosine has neuroprotective properties against glutamatergic excitotoxicity, oxidative stress and convulsion, and has a potential neuroprotective role in hepatic encephalopathy and hyperammonemia. In this thesis, we present two experimental models. In the first, we induced encephalopathy through the administration of ammonia acetate intraperitoneally in rats. The treatment group received guanosine 20 minutes before receiving ammonia acetate. We analyzed hepatic and systemic changes, lethality, neurological scale (normal, pre-coma, coma and death) and electroencephalographic analyzes, cerebrospinal fluid level of glutamate, glutamine, alanine and ammonia, oxidative stress markers in the central nervous system, cortical glutamate uptake and, finally, activity and immunocontent of the enzyme glutamine synthetase. Guanosine dramatically reduced lethality rate (50%) and coma duration (30%). Other outcomes were: improvement in electroencephalographic tracing, normalization of glutamate levels, normalization of glutamate uptake and maintenance of normal levels of oxidative stress in the central nervous system. In the second model, we induced hepatic encephalopathy in rats through subtotal hepatectomy (92%). We aimed to better understand the mechanisms of hepatic encephalopathy and consequent alterations in cerebral metabolism. We evaluated surgical lethality, hepatic and systemic alterations, behavioralal activity in the open field test, electroencephalographic analysis, cerebrospinal fluid levels, immunocontent of glutamatergic transporters, oxidative stress markers, activity of tricarboxylic acid cycle enzymes and glutamate, glucose and lactate oxidation. Subtotal hepatectomy surgery caused profound alterations in the electroencephalographic analysis and in the behavioral profile of the animals, which showed a decrease in locomotion. Also, there were alterations in cerebral metabolism and markers of oxidative stress compatible with increased cerebral proteolysis (increase of glutamine, glutamate and branched-chain amino acids), increased glycolysis, increased cerebral oxidation of glutamate, and decreased glucose and lactate oxidation . With two complementary models, we correlate neurochemical, metabolic, electroencephalographic and behavioral changes, beeter comprehensing the physiopathology of hepatic encephalopathy. This thesis brings new evidence for the use of the nucleoside guanosine in the treatment of hyperammonemia and hepatic encephalopathy.

## Lista de abreviaturas

Acetil-CoA; acetilcoenzima A

a-CGDH; ala-cetoglutarato desidrogenase

ALT; alanina aminotransferase

AST; aspartato aminotransferase

ADP; adenosina-5'-difosfato

AMP; adenosina-5'-monofosfato

ATP; adenosina-5'-trifosfato

BHE; barreira hemato-encefálica

CAT; ciclo dos ácidos tricarboxílicos

CPS; ciclos por segundo

EH; encefalopatia hepática

EEG; eletroencefalografia

GABA; ácido gama-aminobutírico

GMP; guanosina-5'-monofosfato

GMPc; guanosina 3',5'-monofosfato-cíclico

GDP; guanosina-5'-difosfato

GTP; guanosina-5'-trifosfato

i.p.; intraperitoneal

MK-801*; (+)-10,11-dihidro-5-metil-5H-dibenzo[a,d]ciclohepteno-5,10 imina*

SNC; sistema nervoso central

SPS; shunt portossistêmico

Succinil-CoA; Succinilcoenzima A

## Introdução

Encefalopatia hepática,

"A encefalopatia hepática (EH) é uma disfunção cerebral causada por insuficiência hepática e/ou *shunt* portossistêmico (SPS); a EH se manifesta com um abrangente espectro de anormalidades neurológicas ou psiquiátricas, variando de alterações subclínicas à coma". A definição de encefalopatia hepática é ligada ao conceito de que encefalopatias são "distúrbios difusos da função cerebral", e que a palavra "hepática" implica conexão causal entre insuficiência hepática e/ou *shunt* vascular periférico e o distúrbio cerebral (Vilstrup H, et al, 2014).

A prevalência de EH no momento do diagnostico de cirrose é de 10-14% em pacientes estáveis (Saunders JB, *et* al, 1981) e de 16-21% em pacientes descompensados (D`Amico G, *et al*, 1986). Utilizando EEG, estimou-se que aproximadamente 40% dos pacientes cirróticos vão apresentar um episódio de EH, com alta chance de recorrência em poucos meses (Amodio P, et al, 2001), representando um alto econômico que está continuamente a aumentar. Estima-se que aproximadamente 110.000 hospitalizações de pacientes com EH ocorreram entre 2005-2009 nos EUA. (Stepanova M., et al, 2012; Kim WR, et al, 2002).

Insuficiência hepática aguda é caracterizada por perda da função hepática em um paciente sem evidência de doença hepática pré-existente. Os critérios diagnósticos para adultos incluem a presença de coagulopatia [*International normalized ratio* (INR) > 1,5], presença de encefalopatia hepática e doença hepática com duração menor de 24 semanas (Lee WM, et

al, 2008). A incidência de insuficiência hepática aguda em países desenvolvidos é entre 1-6 casos por milhão de pessoa por ano (Bower et al., 2007). A injúria hepática induzida por medicações é a causa mais comum de insuficiência hepática aguda nos países desenvolvidos, sendo que, nos EUA, ao menos metade dos casos são causados por acetaminofeno (Larson et al., 2005).

A classificação da EH pode ser dividida por diversos fatores:

a. De acordo com a doença de base;
   - Tipo A, resultando de insuficiência hepática aguda; que apresenta como característica distinta a presença de aumento de pressão intracraniana e risco de herniação cerebral.
   - Tipo B, resultando predominantemente de *bypass* portossistêmico ou *shunting*
   - Tipo C, resultando de cirrose.
b. De acordo com a severidade da manifestação: (Vilstrup H, et al, 2014)
   - Mínima: presença de alterações psicométricas ou neuropsicológicas em testes que avaliam atividade psicomotora e função executiva ou alterações neurofisiológicas sem sinais de alteração mental.
   - Grau I: Diminuição de atenção, euforia ou ansiedade, diminuição da capacidade de concentração, prejuízo cálculos matemáticos (adição e subtração) e alteração no ciclo sono-vigília.
   - Grau II: Letargia ou apatia, desorientação temporal, alteração de personalidade, comportamento inapropriado, dispraxia, *asterixis*

- Grau III: Sonolência ou estupor, ainda responsivo ao estimulo, confusão, desorientação grosseira e comportamento bizarro.
- Grau IV: Coma

  Graus de EH Mínima e Grau I são considerados subclínicas ("*Covert"*).

c. De acordo com a trajetória temporal;
   - Episódica: referente a episódios isolados;
   - Recorrente: mais de um episódio em menos de 6 meses
   - Persistente: presença de alteração de comportamento persistente, muitas vezes subclínica, intercalado por relapsos de novos episódios de EH

d. De acordo com os fatores desencadeantes:
   - Não precipitada por fatores específicos;
   - Precipitada por fatores específicos, como infecções, sangramento gastrointestinal, alterações eletrolíticas, constipação e outros (Strauss E, da Costa MF, 1998; Vilstrup H, et al, 2014).

Atualmente, não existe indicação de tratamento para EH subclínica. Em 90% das vezes, podemos tratar o episódio de EH apenas com o tratamento dos fatores precipitantes (Strauss E, et al, 1992). Além disso, outros tratamentos para EH não foram testados por ensaios clínicos randomizados rigorosos, muitas vezes apenas utilizando-se de estudos observacionais ou opinião de especialistas. Ainda há um intenso debate sobre terapia em EH, que fica claro quando analisamos correspondências entre especialistas no assunto (Borkakoty A, Kumar P, Taneja , 2017).

Entre os principais tratamentos estabelecidos para EH episódica, recorrente e EH crônica, podemos citar:

- Dissacarídeos não absorvíveis: A lactulose é geralmente utilizada como primeira linha de tratamento, embora uma grande meta-análise não tenha elucidado completamente seu benefício (Als-Nielsen B, Gluud LL, Gluud C, 2004). Essa droga possui dois prováveis mecanismos de ação que, em última instância, provocam uma diminuição na absorção sistêmica de amônia. O primeiro mecanismo é a metabolização da lactulose por bactérias intestinais e consequente acidificação do conteúdo fecal, favorecendo a conversão de amônia a amônio, o qual é aprisionado no lúmen intestinal. O segundo é pelo efeito pró-cinético (aumento da movimentação intestinal) da droga, também diminuindo a absorção sistêmica de amônia. (Patil, D. H, et al, 1987).
- Rifaximina: A superioridade de rifaximina frente a outros antibióticos é estabelecida por diversos estudos (Patidar KR, Bajaj JS. 2013), devendo ser associada à lactulose (Bass NM, et al, 2010). Seu provável mecanismo de ação é relacionado a ser um antibiótico de baixa-absorção oral (ou seja, fica restrito ao trato gastrointestinal se tomado por via oral) com espectro de atividade antibiótica contra bactérias entéricas gram+, gram-, aeróbicos e anaeróbicos, diminuindo a produção de compostos nitrogenados que são subsequentemente absorvidos e causam EH (Flamm SL, 2011).
- Aminoácidos de cadeia ramificada: A utilização de aminoácidos de cadeia ramificada foi estudada em diversos estudos e reavaliada em

recente meta-análise, apresentando efeito benéfico em melhora clínica de pacientes com EH (Gluud LL, et al 2013, Gluud LL, et al 2015).

- Outras terapias também utilizadas são: L-ornitina L-aspartato (LOLA), que promove melhora em testes psicométricos e diminuição dos níveis de amônia pós-prandiais por aumento de metabolização muscular de amônia (Kircheis G, et al, 1997); probióticos, inibidores de glutaminase, metronidazole, flumazenil, e, em alguns casos, transplante hepático (Vilstrup H, et al, 2014, Mpabanzi L, Jalan R., 2012).

A técnica de eletrofisiologia pode ser utilizada para detectar alterações cerebrais presentes em EH, e inclui monitoramento por eletroencefalografia (EEG), potenciais evocados e *critical flicker frequency testing*. O Grau das alterações encontradas em pacientes com EH são relacionadas com a severidade do episódio. Sumariamente, elas consistem em diminuição sincrônica bilateral da frequência de ondas, concomitante a um aumento na amplitude e o desaparecimento no padrão normal de onda do ritmo-alpha [8-12 ciclos por segundo (cps)]. Além disso, análises mais aprofundadas, como as encontradas nos trabalhos desta tese, podem identificar o padrão de onda predominante, a densidade espectral e realizar a quantificação dessas alterações – chamado de *left-index* (Amodio P, et al 1999, Vogels BA, et al, 1997; Paniz LG, et al, 2014).

Fisiopatologia,

Focaremos principalmente em alterações no mecanismo fisiopatogênico de encefalopatia aguda, a qual mais se relaciona com os trabalhos desenvolvidos nessa tese.

Hiperamonemia,

A amônia está classicamente envolvida no desenvolvimento de EH (Traeger, H., et al 1954), sendo fator causal de diversas alterações tais como excitotoxicidade glutamatérgica, estresse oxidativo, alterações em metabolismo energético e metabolismo de aminoácidos (Ott P, Vilstrup H, 2014; Felipo V. 2013). Além disso, crescentes níveis de amônia no sistema nervoso central correlacionam-se com o a gravidade de alterações neurológicas observadas em modelos experimentais (Hermenegildo C, Monfort P, Felipo V. 2000) e em humanos (Lockwood AH, et al, 1991).

Em modelos experimentais em roedores, nos quais os animais são expostos a um rápido aumento no nível plasmático arterial de amônia, observa-se um consequente aumento nos níveis cerebrais de amônia (de 0.2 $\mu mol.g^{-1}$ a 1–3 $\mu mol.g^{-1}$ ) (Felipo V. 2013). Existem duas principais hipótese para um acúmulo de amônia no sistema nervoso central (SNC): a hipótese de transporte passivo assume que o pKa da amônia a 37$^{o}$C é ~8.9, e NH3 constitui uma parcela de cerca de 3.4% da amônia total do plasma arterial a pH de 7.42. Uma vez que o pH é menor no lado cerebral da BHE, a fração de NH3 é mais baixa, dessa forma desvia o equilíbrio da reação para a formação de amônio. Para manter o equilíbrio, mais amônia atravessa a

BHE, levando a um acúmulo de amônia e amônio no SNC (Ott P, Vilstrup H, 2014). A segunda hipótese cursa sobre transporte ativo de $NH4^+$, o qual ocorre predominantemente após ser atingido equilíbrio, explicado pela hipótese de transporte passivo. O transporte ativo de NH4+ é provavelmente mediado por canais de potássio (80%) e cotransportadores de sódio, potássio e cloreto (Ott and Larsen 2004).

Excitotoxicidade glutamatérgica,

O aumento dos níveis de amônia no SNC leva à ativação de receptores NMDA e ao aumento dos níveis de glutamato extracelular. Essas alterações podem ser parcial ou completamente prevenidas com a utilização de bloqueadores NMDA como memantina ou MK-801, melhorando o prognóstico em modelos animais de hiperamonemia. Com o bloqueio de receptores NMDA, também se previne a ativação da formação de GMP cíclico e óxido nítrico, os quais também estão envolvidos nos mecanismos de excitotoxicidade. Dessa forma, sabemos que, inicialmente, a maior ativação de receptores NMDA se deve ao aumento da amônia, a qual age diretamente despolarizando a membrana neuronal e deslocando moléculas de magnésio dos receptores NMDA. Assim, mesmo com concentrações normais de glutamato no espaço extracelular, há despolarização neuronal. Outro fator é a consequente diminuição dos níveis de ATP com ativação desenfreada de receptores NMDA, o que leva à diminuição da captação sináptica de glutamato, resultando em excesso de glutamato na fenda sináptica e excitotoxicidade glutamatérgica (Vogels BA, et al, 1997; Hermenegildo C, Monfort P, Felipo V., 2000).

Estresse oxidativo,

Além de haver um efeito tóxico direto da amônia sobre as membranas neuronais (Butterworth R. F, et al, 1987), o aumento dos níveis de óxido nítrico e glutamato extracelular também promovem estresse oxidativo no SNC. É provável que o estresse oxidativo induzido por elevados níveis de amônia esteja entre os principais mecanismos de EH aguda (Ciećko-Michalska, et al, 2012).

Metabolismo energético,

É sabido que pacientes com EH apresentam níveis liquóricos de lactato elevados. Existem 2 principais teorias contraditórias, que explicam essa alteração:

1) Inibição da enzima alfa-cetoglutarato desidrogenase (a-CGDH) o que leva ao aumento de glutamato a partir de alfa-cetoglutarato, diminuindo o número de cadeias carbonadas no ciclo do ácido tricarboxílico (CAT). Por conta disso, existe uma diminuição na produção de ATP acoplados à oxidação dos carbonos da molécula de glicose. Há duas maneiras principais de reposição de cadeias carbônicas no CAT: a) Aumento de proteólise, levando ao aumento de aspartato e reposição de cadeias carbonadas através do aspartato-malato *shuttle* (Ott P, Clemmesen O, Larsen FS, 2005; Swain M, Butterworth RF, Blei AT, 1992)*;* b) Aumento de glicólise, aumentando anaplerose (síntese de oxalacetato a partir de piruvato) e também lactato (devido ao aumento de metabolismo anaeróbico).

Embora classicamente aceita, existem estudos que mostraram aumento da

atividade do CAT em hiperamonemia, contrariando a hipótese recém apresentada (Rama Rao KV, Norenberg MD, et al 2012; Leke et al. 2011a).

2)Como exposto anteriormente, o aumento da glicólise provavelmente é um dos principais mecanismos causadores do aumento de níveis de lactato. É sabido que em hiperamonemia há maior ativação de enzimas chave na glicólise, como fosfofrutoquinase e aldolase (Ratnakumari and Murthy, 1992, 1993). Com o aumento da amônia, a captação de glutamato extracelular também estimula a glicólise, devido a uma maior ativação da bomba Na/K ATPase. Isso leva à formação de lactato intra astrocitário, o qual é transferido ao neurônio para ser usado como substrato energético preferencial, o que vai ao encontro da teoria lactato *shuttle* (Ott P, Vilstrup H., 2014; Pellerin and Magistretti 2012).

Metabolismo de aminoácidos,

O metabolismo de aminoácidos é extensamente estudado em modelos de hiperamonemia e, utilizando o critério de priorizar os mecanismos mais ligados a este trabalho, focaremos nossa introdução em glutamato, glutamina, alanina e aspartato.

O edema astrocítico causado pela glutamina é considerado um dos principais causadores das alterações na EH. A enzima glutamina sintetase está presente nos astrócitos e sintetiza glutamina a partir de glutamato e amônia. Em modelos de hiperamonemia, há aumento da quantidade citoplasmática de glutamina, que tem propriedade osmótica e, em altas quantidades, provoca edema astrocitário e, consequentemente, edema

cerebral. (Felipo, V. 2013, Desjardins P, Du T, Jiang W, Peng L, Butterworth RF., 2012).

Diversas teorias explicam aumento do glutamato extracelular: 1) despolarização neuronal por elevado nível de amônia, aumentando exocitose de glutamato; 2) diminuição de transportadores glutamatérgicos astrocitários (Lehmann C, Bette S, Engele J., 2009), diminuindo captação de glutamato, acumulando glutamato na fenda sináptica; 3) inibição da enzima a-CGDH, levando ao acúmulo de alfa-cetoglutarato, o qual serve de substrato para formação de glutamato (Ciećko-Michalska I. et al, 2012).

O aumento dos níveis liquóricos de alanina observado em modelos animais de hiperamonemia se deve principalmente a dois mecanismos: primeiramente, pelo aumento de transaminação de glutamina e de piruvato (enzima glutamina transaminase), formando alanina e alfa-cetoglutarato. O segundo mecanismo é a partir do aumento da quantidade de piruvato por maior atividade da glicólise (supracitado) e ação da enzima alanina aminotransferase (Swain M, Butterworth RF, Blei AT, 1992; Ciećko-Michalska I. et al, 2012).

Também se especula que o uso de aminoácidos de cadeia ramificada se torna importante fonte de carbonos para o CAT, uma vez que a partir de sua desaminação, forma-se acetil-CoA e succinil-CoA. Essas moléculas são metabolizadas no CAT em etapas prévias e posteriores ao metabolismo de alfa-cetoglutarato (Ott et al. 2005; Gluud LL, et al, 2013).

A EH apresenta diversos outros mecanismos fisiopatológicos além dos supracitados, que influem em maior ou menor grau do quadro clínico. Fazem parte dos mecanismos não abordados nessa revisão: alteração de permeabilidade na BHE, edema vasogênico, hipótese dos neuro esteróides, acúmulo de toxinas, neuroinflamação, etc. (Vaquero J, Butterworth RF., 2007, Ciećko-Michalska I, et al, 2012, Scott TR, et al, 2013)

Guanosina e o sistema purinérgico,

O sistema purinérgico compreende moléculas relacionadas a bases purínicas adenina e guanina, seus derivados - ATP, ADP, AMP, adenosina, GTP, GDP, GMP e guanosina; seus metabólitos - xantina, hipoxantina, ácido úrico e inosina; e seus transportadores e receptores. O sistema purinérgico está relacionado a funções como segundo mensageiros e metabolismo energético, mas também apresenta efeitos extracelulares, modulando atividade glutamatérgica (Schmidt AP, Lara DR, Souza DO. 2007).

O sistema purinérgico frente à excitotoxicidade glutamatérgica já vem sendo estudado e derivados da guanina, principalmente a guanosina, apresentam efeitos anticonvulsivantes (Schmidt et al., 2010). Guanosina também preveniu diminuição da captação de glutamato em estudos *ex-vivo* (Vinadé et al., 2005). Além disso, o efeito da guanosina e do sistema purinérgico vem sendo estudado em trauma, isquemia, hipóxia e hipoglicemia (Schmidt AP, Lara DR, Souza DO. 2007). Recentemente foi publicado por nosso grupo um estudo sobre os efeitos neuroprotetores da administração de guanosina em um modelo de EH crônica (Paniz LG, et al, 2014)

**Objetivos desta Tese**

Objetivos gerais,

Estudar o efeito da guanosina em um modelo animal de hiperamonemia aguda;

Padronizar um modelo animal de encefalopatia hepatica induzida por hepatectomia subtotal, com objetivo de compreender melhor as alterações no metabolismo do SNC devido à EH;

Objetivos específicos,

Modelo animal de hiperamonemia aguda: estudar os efeitos da guanosina sobre letalidade e morbidade, eletrofisiologia, marcadores de estresse oxidativo, captação de glutamato, imunoconteúdo e atividade da enzima glutamina sintetase, níveis liquóricos de glutamato, glutamina, alanina e amônia,

Modelo animal de EH induzida por hepatectomia subtotal: estudar letalidade cirúrgica, alterações comportamentais, eletrofisiologia, marcadores de estresse oxidativo, imunoconteúdo de GLAST e GLT-1, quantificação de oxidação de glicose, glutamato e lactato no SNC, atividade das enzimas do ciclo dos ácidos tricarboxílicos.

# PARTE 2

**“A GUANOSINA CONTRA ATACA”**

# CAPÍTULO 1

## Guanosine Exerts Neuroprotective Effect in an Experimental Model of Acute Ammonia Intoxication

Giordano Fabricio Cittolin-Santos, Adriano Martimbianco de Assis, Pedro A. Guazzelli, Lucas G. Paniz, Jussemara S. da Silva, Maria Elisa Calcagnotto, Gisele Hansel, Kamila C. Zenki, Eduardo Kalinine, Marta M. Duarte, Diogo O. Souza

*Giordano Fabricio Cittolin-Santos e Adriano Martimbianco de Assis contribuíram igualmente para esse trabalho.

**MANUSCRITO PUBLICADO NA REVISTA MOLECULAR OF NEUROBIOLOGY**

Submetido em 06 de março de 2016

Aceito em 28 de março de 2016

Mol Neurobiol
DOI 10.1007/s12035-016-9892-4

# Guanosine Exerts Neuroprotective Effect in an Experimental Model of Acute Ammonia Intoxication

G. F. Cittolin-Santos[1] · A. M. de Assis[1] · P. A. Guazzelli[1] · L. G. Paniz[1] · J. S. da Silva[1] · M. E. Calcagnotto[1,2] · G. Hansel[1] · K. C. Zenki[1,3] · E. Kalinine[1,3] · M. M. Duarte[4] · D. O. Souza[1,2]

Received: 6 March 2016 / Accepted: 28 March 2016


**Abstract** The nucleoside guanosine (GUO) increases glutamate uptake by astrocytes and acts as antioxidant, thereby providing neuroprotection against glutamatergic excitotoxicity, as we have recently demonstrated in an animal model of chronic hepatic encephalopathy. Here, we investigated the neuroprotective effect of GUO in an acute ammonia intoxication model. Adult male Wistar rats received an intraperitoneal (i.p.) injection of vehicle or GUO 60 mg/kg, followed 20 min later by an i.p. injection of vehicle or 550 mg/kg of ammonium acetate. Afterwards, animals were observed for 45 min, being evaluated as normal, coma (i.e., absence of corneal reflex), or death status. In a second cohort of rats, video-electroencephalogram (EEG) recordings were performed. In a third cohort of rats, the following were measured: (i) plasma levels of glucose, transaminases, and urea; (ii) cerebrospinal fluid (CSF) levels of ammonia, glutamine, glutamate, and alanine; (iii) glutamate uptake in brain slices; and (iv) brain redox status and glutamine synthetase activity in cerebral cortex. GUO drastically reduced the lethality rate and the duration of coma. Animals treated with GUO had improved EEG traces, decreased CSF levels of glutamate and alanine, lowered oxidative stress in the cerebral cortex, and increased glutamate uptake by astrocytes in brain slices compared with animals that received vehicle prior to ammonium acetate administration. This study provides new evidence on mechanisms of guanine-derived purines in their potential modulation of glutamatergic system, contributing to GUO neuroprotective effects in a rodent model of by acute ammonia intoxication.

**Keywords** Acute ammonia intoxication · Glutamate excitotoxicity · Hyperammonemia · Guanosine

## Introduction

Encephalopathy is a global disturbance of cerebral function characterized by an altered mental state also known as delirium. These alterations in mental state range from mild disorientation to severe coma [1]. The underlying disease etiologies are diverse and include metabolic and systemic causes (e.g., hepatopathies and nephropathies), brain ischemia, hypertension, intoxication, traumatic brain injury (TBI), epilepsy, and infections [2]. Encephalopathy is associated with high morbidity and mortality unless it is promptly treated, and in some cases, the only option for stabilizing the patient is liver transplantation [3].

Hepatic encephalopathy (HE) is considered one of the main subtypes of the encephalopathy syndrome, with a characteristic alteration in cerebral function that occurs due to liver failure (both acute and chronic) or portacaval shunt [4–6]. It is

G. F. Cittolin-Santos and A. M. de Assis contributed equally to this work.

✉ D. O. Souza
diogo@ufrgs.br

[1] Postgraduate Program in Biological Sciences: Biochemistry, ICBS, Federal University of Rio Grande do Sul, Porto Alegre, RS 90035-003, Brazil

[2] Department of Biochemistry, Federal University of Rio Grande do Sul, Porto Alegre, RS 90035-003, Brazil

[3] Department of Physiology, Federal University of Sergipe, São Cristovão, SE 49100-000, Brazil

[4] Health Sciences Center, Lutheran University of Brazil (ULBRA), Campus Santa Maria, Santa Maria, RS 97020-001, Brazil

Published online: 06 April 2016

known that approximately 40 % of cirrhotic patients will present with overt HE during their clinical course and that these patients have a high chance of HE recurrence within months [7, 8]. Therefore, HE is one of the main reasons for hospitalization in patients with liver dysfunction, and its management represents a high economic burden [9].

It is likely that ammonia plays a central role in episodic (i.e., acute) HE. The hyperammonemia caused by liver failure leads to increased levels of ammonia in the brain, with consequent brain edema that induces behavioral changes, coma, and death [10–12]. High levels of ammonia in the brain lead to activation of NMDA receptors, thereby triggering the glutamate-nitric oxide-cGMP pathway [13]. This effect activates the glutamatergic system excitotoxicity mechanism through decreased glutamate transporter activity and levels, as well as increased extracellular glutamate levels, resulting in hyperactivation of NMDA receptors and consequent brain oxidative stress damage [14–16].

Previous studies have shown that neuroprotective strategies against glutamatergic excitotoxicity contribute to decreasing the deleterious effect of hyperammonemia on the central nervous system (CNS) [17–19]. One such strategy can be achieved through the use of MK801, which reduces glutamatergic activity [18, 19]. Accordingly, the nucleoside guanosine exhibits several neuroprotective effects in experimental models of brain injuries involving glutamatergic excitotoxicity, such as HE, seizures, brain ischemia, and pain [17, 20–22].

We hypothesize that the intraperitoneal (i.p.) injection of ammonia at a high concentration induces neurological alterations followed by brain disorders and that the nucleoside guanosine could exert a neuroprotective effect in this situation. To test our hypothesis, we evaluated the effects of acute ammonium exposure and the neuroprotective effects of guanosine administration on (i) the mortality and coma rates, (ii) electrophysiological recordings, (iii) glutamatergic brain parameters, (iv) brain redox status, and (v) biochemical parameters in cerebrospinal fluid (CSF) and serum.

## Materials and Methods

### Animals

Adult male Wistar rats (90 days old), from the Central Animal House of the Department of Biochemistry—UFRGS, were maintained under a standard light/dark cycle (light between 7:00 a.m. and 7:00 p.m.) at room temperature (22 ± 2 °C). The rats were housed in plastic cages (five rats per cage), with tap water and commercial food available ad libitum. These conditions were kept constant throughout the experiments.

### Drugs

Guanosine, ammonium acetate, and all other chemicals were from Sigma-Aldrich (St. Louis, MO, USA). L-[3,4-$^{3}$H]-Glutamic acid (50 Ci/mmol) was from Perkin Elmer Life Sciences (Boston, MA, USA).

Ammonium acetate (150–750 mg/ml) was dissolved in distilled water and administered via i.p. injection. Concentrations of ammonium acetate solutions were adjusted to reach the desired dose by injecting 3 mL/kg of body weight, as previously described [10]. Guanosine was dissolved in 0.1 mM NaOH and used as a pretreatment 20 min before the ammonium acetate injection. A vehicle solution of 0.1 mM NaOH was used as a control. Both solutions were adjusted to pH 7.4. The guanosine solutions and the vehicle solution were administered by i.p. injection at a dose of 2 mL/kg of body weight.

### Experimental Design

The experiments were divided into three protocols (Fig. 1).

#### *Protocol 1—Neurological Parameters*

For evaluation of neurological parameters, the animals were divided into four groups. Each group received a combination of pretreatment (i.p. injection of either guanosine or vehicle) and insult (i.p. injection of either ammonium acetate or distilled water). The four groups of animals were as follows: control (vehicle + distilled water), ammonium (vehicle + ammonium acetate), guanosine (guanosine + distilled water), and guanosine + ammonium (guanosine + ammonium acetate). The animals were monitored for 20 min after the pretreatment injection and 45 min after the insult injection.

Neurological evaluation was performed every 3 min during the 45 min after ammonium acetate injection. The time point at which the animals entered the comatose state (i.e., loss of corneal reflex), as well as the duration of coma and the time of death, was recorded.

### Dose Curve of Ammonium Acetate and Guanosine Administration

The established dose of i.p. ammonium acetate was 550 mg/kg according to a dose response curve (Fig. 2a). The animals were pretreated using different doses of guanosine 20 min before the insult to evaluate the effect of guanosine on the mortality rate (Fig. 2b). The dose of i.p. guanosine 60 mg/kg was used in the further experiments.

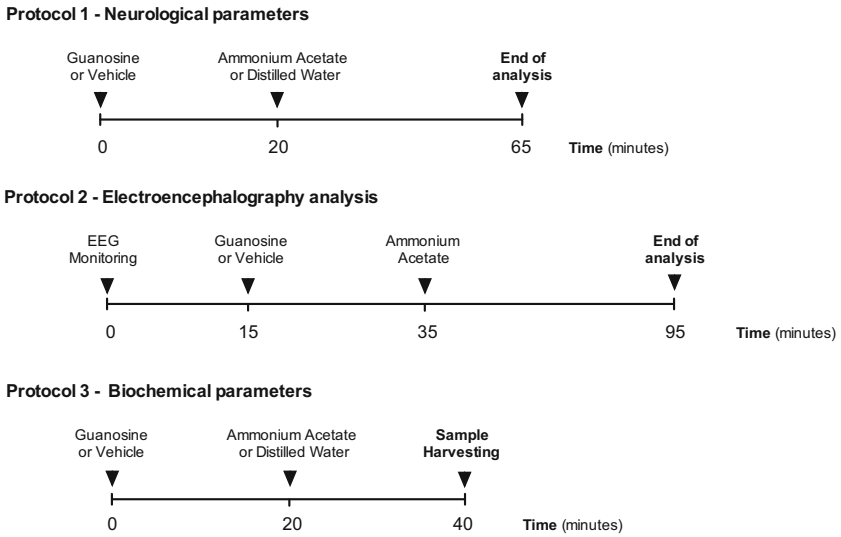


**Fig. 1** *Protocol 1* Pretreatment (with guanosine or vehicle) set the time at 0. Ammonium acetate or distilled water was injected 20 min later for neurological evaluation during a 45-min period. *Protocol 2* The EEG monitoring set the time at 0. Pretreatment (with guanosine or vehicle) was injected 15 min later of the beginning of recording. Ammonium acetate was injected 20 min later of pretreatment. EEG was recorded 15 min before pretreatment and 80 min after the first injection (pretreatment). *Protocol 3* Pretreatment (with guanosine or vehicle) set the time at 0. Ammonium acetate or distilled water was injected 20 min later. The sample harvesting happened after 40 min after the first injection (pretreatment)

*Protocol 2—Electroencephalographic Analysis*

For EEG analysis, the animals were divided into two groups. The animals received either vehicle or GUO as a pretreatment, and 20 min later both groups received an ammonium acetate injection (Fig. 1). Both groups were monitored by recording the video EEG at 15 min before pretreatment administration (i.e., baseline EEG), 20 min after guanosine (60 mg/kg) or vehicle injection, and 60 min after the ammonium acetate injection. The animals used for the EEG analysis were not included in the clinical evaluation or the neurochemical analysis.

Epidural electrodes were implanted 1 week before the video-EEG recording. To place the electrodes on the cortical surface, the animals were anesthetized with i.p. injections of ketamine (80 mg/kg–0.8 mL/kg) and xylazine (10 mg/kg–0.5 mL/kg) and placed on a stereotaxic instrument. The three stainless steel screw electrodes (1.0-mm diameter) were placed according to the coordinates from Paxinos and Watson [23]. Two of them were placed LL +/− 2.0 mm, AP −1.0 mm from bregma; the third (the reference) electrode was placed on the midline of the occipital bone and kept in contact with cerebrospinal fluid. The ground (small screw) was placed over the frontal bone and was used for fixation of the dental acrylic helmet to the skull [17].

One week after implanting the electrodes, each animal was individually transferred to an observation cage to perform the video-EEG recordings. The EEG was recorded with a standard data acquisition system (Multichannel Plexon Acquisition Processor System). EEG signals were filtered at 0.01–100 Hz, followed by digitization at 1 kHz for posterior analysis. All analyses were performed using built-in and custom-written routines in MATLAB (Mathworks, Inc.). The power density spectra were obtained to calculate the EEG left index at baseline, after injection of guanosine or vehicle, after ammonium acetate injection and at the end of the video-EEG recording. The EEG left index was calculated as the logarithm of the ratio between the power of the low frequency (1–7.4 Hz) and the high frequency (13.5–26.5 Hz). Normal rats have an EEG left index of approximately 0.60, and rats in coma have an index of approximately 0.80–0.90 [24].

*Protocol 3—Biochemical Analyses*

For biochemical analyses, we used the four groups as described above for protocol 1 (control, ammonium, guanosine, and guanosine + ammonium). At the 40-min time mark, the animals were euthanized to collect cerebrospinal fluid (CSF) and blood samples, as well as cerebral cortex tissues.

## CSF Analysis

The animals were anesthetized with inhaled isoflurane and placed on a stereotaxic apparatus to collect CSF samples (40–80 μL per rat) by direct puncture of the cisterna magna with an insulin syringe (27 gauge × 1/2-in. length) [25]. The CSF was centrifuged at 1000×*g* for 10 min, and the supernatant was stored at −80 °C for further evaluation of (i) ammonia, measured using a commercial kit (Sigma-Aldrich, St.

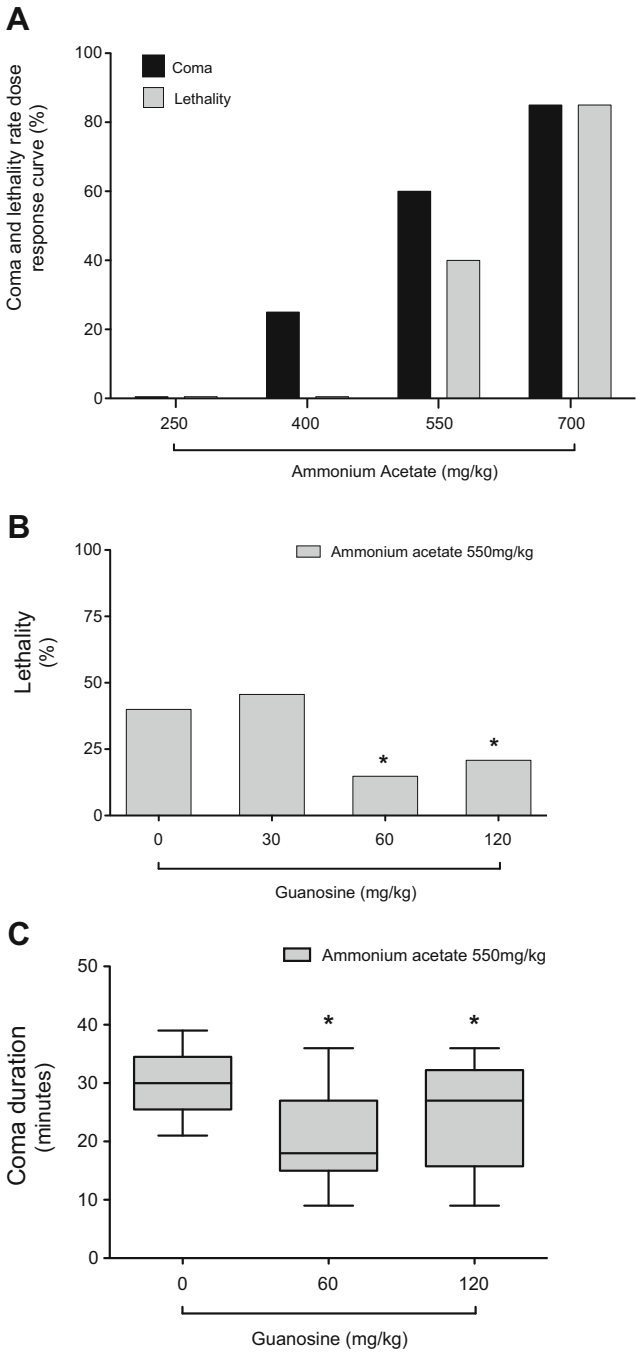


**Fig. 2** Ammonium acetate effect on rates of coma and death (**a**), guanosine effect on lethality rate (**b**), and on coma duration of animals entering in comatose state and did not die (**c**). The Spearman correlation coefficient for coma is $r = 1$ and for mortality is $r = 0.9747$ (**a**). *Asterisk* indicates a difference from 0 to 30 mg/kg guanosine groups, $p < 0.05$, one-way ANOVA (**b**). The results are expressed as the median and 5–95 % range (minutes), *Asterisk* indicates a difference from the control group, $p < 0.05$, Kruskal–Wallis test with Dunn's multiple comparison test (**c**)

Louis, MO, USA) according to the manufacturer's protocol and (ii) glutamine, glutamate, and alanine levels, measured by HPLC [26].

### Plasma Biochemical Analysis

Blood samples were drawn into EDTA tubes, followed by centrifugation at 5000×*g* for 10 min. Plasma was stored at −80 °C for further evaluation of alanine aminotransferase (ALT) and aspartate aminotransferase (AST) activities, as well as the levels of glucose and urea. These evaluations were performed using commercial kits (Labtest, MG, Brazil).

### Glutamate Uptake

After decapitation, the cortex was immediately dissected on ice (4 °C). Frontoparietal cortical slices (0.2-mm thickness) were rapidly obtained using a McIlwain Tissue Chopper and immersed at 4 °C in HBSS buffer ph 7.2. Frontoparietal cortical slices were preincubated with HBSS at 37 °C for 15 min. The incubation was started by the addition of 0.33 μCi/mL of L-[$^3$H] glutamate, and stopped after 7 min with two ice-cold washes using 1 mL of HBSS. After washing, 0.5 N NaOH was immediately added to the slices and they were stored overnight. The $Na^+$-independent uptake of glutamate was measured. $Na^+$-dependent uptake of glutamate was measured as the difference between the total uptake and the $Na^+$-independent uptake [27].

### Glutamine Synthetase Activity

The glutamine synthetase (GS) enzymatic activity assay was performed as described previously by Quincozes-Santos et al. [28]. Synthetic γ-glutamylhydroxamate was used as the standard. GS activity was expressed as micromole per hour per milligram of protein of formed product.

### Redox Parameters

The oxidative stress parameters were evaluated in the cerebral cortex. The cortices were homogenized in PBS (20 mM, pH 7.4) for analysis of the following redox parameters.

### Dichlorodihydrofluorescein Oxidation

The levels of reactive oxygen species were measured as described before [17]. A calibration curve was calculated with standard dichlorodihydrofluorescein DCFH, and the levels of reactive species were expressed as micromole of DCF formed per milligram of protein.

### Thiobarbituric Acid Reactive Species

To assess the extent of lipoperoxidation, the levels of thiobarbituric acid reactive species (TBARS) were measured according to Paniz et al. [17]. The results are expressed as nanomole of TBARS per milligram of protein.

### Antioxidant Enzyme Activities

Superoxide dismutase (EC 1.15.1.1) activity was assessed as described previously [29]. The results were expressed as units of SOD per milligram of protein. The glutathione peroxidase (EC 1.11.1.9) [30] (GSH-Px) activity was measured according to Wendel. One unit of GSH-Px activity was defined as 1 μmol of NADPH consumed per minute, and the specific activity was expressed as units per milligram of protein.

### Western Blotting of Glutamine Synthetase

Cerebral cortex was homogenized in Laemmli sample buffer (20 μg) and separated by SDS-PAGE on 10 % (*w*/*v*) acrylamide and 0.275 % (*w*/*v*) bisacrylamide gels. The proteins were then electrotransferred onto nitrocellulose membranes. The membranes were incubated for 1 h at 25 °C in Tris/saline buffer Tween-20 (TSB-T 20 mM Tris-HCl, pH 7.5, 137 mM NaCl and 0.05 % (*v*/*v*) Tween 20) that contained 1 % (*w*/*v*) non-fat milk powder. The membranes were subsequently incubated for 12 h with the appropriate primary antibody (glutamine synthetase, 1:10,000). After washing in TBS-T, the blots were incubated with HRP-linked anti-immunoglobulin G (IgG) antibodies for 1.5 h at 25 °C [31]. Chemiluminescent bands were detected, and a densitometric analysis was performed with ImageJ software (NIH, Bethesda, MD, USA).

### Statistical Analysis

Data are expressed as the means ± S.E.M. To compare the groups, we used the following statistical methods, as appropriate: one-way ANOVA followed by Tukey test, chi-square test, Spearman correlation coefficient, Newman–Keuls post-test, Kruskal–Wallis test, Dunn's multiple comparison test, and Student's *t* test, when mentioned, using GraphPad Prism vs. 5 (La Jolla, CA, USA). The level of significance was considered to be $p < 0.05$.

## Results

### Neurological Evaluation

There were no neurological alterations in the control or guanosine groups. However, guanosine had a strong effect on mortality in the groups that received ammonium acetate. The lethality rate of the ammonium acetate group was 36 %, but 60 and 120 mg/kg guanosine (in the guanosine + ammonium acetate group) decreased this rate to 15 % ($n = 52$) (Fig. 2b, $p < 0.05$). There was no difference in the percentage of animals entering in comatose state between the guanosine + ammonium acetate group ($n = 41$) and the ammonium acetate group ($n = 42$), 75 and 69 %, respectively. However, guanosine

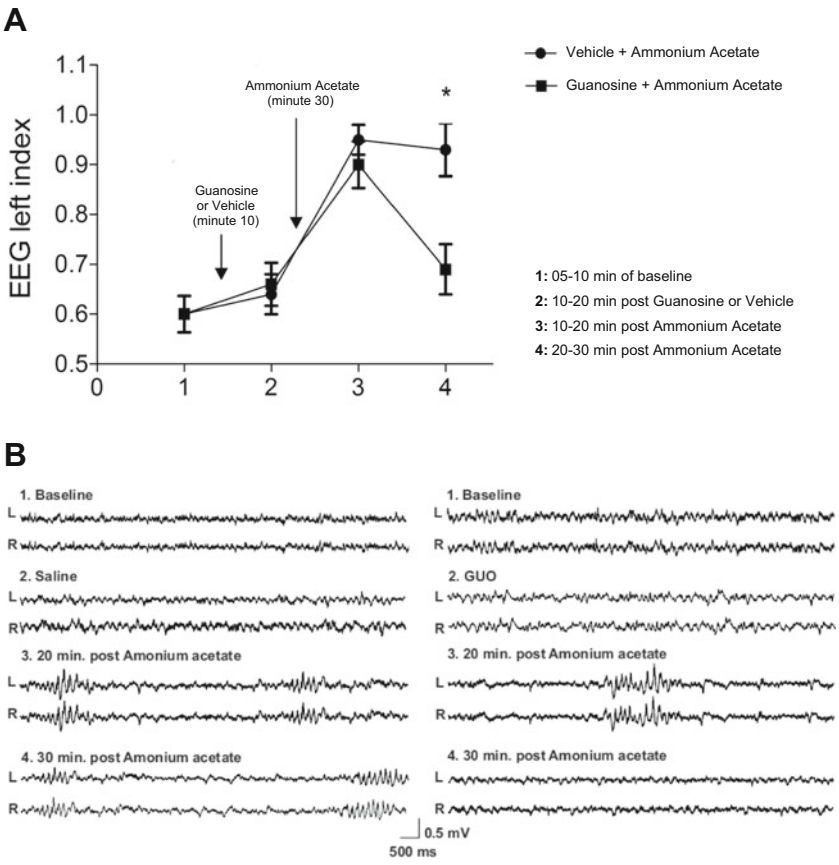


**Fig. 3** EEG analysis: **a** EEG left index values for ammonium acetate group and guanosine + ammonium acetate group at four different times. **b** Representative EEG traces for each analyzed period of both groups. *Asterisk* Indicates a difference from the guanosine + ammonium acetate other group, $p < 0.01$, Student's *t* test

significantly reduced the coma duration of animals that survived in the time evaluated (ammonium acetate group, 29.1 ± 1.5 min. vs. guanosine + ammonium acetate group, 22.8 ± 1.9 min, Fig. 2c, $p < 0.005$, $t$ test). Concerning the mortality rates of this experimental model, the rats were only evaluated neurologically for up to 45 min following ammonium acetate administration, as after this period, no animal died. However, at this time mark, most of the ammonium group maintained the same neurological status, which was coma. In contrast, the guanosine + ammonium group had already begun to show neurological improvement at 33–35 min by starting to walk again. Thus, it can be inferred that the reduction of coma duration (Fig. 2c, $p < 0.05$) that we observed would be even more pronounced if the rats had been assessed for longer than 45 min.

## EEG

Guanosine per se had no effect on the EEG left index (guanosine or vehicle, Fig. 3), which became abnormally higher in the first 10 min after ammonium administration (Fig. 3a) in both groups (guanosine + ammonium group, 0.90 + 0.05, $n = 9$; ammonium group, 0.95 + 0.03, $n = 9$). However, during the 20–30-min interval after ammonium acetate administration, the EEG left index in the ammonium group remained high up to the end of the recording time (0.93 + 0.05, $n = 8$; $p < 0.005$), but guanosine reversed this ammonium effect because the EEG left index returned to normal values in the guanosine + ammonium group (0.69 + 0.05, $n = 9$). This finding could be related to the fact that the animals in the guanosine + ammonium group remained in severe coma for a shorter duration than those in the ammonium group. One animal in the ammonium group died before the 20-min time mark after ammonium acetate administration. Figure 3b shows the representative EEG traces of both groups.

## Plasma Biochemical Parameters

The injection of ammonium acetate decreased the plasma levels of glucose (~30 %, Fig. 4a, $p < 0.05$) and increased the plasma levels of ALT and AST (~70 %, Fig. 4b; ~70 %, Fig. 4c, $p < 0.05$) without affecting plasma urea levels (Fig. 4d). Pretreatment with guanosine had no effect on the analyzed parameters. These results indicate that systemic and hepatic parameters were not affected by guanosine.

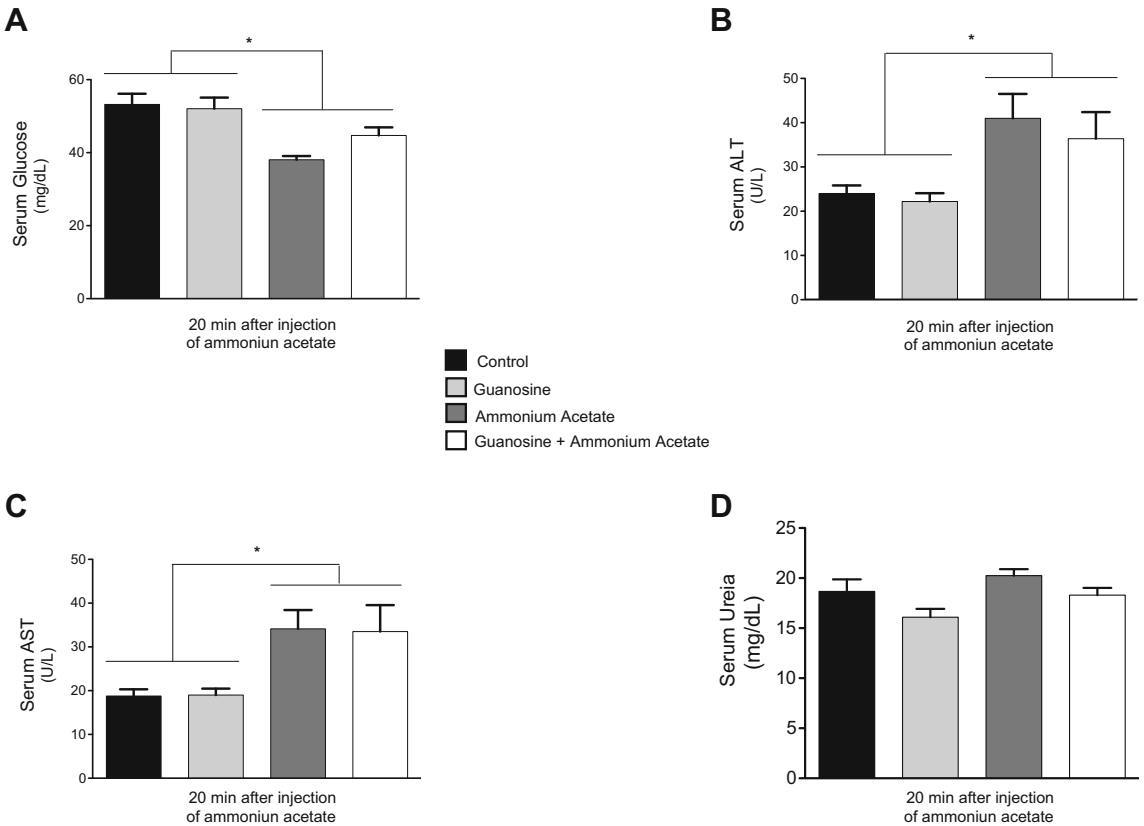


**Fig. 4** Plasma biochemical levels of **a** glucose, **b** ALT, **c** AST, and **d** urea. The results are expressed in milligram per decaliter (**a** and **d**) and U/L (**b** and **c**) and as the means ± S.E.M. ($n = 8$ per group). *Asterisk* Indicates a difference among ammonium acetate groups (guanosine or vehicle) and distilled water groups (guanosine or vehicle), $p < 0.05$, one-way ANOVA

### CSF Biochemical Parameters

Ammonia levels in the CSF (μmol/L) (Fig. 5a) increased in the ammonium group (6.87 ± 1.3) compared to the control (3.06 ± 0.91) and guanosine (3.53 ± 1.20) groups ($p < 0.001$). This increase was not affected by guanosine administration (guanosine + ammonium group 6.17 ± 1.47) ($p < 0.001$). Interestingly, the increase in CSF levels of glutamate (4.75 ± 1.62, $n = 11$) and alanine (26.3 ± 5.4, $n = 6$) observed in the ammonium group was reversed by pretreatment with guanosine. The CSF amino acid levels in the guanosine + ammonium group were 3.37 ± 0.80 and 19.6 ± 2.70, respectively ($n = 10$) (Fig. 5c and d, $p < 0.001$). CSF glutamine levels were similar for all groups (Fig. 5b).

### Brain Glutamatergic Parameters

#### *Glutamate Uptake*

The glutamate uptake activity in cortical slices decreased in the ammonium group, compared with the control group (~30 %, Fig. 6a, $p < 0.05$). Guanosine administration partially reversed this increase.

#### *Glutamine Synthetase Activity and Immunocontent*

The GS activity decreased in the ammonium group (Fig. 6b, $p < 0.001$) when compared with the control group. Guanosine administration abolished this decrease. The GS immunocontent was similar for all groups (Fig. 6c).

### Brain Redox Parameters

Concerning the activity of antioxidant enzymes, in the ammonium group compared with the control group, there was a decrease in SOD activity and an increase in GSH-Px activity. Pretreatment with guanosine prevented both of these effects (Fig. 7a and b, $p < 0.05$). TBARS (Fig. 7c) and DCFH (Fig. 7d) levels were similar in all groups. Guanosine per se had no effect on any parameter investigated, which is in accordance with previous results from our group [20].

## Discussion

We used an effective experimental model of acute ammonia intoxication [13] that exhibited neurological and EEG pattern

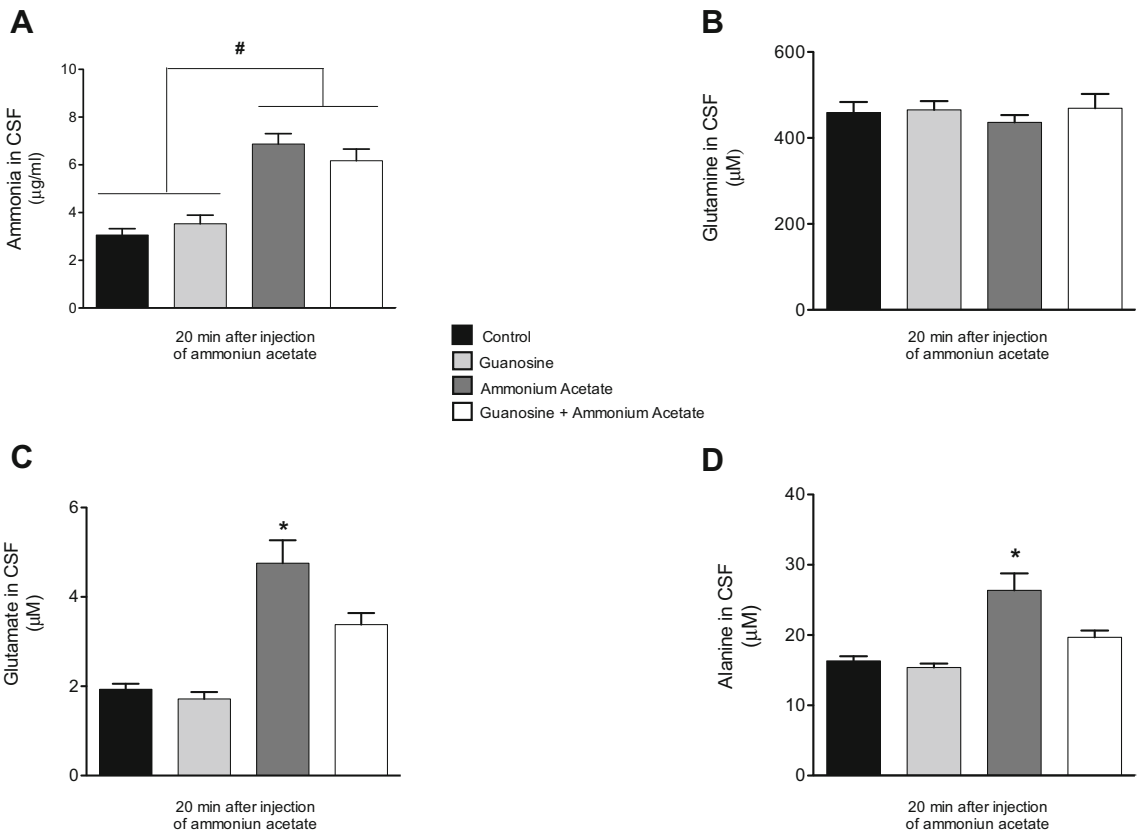


**Fig. 5** CSF levels of **a** ammonia, **b** glutamine, **c** glutamate, and **d** alanine. The results are expressed in microgram per milliliter (**a**) and micromolar (**b**, **c**, **d**) as the means ± S.E.M. ($n = 8$ per group). *Octothorpe* indicates difference among ammonium acetate groups (guanosine or vehicle) and distilled water groups (guanosine or vehicle) (**a**); *Asterisk* indicates difference from all other groups (**c**, **d**), $p < 0.05$, one-way ANOVA

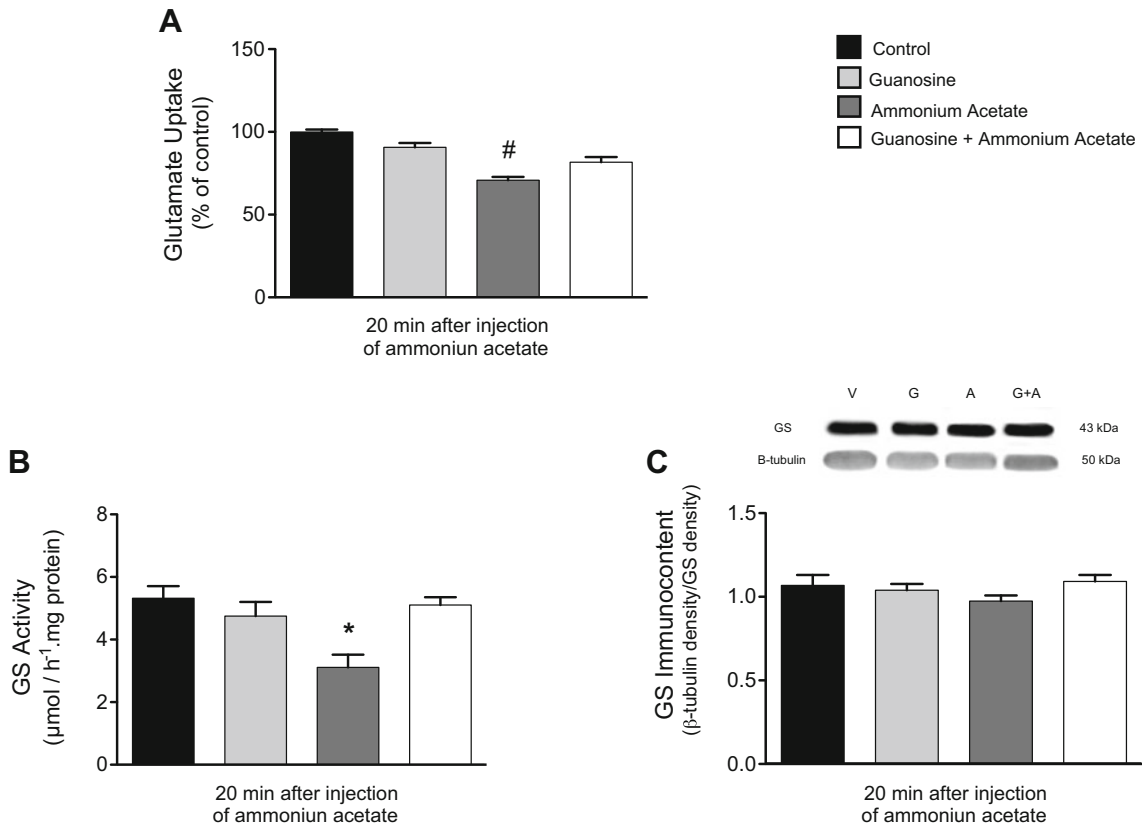


**Fig. 6** Cortical (**a**) glutamate uptake, (**b**) glutamine synthetase activity, and (**c**) glutamine synthetase immunocontent. The results are expressed as percent of control (control group value = 1393.5 ± 149.7 cpm/min/mg of protein) (**a**), micromole per hour per milligram of protein (**b**), and ratio of the control/β-tubulin (**c**), as the means ± S.E.M. ($n = 6$ per group). *Octothorpe* indicates difference from the control and guanosine groups; *Asterisk* indicates difference from all other groups, $p < 0.05$, one-way ANOVA

alterations similar to those in human acute HE [32]. This experimental model of ammonium acetate injection reproduces the increase in CSF ammonia levels, which is likely the main alteration described in HE pathophysiology [33]. The increase in total brain extracellular glutamate due to high ammonia levels is well described in HE [34], including the rise in brain extracellular glutamate after ammonium acetate administration [13]. Moreover, it has been shown that preventing the increase in brain extracellular glutamate using MK-801 [13] or memantine [24] could diminish the clinical and electrophysiological alterations following ammonium acetate administration. Furthermore, Rose and colleagues [15] have suggested that the pathophysiology of hyperammonemic encephalopathy in acute hepatic dysfunction could be related to a decrease in glutamate uptake in the CNS. Because MK-801 and memantine alter glutamate metabolism routes by decreasing the brain extracellular glutamate pool, it is reasonable that the use of guanosine, previously shown to exert neuroprotective effects against glutamatergic excitotoxicity in experimental models of brain injury [17, 22, 25–28, 31, 35], could potentially alter the course of ammonium acetate intoxication in vivo.

To our knowledge, this is the first report that indicates the neuroprotective effects of guanosine in acute hyperammonemic encephalopathy. The systemic administration of guanosine reversed/diminished the following effects of ammonium administration: mortality rate and coma duration (protocol 1), alterations in the EEG left index (protocol 2); increase in alanine CSF levels and alterations in various glutamatergic parameters (increased CSF glutamate levels, decreased ex vivo brain glutamate uptake (partially reversed), decreased brain GS activity) (protocol 3); and alterations in some brain redox parameters (increased SOD activity and decreased GSH-Px activity) (protocol 3). These findings reinforce previous data from our group and others showing that guanosine exerts neuroprotective effects in various in vivo animal models of glutamate excitotoxicity, such as seizures, brain ischemia, glutamatergic nociception, and chronic HE [17, 22, 26, 35–37]. It is also well known that guanosine has the ability to increase glutamate uptake by astrocytes, although the specific protein carriers have not yet been identified.

Some systemic metabolic parameters, such as plasma levels of glucose, ALT, and AST, were affected by ammonium acetate administration, but guanosine did not reverse

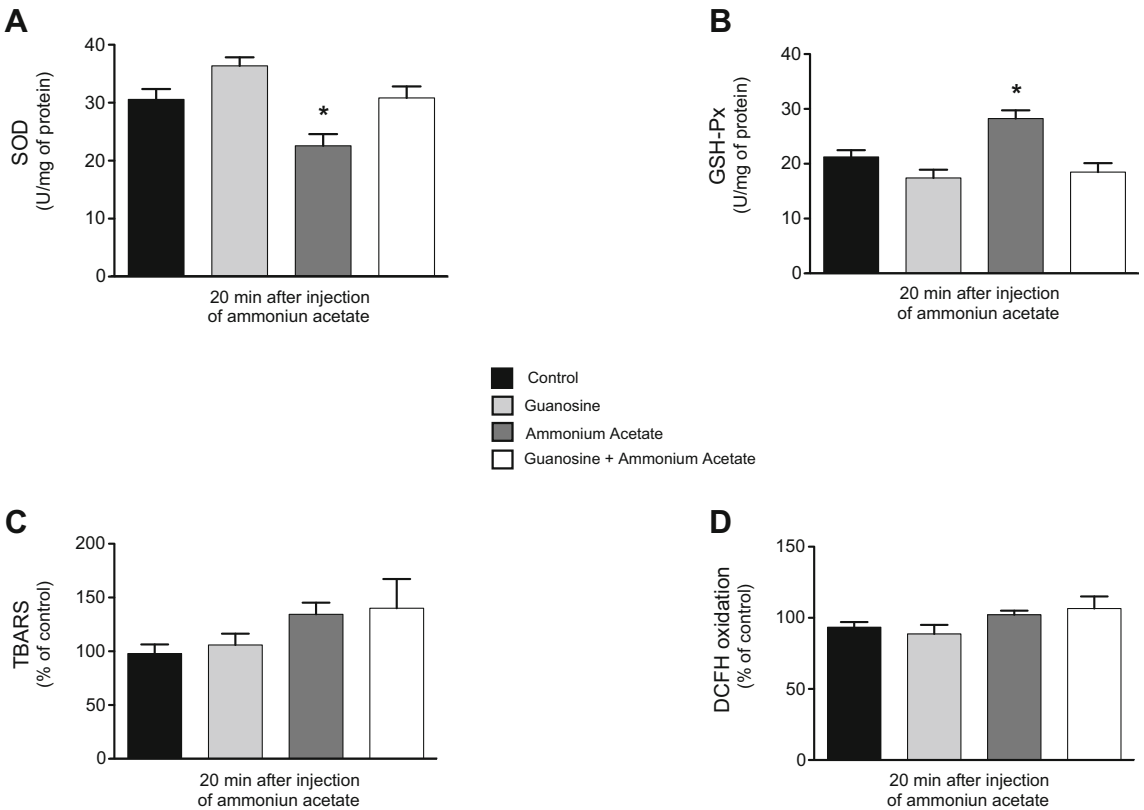


**Fig. 7** Oxidative stress parameters in cortical homogenate of **a** SOD activity, **b** GSH-Px activity, **c** TBARS levels, and (**d**) DCFH levels. The results are expressed as units per milligram of protein (**a** and **b**) and percent of control (TBARS: control group value = 0.160 ± 0.01 nmol/mg of protein; DCFH: control group value = 3385.1 ± 94.3 nmol/mg of protein) (**c** and **d**) as the means ± S.E.M. ($n = 8$ per group). *Asterisk* indicates difference from all other groups, $p < 0.05$, one-way ANOVA

these alterations. Although it could be postulated that the decrease in serum glucose levels in groups treated with ammonium acetate could contribute to the observed mortality rate, this possibility is unlikely because guanosine administration did not affect the decrease in serum glucose levels but did decrease the mortality rate by approximately 50 %.

CSF analysis is extensively used in translational research to identify some markers of brain disorders [38–40]. Here, it was observed that ammonium administration increased the CSF levels of ammonia as well as of the amino acids glutamate and alanine. In accord with our results, Therrien and Butterworth [41] observed the same increase in CSF amino acids levels (glutamate and alanine) in an experimental model of portal systemic encephalopathy. Intriguingly, the increase in ammonia CSF levels here observed in the ammonium group was not reversed by guanosine administration, while the increases in CSF levels of the amino acids glutamate and alanine was reversed.

Ammonia is considered the major toxin responsible for brain disorder in patients with liver disease. The role of brain glutamine and amino acids (e.g., glutamate and alanine) and consequently the role of brain transaminases and of tricarboxylic acid cycle intermediates on ammonia metabolization (potentially affecting the levels of amino acids as glutamate and alanine) are controversial [42–44]. Here, guanosine decreased the CSF glutamate and alanine levels without affecting the ammonia levels, pointing that guanosine administration affected the amino acid levels (favoring a neuroprotective effect against glutamatergic excitotoxicity) probably without affecting brain transaminases activity. Therefore, the source (if central or systemic) of CSF glutamate and alanine and the variation in the levels of other amino acids in CSF and BBB alterations to amino acid permeability are, among other issues, under investigation by our group.

Several studies have shown that EEG is the most adequate method for detecting and monitoring oscillatory changes of neural networks in patients with HE [24, 45, 46]. In this study, the EEG analysis showed intermittent slow activity and an increased EEG left index in animals receiving the ammonium acetate injection, indicating a decline in the conscious level [24, 45]. However, the animals pretreated with guanosine had a shorter period of EEG abnormalities and presented a subsequent normalization of the EEG profile at 20 to 30 min after ammonium administration. These EEG findings corroborate with the observation that the animals pretreated with guanosine spent less time in the comatose state.

The involvement of disturbances in the redox and glutamatergic brain homeostasis has been demonstrated in acute HE [6]. Our group and other groups have previously indicated, using both in vitro and in vivo protocols, that guanosine has neuroprotective effects against glutamatergic excitotoxicity and oxidative stress [17, 21, 22, 28, 47]. These roles have been attributed to the action of guanosine: (i) stimulating glutamate uptake by astrocytes in experimental in vivo and in vitro models of brain injury [48] and (ii) exerting antioxidant effects [28, 31]. Our study shows that ammonium acetate administration decreased the ex vivo glutamate uptake and caused the dysfunction of antioxidant enzymes in the CNS, both of which were reversed by guanosine administration.

In an additional group of animals, we followed the same experimental protocol as in protocol 3, with the difference of harvesting the samples at 10 min after the ammonium acetate injection to evaluate the earlier effect of guanosine on biochemical parameters. We observed the same effect of a reduction in glutamate uptake, but we found no difference in the redox status (data not shown). It seems that the decrease in glutamate uptake occurs before the oxidative stress alterations in the pathophysiology of acute hyperammonemia. In accordance with our results, Butterworth and colleagues [49, 50] proposed that the increase of ammonia levels in the brain of patients with acute HE leads to an inhibition of glutamate removal by astrocytes, with consequent increases in extracellular brain glutamate levels and posterior oxidative/nitrosative stress [49]. We can speculate that the antioxidant effect of guanosine is a consequence of its ability to enhance glutamate uptake and thereby prevent oxidative/nitrosative stress.

In conclusion, this study shows the well-known involvement of the glutamatergic system and oxidative stress in the pathophysiology of acute ammonia intoxication, which is probably the main factor underlying acute HE. Most importantly, our data suggest a remarkable neuroprotective effect of guanosine in acute encephalopathy as shown by neurological, electrophysiological, and neurochemical parameters, with a very significant decrease in mortality rate. Considering that HE still has high morbidity and mortality rates unless promptly treated, here, we presented valuable evidence to further understand the pathophysiology of this condition and the possible use of guanosine as a treatment for acute encephalopathy.

**Acknowledgments** This work was supported by Brazilian agencies and grants: Conselho Nacional de Desenvolvimento Científico e Tecnológico (CNPq), Coordenação de Aperfeiçoamento de Pessoal de Nível Superior (CAPES), Fundação de Amparo à Pesquisa do Estado do Rio Grande do Sul (FAPERGS), and Brazilian Institute of Neuroscience—IBN Net FINEP, INCT—Excitotoxicity and Neuroprotection (573577/2008-5).

**Compliance with Ethical Standards** All experiments were approved by the Ethics Commission (CEUA/UFRGS) under project number 29468 and followed the National Institutes of Health "Guide for the Care and Use of Laboratory Animals" (NIH publication No. 80-23, revised 1996).

**Conflict of Interest** The authors declare that they have no competing financial interests.

## References

1. Daroff RB, Bradley WG (2012) Bradley's neurology in clinical practice, 6th edn. Elsevier/Saunders, Philadelphia
2. Jackson P, Khan A (2015) Delirium in critically ill patients. Crit Care Clin 31(3):589–603. doi:10.1016/j.ccc.2015.03.011
3. Liu A, Perumpail RB, Kumari R, Younossi ZM, Wong RJ, Ahmed A (2015) Advances in cirrhosis: optimizing the management of hepatic encephalopathy. World J Hepatol 7(29):2871–2879. doi:10.4254/wjh.v7.i29.2871
4. Poordad FF (2007) Review article: the burden of hepatic encephalopathy. Aliment Pharmacol Ther 25(Suppl 1):3–9. doi:10.1111/j.1746-6342.2006.03215.x
5. Felipo V (2013) Hepatic encephalopathy: effects of liver failure on brain function. Nat Rev Neurosci 14(12):851–858. doi:10.1038/nrn3587
6. Ciecko-Michalska I, Szczepanek M, Slowik A, Mach T (2012) Pathogenesis of hepatic encephalopathy. Gastroenterol Res Pract 2012:642108. doi:10.1155/2012/642108
7. Amodio P, Del Piccolo F, Petteno E, Mapelli D, Angeli P, Iemmolo R, Muraca M, Musto C et al (2001) Prevalence and prognostic value of quantified electroencephalogram (EEG) alterations in cirrhotic patients. J Hepatol 35(1):37–45
8. Agrawal A, Sharma BC, Sharma P, Sarin SK (2012) Secondary prophylaxis of hepatic encephalopathy in cirrhosis: an open-label, randomized controlled trial of lactulose, probiotics, and no therapy. Am J Gastroenterol 107(7):1043–1050. doi:10.1038/ajg.2012.113
9. Stepanova M, Mishra A, Venkatesan C, Younossi ZM (2012) In-hospital mortality and economic burden associated with hepatic encephalopathy in the United States from 2005 to 2009. Clin Gastroenterol Hepatol 10(9):1034–1041. doi:10.1016/j.cgh.2012.05.016, **e1031**
10. Desjardins P, Du T, Jiang W, Peng L, Butterworth RF (2012) Pathogenesis of hepatic encephalopathy and brain edema in acute liver failure: role of glutamine redefined. Neurochem Int 60(7):690–696. doi:10.1016/j.neuint.2012.02.001
11. Felipo V, Butterworth RF (2002) Neurobiology of ammonia. Prog Neurobiol 67(4):259–279
12. Ott P, Vilstrup H (2014) Cerebral effects of ammonia in liver disease: current hypotheses. Metab Brain Dis 29(4):901–911. doi:10.1007/s11011-014-9494-7
13. Hermenegildo C, Monfort P, Felipo V (2000) Activation of N-methyl-D-aspartate receptors in rat brain in vivo following acute ammonia intoxication: characterization by in vivo brain microdialysis. Hepatology 31(3):709–715. doi:10.1002/hep.510310322
14. Bruck J, Gorg B, Bidmon HJ, Zemtsova I, Qvartskhava N, Keitel V, Kircheis G, Haussinger D (2011) Locomotor impairment and cerebrocortical oxidative stress in portal vein ligated rats in vivo. J Hepatol 54(2):251–257. doi:10.1016/j.jhep.2010.06.035
15. Rose C (2002) Increased extracellular brain glutamate in acute liver failure: decreased uptake or increased release? Metab Brain Dis 17(4):251–261

16. Chan H, Butterworth RF (2003) Cell-selective effects of ammonia on glutamate transporter and receptor function in the mammalian brain. Neurochem Int 43(4-5):525–532
17. Paniz LG, Calcagnotto ME, Pandolfo P, Machado DG, Santos GF, Hansel G, Almeida RF, Bruch RS et al (2014) Neuroprotective effects of guanosine administration on behavioral, brain activity, neurochemical and redox parameters in a rat model of chronic hepatic encephalopathy. Metab Brain Dis 29(3):645–654. doi:10.1007/s11011-014-9548-x
18. Cauli O, Gonzalez-Usano A, Cabrera-Pastor A, Gimenez-Garzo C, Lopez-Larrubia P, Ruiz-Sauri A, Hernandez-Rabaza V, Duszczyk M et al (2014) Blocking NMDA receptors delays death in rats with acute liver failure by dual protective mechanisms in kidney and brain. Neruomol Med 16(2):360–375. doi:10.1007/s12017-013-8283-5
19. Rodrigo R, Cauli O, Boix J, ElMlili N, Agusti A, Felipo V (2009) Role of NMDA receptors in acute liver failure and ammonia toxicity: therapeutical implications. Neurochem Int 55(1-3):113–118. doi:10.1016/j.neuint.2009.01.007
20. Schmidt AP, Lara DR, Souza DO (2007) Proposal of a guanine-based purinergic system in the mammalian central nervous system. Pharmacol Ther 116(3):401–416. doi:10.1016/j.pharmthera.2007.07.004
21. Connell BJ, Di Iorio P, Sayeed I, Ballerini P, Saleh MC, Giuliani P, Saleh TM, Rathbone MP et al (2013) Guanosine protects against reperfusion injury in rat brains after ischemic stroke. J Neurosci Res 91(2):262–272. doi:10.1002/jnr.23156
22. Hansel G, Tonon AC, Guella FL, Pettenuzzo LF, Duarte T, Duarte MM, Oses JP, Achaval M et al (2015) Guanosine protects against cortical focal ischemia. Involvement of inflammatory response. Mol Neurobiol 52(3):1791–1803. doi:10.1007/s12035-014-8978-0
23. Paxinos G, Watson C (2007) The rat brain in stereotaxic coordinates, 6th edn. Elsevier, Amsterdam; Boston
24. Vogels BA, Maas MA, Daalhuisen J, Quack G, Chamuleau RA (1997) Memantine, a noncompetitive NMDA receptor antagonist improves hyperammonemia-induced encephalopathy and acute hepatic encephalopathy in rats. Hepatology 25(4):820–827. doi:10.1002/hep.510250406
25. Almeida RF, Comasseto DD, Ramos DB, Hansel G, Zimmer ER, Loureiro SO, Ganzella M, Souza DO (2016) Guanosine anxiolytic-like effect involves adenosinergic and glutamatergic neurotransmitter systems. Mol Neurobiol. doi:10.1007/s12035-015-9660-x
26. Schmidt AP, Tort AB, Silveira PP, Bohmer AE, Hansel G, Knorr L, Schallenberger C, Dalmaz C et al (2009) The NMDA antagonist MK-801 induces hyperalgesia and increases CSF excitatory amino acids in rats: reversal by guanosine. Pharmacol Biochem Behav 91(4):549–553. doi:10.1016/j.pbb.2008.09.009
27. Thomazi AP, Godinho GF, Rodrigues JM, Schwalm FD, Frizzo ME, Moriguchi E, Souza DO, Wofchuk ST (2004) Ontogenetic profile of glutamate uptake in brain structures slices from rats: sensitivity to guanosine. Mech Ageing Dev 125(7):475–481. doi:10.1016/j.mad.2004.04.005
28. Quincozes-Santos A, Bobermin LD, Souza DG, Bellaver B, Goncalves CA, Souza DO (2014) Guanosine protects C6 astroglial cells against azide-induced oxidative damage: a putative role of heme oxygenase 1. J Neurochem 130(1):61–74. doi:10.1111/jnc.12694
29. Boveris A (1984) Determination of the production of superoxide radicals and hydrogen peroxide in mitochondria. Methods Enzymol 105:429–435
30. Wendel A (1981) Glutathione peroxidase. Methods Enzymol 77:325–333
31. Bellaver B, Souza DG, Bobermin LD, Goncalves CA, Souza DO, Quincozes-Santos A (2015) Guanosine inhibits LPS-induced pro-inflammatory response and oxidative stress in hippocampal astrocytes through the heme oxygenase-1 pathway. Purinergic signalling 11(4):571–580. doi:10.1007/s11302-015-9475-2
32. Clay AS, Hainline BE (2007) Hyperammonemia in the ICU. Chest 132(4):1368–1378. doi:10.1378/chest.06-2940
33. Rama Rao KV, Jayakumar AR, Norenberg MD (2014) Brain edema in acute liver failure: mechanisms and concepts. Metab Brain Dis 29(4):927–936. doi:10.1007/s11011-014-9502-y
34. Palomero-Gallagher N, Zilles K (2013) Neurotransmitter receptor alterations in hepatic encephalopathy: a review. Arch Biochem Biophys 536(2):109–121. doi:10.1016/j.abb.2013.02.010
35. Schmidt AP, Bohmer AE, Schallenberger C, Antunes C, Pereira MS, Leke R, Wofchuk ST, Elisabetsky E et al (2009) Spinal mechanisms of antinociceptive action caused by guanosine in mice. Eur J Pharmacol 613(1-3):46–53. doi:10.1016/j.ejphar.2009.04.018
36. Ramos DB, Muller GC, Rocha GB, Dellavia GH, Almeida RF, Pettenuzzo LF, Loureiro SO, Hansel G, Horn AC, Souza DO, Ganzella M (2015) Intranasal guanosine administration presents a wide therapeutic time window to reduce brain damage induced by permanent ischemia in rats. Purinergic signalling. doi:10.1007/s11302-015-9489-9
37. Dal-Cim T, Ludka FK, Martins WC, Reginato C, Parada E, Egea J, Lopez MG, Tasca CI (2013) Guanosine controls inflammatory pathways to afford neuroprotection of hippocampal slices under oxygen and glucose deprivation conditions. J Neurochem 126(4):437–450. doi:10.1111/jnc.12324
38. Palsson E, Jakobsson J, Sodersten K, Fujita Y, Sellgren C, Ekman CJ, Agren H, Hashimoto K et al (2015) Markers of glutamate signaling in cerebrospinal fluid and serum from patients with bipolar disorder and healthy controls. Eur Neuropsychopharmacol 25(1):133–140. doi:10.1016/j.euroneuro.2014.11.001
39. Rodan LH, Gibson KM, Pearl PL (2015) Clinical use of CSF neurotransmitters. Pediatr Neurol 53(4):277–286. doi:10.1016/j.pediatrneurol.2015.04.016
40. Struyfs H, Niemantsverdriet E, Goossens J, Fransen E, Martin JJ, De Deyn PP, Engelborghs S (2015) Cerebrospinal fluid P-Tau181P: biomarker for improved differential dementia diagnosis. Front Neurol 6:138. doi:10.3389/fneur.2015.00138
41. Therrien G, Butterworth RF (1991) Cerebrospinal fluid amino acids in relation to neurological status in experimental portal-systemic encephalopathy. Metab Brain Dis 6(2):65–74
42. Rothman DL, De Feyter HM, Maciejewski PK, Behar KL (2012) Is there in vivo evidence for amino acid shuttles carrying ammonia from neurons to astrocytes? Neurochem Res 37(11):2597–2612. doi:10.1007/s11064-012-0898-7
43. Rama Rao KV, Norenberg MD (2014) Glutamine in the pathogenesis of hepatic encephalopathy: the trojan horse hypothesis revisited. Neurochem Res 39(3):593–598. doi:10.1007/s11064-012-0955-2
44. Cooper AJ, Kuhara T (2014) alpha-Ketoglutaramate: an overlooked metabolite of glutamine and a biomarker for hepatic encephalopathy and inborn errors of the urea cycle. Metab Brain Dis 29(4):991–1006. doi:10.1007/s11011-013-9444-9
45. Amodio P, Gatta A (2005) Neurophysiological investigation of hepatic encephalopathy. Metab Brain Dis 20(4):369–379. doi:10.1007/s11011-005-7921-5
46. Amodio P, Montagnese S (2015) Clinical neurophysiology of hepatic encephalopathy. J Clin Exp Hepatol 5(Suppl 1):S60–S68. doi:10.1016/j.jceh.2014.06.007
47. Petronilho F, Perico SR, Vuolo F, Mina F, Constantino L, Comim CM, Quevedo J, Souza DO et al (2012) Protective effects of

guanosine against sepsis-induced damage in rat brain and cognitive impairment. Brain Behav Immun 26(6):904–910. doi:10.1016/j.bbi.2012.03.007

48. Giuliani P, Ballerini P, Buccella S, Ciccarelli R, Rathbone MP, Romano S, D'Alimonte I, Caciagli F et al (2015) Guanosine protects glial cells against 6-hydroxydopamine toxicity. Adv Exp Med Biol 837:23–33. doi:10.1007/5584_2014_73
49. Butterworth RF (2015) Pathogenesis of hepatic encephalopathy in cirrhosis: the concept of synergism revisited. Metab Brain Dis. doi:10.1007/s11011-015-9746-1
50. Bemeur C, Desjardins P, Butterworth RF (2010) Evidence for oxidative/nitrosative stress in the pathogenesis of hepatic encephalopathy. Metab Brain Dis 25(1):3–9. doi:10.1007/s11011-010-9177-y

## Supplementary Figure 1

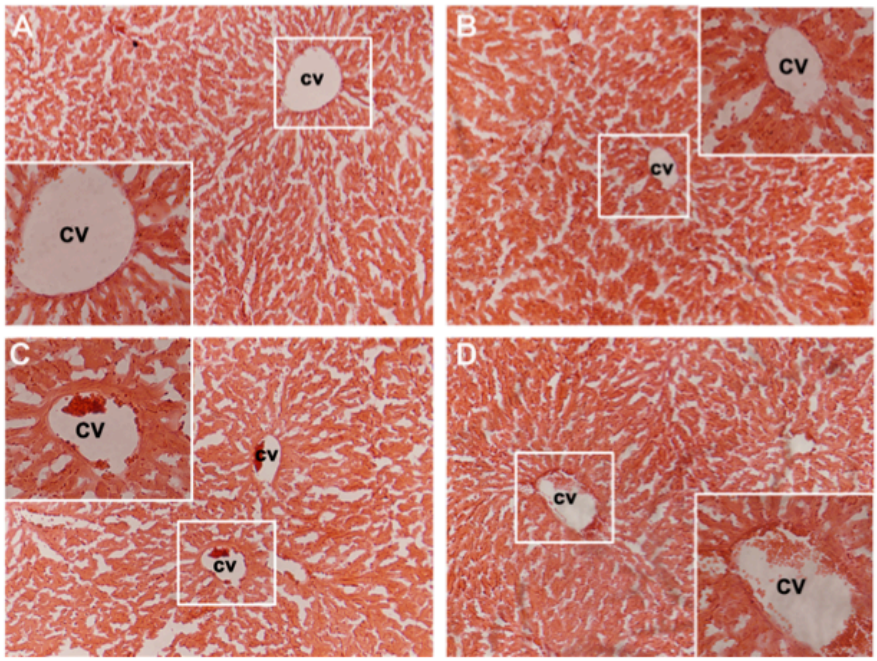


**Liver histology.** Briefly, liver samples from treated and untreated animals were dissected and overnight fixed with 4% paraformaldehyde buffered with sodium phosphate (pH 7,4). Then, all specimens were immersed into 30% of sucrose solution. Thin sagittal sections of 10 µm were obtained using a cryostat (-25º C). Six histological slides from each group were prepared and stained with haematoxylin and eosin, accordingly to the basic protocols. Structural analyses were performed for each group on aleatory fields. Images were obtained through a CCD camera coupled in an optical microscope (Nikon Eclipse E600; whole images: 100x; highlighted square: 400x), using the NIS Elements AR 3.2 software. No structural abnormalities or differences were observed in treated or untreated groups, which presented well-structured hepatocytes delimiting the hepatic sinusoids. **A**- Vehicle; **B**- Vehicle+GUO60mg/kg; **C**- Ammonia; **D**- Ammonia+GUO60mg/kg; **CV**- Central Vein.

## CAPITULO 2

# Behavioural, neurochemical and brain oscillation abnormalities in rats submitted to subtotal hepatectomy

Giordano F. Cittolin-Santos, Pedro A. Guazzelli, Yasmine Nonose, Fernanda U. Fontella, Mayara V. Pasquetti, Roberto F. Almeida, Francisco J. Ferreira-Lima, Rafael M. Berlezi, Alessandro B. Osvaldt, Adriano M. de Assis, Maria Elisa Calcagnotto, Diogo O Souza

**Manuscrito submetido para o periódico SCIENTIFIC REPORTS**

Submetido em 3 de novembro de 2016

*CURRENT STATE*: “Manuscript Assigned to Editor”

# Behavioural, neurochemical and brain oscillation abnormalities in rats submitted to subtotal hepatectomy

Giordano F. Cittolin-Santos [1], Pedro A. Guazzelli [1], Yasmine Nonose [1], Fernanda U. Fontella [1], Mayara V. Pasquetti [1], Roberto F. Almeida [1], Francisco J. Ferreira-Lima [3], Rafael M. Berlezi [3], Alessandro B. Osvaldt [3], Adriano M. de Assis [1], Maria Elisa Calcagnotto [1,2], Diogo O Souza [1,2 *]

[1] Postgraduate Program in Biological Sciences: Biochemistry, ICBS, Universidade Federal do Rio Grande do Sul, Porto Alegre, RS 90035-003, Brazil;

[2] Department of Biochemistry, Universidade Federal do Rio Grande do Sul, Porto Alegre, RS 90035-003, Brazil;

[3] Division of Gastrointestinal Surgery, Hospital de Clínicas de Porto Alegre, Porto Alegre, RS 90035-003, Brazil.

Giordano Fabrício Cittolin-Santos and Pedro Arend Guazzelli contributed equally to this work.

The authors declare no competing financial interests.

Corresponding author:
Diogo Onofre Souza, Ph.D.
Department of Biochemistry, Postgraduate Program in Biochemistry
ICBS, Universidade Federal do Rio Grande do Sul, UFRGS
Ramiro Barcelos St 2600 Annex Building, 90035-003, Porto Alegre, RS, Brazil. Tel.: +55 51 3308 5559
Fax: +55 51 3308 5540
E-mail: diogo@ufrgs.br

## Abstract

Concerning the pathophysiology of Hepatic Encephalopathy (HE), ammonia levels and glutamatergic system dysfunction seem to be strongly involved in brain function impairment. Here, we used an animal model of acute liver failure (ALF) induced via subtotal hepatectomy (92%) to evaluate changes in behaviour, electroencephalograms (EEGs) and neurochemistry during HE. Hepatectomized rats presented increased serum levels of ammonia, ALT, AST, gamma-GT, lactate and bilirubin associated with reduced glycaemia, classical features of ALF. EEG abnormalities were observed as early as 30 minutes after surgery, mainly characterized by a predominance of delta oscillations and increased EEG left index. Although rats maintained nearly normal movement abilities after surgery, they presented behavioural changes characterized by decreased locomotion in OFTs. The expression of glutamate transporters (GLT-1 and GLAST) was diminished in the brain. The levels of 12 of 15 amino acids analysed in the CSF were increased. Using an animal model of ALF induced via subtotal hepatectomy, this work provides new insights into the pathophysiology of HE, demonstrating the involvement of alterations in three important aspects of the disease: neurochemistry, behaviour and brain oscillations. Our study strengthens the idea that imbalanced amino acids levels and glutamatergic system alterations are involved in the pathophysiology of HE.

## Introduction

Hepatic encephalopathy (HE) is characterized by brain dysfunction directly caused by acute or chronic liver insufficiency or portosystemic shunting and exhibits a wide spectrum of neurological and psychiatric deficits, ranging from subclinical manifestations to coma [1]. HE occurs as overt episodes in approximately 40% of patients with chronic liver disease [2] and results in a significant reduction in quality of life, as well as high costs for patients and medical systems [3,4].

Although the exact mechanism underlying HE remains uncertain, elevated serum ammonia levels are considered a trigger [5]. In addition to hyperammonaemia, glutamatergic system dysfunction plays an important role in the development of HE [6,7]. We have recently shown that experimental hyperammonaemia is accompanied by a decrease in glutamatergic uptake by astrocytes and increased cerebrospinal fluid (CSF) glutamate levels [8]. The increased extracellular levels of glutamate lead to intracellular glutamine accumulation, mainly in astrocytes, which seems to be the main factor responsible for cell swelling and mitochondrial dysfunction [9,10]. Accordingly, brain oedema and subsequent brain herniation has been suggested as a possible cause of impaired consciousness and death in HE patients [11,12].

Electroencephalograms (EEGs) can provide accurate and sensitive measures of CNS dysfunction in neurological and psychiatric diseases, including HE [13-16]. In addition, they can often be a reliable predictor of the severity and outcome for HE [17]. Changes in EEGs are characterized by a gradual decrease in frequency and a continuous slowing of background activity (theta, theta/delta, and delta activities) and episodic transients, such as triphasic waves (TWs) or frontal intermittent rhythmic delta activity (FIRDA) [18]. TWs are frequently seen in HE [19]; however, they are best seen in association with deeper levels of brain dysfunction and higher levels of ammonia [17,18]. EEGs in patients with acute encephalopathy generally reveal a slowing of background frequencies with or without the presence of TWs and FIRDA [20,21]. These patterns are widely believed to reflect an underlying structural or metabolic impairment in the brain [18]. Therefore, the quantitative analysis of EEG brain oscillations is a powerful tool, in conjunction with assessments of clinical manifestations, for evaluating the development and severity of HE [13-15,22].

For almost 40 years, the relationship between amino acid imbalances and the onset of HE has been studied [23-25]. The large neutral amino acid (LNAA) group includes

the aromatic amino acids (AAAs; tyrosine, phenylalanine and tryptophan), the branched chain amino acids (BCAAs; leucine, isoleucine and valine), methionine, threonine and histidine. All LNAAs share a common blood-brain transport system [26], and it is known that hyperammonaemia in association with liver disease is responsible for alterations in the metabolism and transport of amino acids through the blood-brain barrier (BBB) [27,28]. The efflux of excess CSF glutamine, which has been demonstrated under hyperammonaemic conditions, competes with other LNAAs in crossing the BBB through the common LNAA transport system [23] and may result in changes in the CSF levels of several other amino acids.

The surgical resection of the liver is a well-established and extensively studied animal model of acute liver failure (ALF) in different species, and it has some fundamental features that are useful for studying the consequences of ALF, such as HE [29]. Subtotal hepatectomy in rats is a reproducible model that induces death from liver failure and presents a therapeutic window for assessing treatments [30-32].

The objective of this study was to investigate the pathophysiology of HE by evaluating, in an unprecedented integrative manner, the behavioural, electroencephalographic and neurochemical abnormalities caused by an experimental model of ALF induced via subtotal hepatectomy (92% of the liver removed). Accordingly, the following concurrent features of acute HE were evaluated: 1) survival rate, 2) behavioural performance, 3) EEG patterns, 4) biochemical parameters in the blood, and 5) biochemical parameters in the CSF and cerebral cortex. In this work, we provide evidence that strengthens the correlation among the changes in brain oscillations, behavioural performance, CSF amino acid levels and the glutamatergic system that occur in association with HE.

## Results

### Survival Rate

Only 4 (20%) out of 20 rats submitted to subtotal hepatectomy survived after 60 hours (Figure 1A), and the mean latency to death after the surgery was 43.9 hours (Figure 1B).

All deaths occurred between 30 and 60 hours after the surgery. Rats that died within the first 6 hours after surgery were excluded from the study because they likely

died from complications of the surgical procedure (e.g., excessive bleeding). No sham operated rats died during the experiment.

**Serum biochemical parameters**

Subtotal hepatectomy altered several serum parameters when compared with the parameters in sham rats, similar to previously described results [30,32]. Hepatectomized rats showed a reduced glycaemia and higher serum levels of AST, ALT, GGT, total bilirubin, direct bilirubin, LDH, lactate, and ammonia than sham animals (Table 1).

**EEG analysis**

EEG data show that hepatectomized rats presented an elevated left index from 1 hour after subtotal hepatectomy, which persisted for 56 h (Figure 2A). Figure 2B shows representative EEG traces of the 3 groups. Hepatectomized rats had significant increases in their left index, ranging from 0.700 to 0.900 (0.750±0.004; n=8), whereas sham and naive rats presented normal values, ranging from 0.550 to 0.650 (0.610±0.006, n=3 and 0.600±0.005, n=3, respectively, $p<0.0001$) (Figure 2C). The hepatectomy group also presented a significant increase ($p<0.0001$) in the percentage of the power of delta oscillations in relation to baseline (42%) when compared with the sham (36%, n=3) and naïve (33%, n=3) groups (Figure 2D). Furthermore, a spectral analysis of power frequencies over time revealed a predominance of delta oscillations in the EEGs of the hepatectomized group when compared with the other groups (a representative spectrogram of each group shows how the EEGs changed over time (Supplementary Figure 1).

**Behavioural analysis**

In OFTs, all groups showed a decrease in the distance travelled from the first to the fourth minute of the session, indicating habituation to the novel environment. Regarding locomotor activity, both the sham and hepatectomy surgeries caused a decrease in the total distance travelled (Figures 3A and 3D) and an increase in the time spent immobile (Figures 3B) when compared with performances before surgery (naïve), and these effects were more pronounced in the hepatectomy group than in the sham group. Additionally, the hepatectomy group spent significantly less time in the centre of the arena (Figure 3C, Supplementary Figure 2A and Supplementary Figure 2B) than the sham group. No difference was found in the average speed of the animals (Supplementary Figure 2C).

**CSF amino acid profile**

Subtotal hepatectomy caused significant increases in most of the amino acids analysed. There was an overall increase in CSF amino acid levels of approximately 70-100%. Glutamine and methionine increased by approximately 200%, and tyrosine and phenylalanine showed even larger increases, increasing by 668% and 272%, respectively. No alterations were found in aspartic acid, alanine and ornithine levels (Table 2).

**Glutamate transporter immunocontent**

Subtotal hepatectomy reduced the cortical content of the main astrocytic glutamate transporters in adult rats, GLAST and GLT-1, compared with the levels in the sham group (0.28±0.05 to 0.17±0.01 and 0.36±0.07 to 0.22±0.03, respectively, Figure 4) measured 24 hours after the surgeries.

## Discussion

Several animal models of HE induced via hepatectomy have been well-described [30,32,33]. Our group recently studied HE using both acute metabolic (hyperammonaemia) and chronic models [9,34]. Here, we used an experimental model of ALF induced via subtotal hepatectomy (92% of the liver removed) to characterize three important aspects of HE: i) behavioural performance, ii) biochemical parameters in the blood and CSF and iii) brain oscillatory activity. The main findings were (1) a high lethality rate, (2) decreased locomotor activity, (3) mild hypoglycaemia associated with increased serum levels of ALT, AST, bilirubin, GGT, LDH, lactate and ammonia, (4) an increase in delta oscillations and EEG left index, (5) increased levels of amino acids in the CSF, and (6) reduced brain cortical content of glutamate transporters, GLAST and GLT-1.

Similar to previous reports [30,32,35], subtotal (92%) hepatectomy resulted in a high mortality rate (80%, Figure 1A) over a relatively small time frame (from 30 hours to 60 hours after hepatectomy, Figure 1B). This is an essential parameter for evaluating the efficacy of the ALF model used as the removal of more of the liver increases the lethality rates to 100%, whereas removing less than 90% of the liver may not result in the adequate development of HE [31].

Here, hepatectomized rats exhibited an increase in serum levels of markers of liver damage (ALT, AST and GGT), which is characteristic of rat models of hepatic failure. However, the changes were milder when compared to the results presented in

previous publications [30,32], likely because ischaemic right lobes were not left inside the abdomen, as was done in the previous studies. Furthermore, subtotal hepatectomy caused some degree of hypoglycaemia, as previously described in this surgical model [35]. In rat models of diabetes, links between hypoglycaemia and clinical and electrographic seizures have been described [36]. However, seizures correlated with reduced glycaemia occurred at blood glucose levels of approximately 20 mg/dL. In our study, serum glucose levels in hepatectomized rats averaged 39.85 ± 1.19 mg/dL, which was probably not low enough to affect behaviour, EEG patterns or the survival rate [36].

EEGs are the examination of choice for establishing a diagnosis of metabolic encephalopathy as they can exclude other pathologies. EEG signal frequency, amplitude, and distribution patterns may indicate generalized, cortical, subcortical or arousal dysfunctions, and the background reactivity provides important information about the prognosis in both human and experimental HE [9,13,14,20,34,37,38]. In this study, HE rats presented higher EEG left index values than naive and sham groups, indicating a predominance of slow wave EEG patterns associated with a decrease in consciousness levels (Figure 2). The elevated EEG left index found in hepatectomized rats is in accordance with previous studies using experimental models of acute and chronic HE. It has been reported that animals with chronic HE reach values of 0.7, and those with acute encephalopathy reach values of 0.9, corresponding to a comatose state [9,34]. The power spectrum analysis of EEGs over time showed a predominance of delta oscillatory activity in hepatectomized rats (Supplementary Figure 1). This supports the gradual decrease in frequency and the continuous slowing of background activity observed in association with HE [39]. The continuous slowing of background activity and episodic transients are best seen with deeper levels of dysfunction and higher levels of ammonia [17,20]. Accordingly, impairments in the level of consciousness in hepatectomized rats were detected as soon as 30 minutes after surgery, and these changes persisted throughout the analysis (Figure 2A). The sudden increases in EEG left index and delta oscillation values coincide with the sudden onset of hyperammonaemia, indicating an encephalopathic state [9,40].

Along with the EEG alterations, clear behavioural changes in OFTs were observed. Sham and hepatectomy procedures did not affect the habituation to novelty, as both groups presented a decrease in exploratory activity from the 1$^{st}$ to the 4$^{th}$ minute (Figure 3D) [41]. However, the sham and hepatectomy groups exhibited a decrease in both locomotor parameters. This finding indicates a direct effect of the surgery on locomotor

activity. Compared with the sham group, the hepatectomized animals presented a greater decrease in the total travelled distance. This diminished locomotion appeared to be due to an increase in time spent immobile because there was no difference in the average speed of movement (Supplementary Figure 2C). Additionally, hepatectomized rats spent less time in the centre of the arena, indicating a greater degree of anxiety (Figure 3C). We acknowledge that it is difficult to make conclusions regarding changes in anxiety for two main reason: i) patterns of anxiety are obfuscated in a repeated analysis of OFTs since the animals were previously exposed to the arena, and ii) the severe reduction in locomotor activity affects observations of exploratory patterns. Hence, we conclude that rats with HE had a clear reduction in locomotor activity and that this may have caused an anxious-like behaviour, without affecting the habituation to novelty [41-43].

In the present study, we observed a wide-ranging increase in the levels of glutamine (approximately 200%) and in the levels of most amino acids (Table 2) in the CSF. The high glutamine levels in the CSF of hepatectomized animals could have altered the concentration of different amino acids in the brain, which may explain the increased levels of most amino acids, such as methionine, phenylalanine and tyrosine, in the CSF. Several studies have also suggested that a decrease in the BCAA/AAA ratio, known as Fischer's ratio [23], is considered an important pathogenic factor in HE [44,45]. In this study, although the CSF of hepatectomized rats presented an important increase in BCAA levels, there was a significant decrease in Fischer's ratio due to a greater increase in AAA levels, mainly tyrosine. The increase in AAA levels is related to the false neurotransmitters theory, as AAAs are involved in the synthesis of octopamine and tryptamine [46,47]. Additionally, high levels of tryptophan are related to the excessive synthesis of serotonin, which has been demonstrated in experimental models of HE [23,48,49]. Thus, it is likely that the pathological increase in extracellular levels of glutamine and the related increase in AAA levels play a role in the observed alterations in the EEG oscillations and behavioural performance.

As mentioned before, glutamatergic system dysfunction is also an important feature in HE's development. Supraphysiological increase in CSF levels of cerebral extracellular glutamate, which may lead to a condition known as glutamate excitotoxicity, is well described in HE [34,50,51]. Our group also demonstrated that hyperammonemia induces a decrease in astrocytic glutamate uptake and glutamine synthetase activity [9], key processes on the metabolism of ammonia and glutamate in the

brain. Here, we observed and increase in glutamate CSF levels alongside with a reduction in the immunocontent of glial glutamate transporters (GLAST and GLT-1, Figure 4). This decrease in glutamate transporter expression together with high CSF glutamate and glutamine levels strengthen the relation between glutamatergic system dysfunction and HE and are probably related to the neurological changes evaluated on behavioural performance and EEG patterns, as well as in the lethality rate.

HE is a multifactorial syndrome [44,52] that includes hyperammonaemia, amino acid imbalance, glutamatergic system alterations, changes in energy metabolism, brain oedema, and inflammation. Here, a correlation among liver insufficiency and neurochemical, behavioural, and EEG pattern alterations is presented, emphasizing the important role of amino acid imbalance and glutamatergic system modifications in the pathophysiology of HE, which cause the characteristic changes demonstrated in brain oscillations.

## Methods

### Ethics statement

All experiments were approved by the Ethics Commission (CEUA/UFRGS) under project number 29468 and followed the National Institutes of Health "Guide for the Care and Use of Laboratory Animals" (NIH publication Nº. 80-23, revised 1996).

### Animals

Adult male Wistar rats (90 days old) were acquired from the Central Animal House of the Department of Biochemistry, ICBS, UFRGS. The animals were housed in plastic cages (5 per cage), maintained under a standard dark/light cycle (lights were on between 7:00 a.m. and 7:00 p.m.) at room temperature (22 ± 2°C), with tap water and commercial food available *ad libitum*.

Rats were divided into 3 experimental cohorts to assess the following factors: i) survival rate, ii) video-electroencephalogram (video-EEG) recordings, and iii) behavioural performance and biochemical measurements.

### Subtotal Hepatectomy

Subtotal hepatectomies were performed as described previously [30,35], with modifications. Anaesthesia was induced and maintained with 3% isoflurane in oxygen

at a flow rate of 1 L/min during the whole procedure. A median laparotomy was performed to expose the liver. The pedicle of the left anterior lobe was ligated and resected. The same procedure was performed on the right anterior lobe and then on the right lobe. After resection, all lobes were removed to prevent inflammatory and necrotic processes in the abdominal cavity. Only the omental lobes (8% of liver mass) remained functional [32].

After suturing the abdominal wall, 0.5 ml of lidocaine was administered intramuscularly in the wound borders. The rats had free access to drinking water supplemented with 20% glucose; additionally, 2 ml/kg of the same glucose solution was administered i.p. 3 times (0, 6, and 12 hours) after the surgery [35]. Before being returned to their home cages, the rats were kept in a heated box for 30 minutes after the surgery. Sham operations were performed with the exact same protocol, except pedicle ligation and liver resection were not performed. The rats were observed every 6 hours over 96 hours to evaluate the mortality rate following surgery.

We chose 24 hours after hepatectomy or sham surgery to perform the behavioural tests and to harvest blood, CSF and brain samples as all rats were still alive at this time.

For EEG recordings, electrodes were implanted 1 week before subtotal hepatectomies were performed.

**Serum biochemical analysis**

Rats were euthanized via decapitation, and blood was immediately collected into EDTA tubes, centrifuged at 5000 x *g* for 10 minutes. Serum was stored at -80°C for subsequent measurements of alanine aminotransferase (ALT), aspartate aminotransferase (AST), gamma-glutamyl transpeptidase (GGT), lactate dehydrogenase, lactate, glucose and ammonia levels [9] using commercial kits (Labtest, MG, Brazil).

***In Vivo* Electrophysiology (EEG)**

Electrode implantation: Each animal was anesthetized with ketamine (100 mg/kg, i.p) and xylazine (10 mg/kg, i.p.) and placed on a stereotaxic apparatus. Five stainless steel screw electrodes (1.0 mm diameter) were implanted at the following coordinates: LL +/- 2.0 mm, AP -1.0 mm; LL +/- 2.0 mm, AP + 1.0 mm [53], and the reference electrode was implanted on the occipital bone and kept in contact with the CSF. A small screw was implanted over the frontal bone and was used for fixing the

dental acrylic helmet to the skull, as described in previous studies from our group [9,34]. After surgery, each animal was placed back in their cage and left to recover for one week. Video-EEG recording: One week later, each animal was transferred to an observation cage to perform the baseline video-EEG recordings for 20 min. Rats were then divided into 3 groups: naïve (with no abdominal surgery), sham (with abdominal surgery but no pedicle ligation and subtotal liver resection) and hepatectomy (with abdominal surgery, pedicle ligation and subtotal liver resection). Immediately after the surgical procedures (hepatectomy or sham) and after recovering from the anaesthesia, naïve, sham and hepatectomized rats were individually transferred to an observation cage for video-EEG recordings for 72 hours or until death, and 56 consecutive hours of EEG data were extracted for analysis.

EEG signals were recorded with a standard data acquisition system (MAP-32, Plexon Inc.) and were filtered at 0.01-100 Hz, followed by digitization at 1 kHz for posterior analysis. All analyses were performed using built-in and custom-written routines in MATLAB (Mathworks, Inc). The power spectra density was obtained, and the EEG left index (EEG index of consciousness level) was calculated as the logarithm of the ratio between the power of the low frequency (1–7.4 Hz) and high frequency (13.5–26.5 Hz) signals. Normal rats have an EEG left index of approximately 0.60, and values above 0.70 indicate changes in the consciousness level up to a coma (approximately 0.80–0.90)[9,22,34].

For the quantitative spectral analysis, the signal was decomposed into four frequencies bands: delta (1-4 Hz), theta (4-10 Hz), low gamma (20-50 Hz) and high gamma (60-100 Hz). The analysis was performed in two-minute epochs every 30 minutes of the recording in hepatectomized rats and two-minute epochs every 90 minutes in the control groups (naïve and sham) while the rats were awake and in a resting state.

**Open Field Task**

The rats' behavioural performance was evaluated as describe by Almeida, et al. [41], with minor modifications. Rats were individually placed in a black arena (50 × 50 × 50 cm, length × width × height, respectively), which they could freely explore for 10 minutes. Each animal was submitted to 2 OFT sessions. The first was performed before the surgery (naïve group), and the second was performed 24 hours after the surgery (sham operated and subtotal hepatectomy groups).

The OFT was used to measure the following relevant behavioural parameters: i) habituation to a novel environment, ii) locomotor activity, and iii) the behavioural response to a natural conflict between the *exploration of* and the *aversion to* the central area of the arena (an anxiety-related parameter). Habituation to a novel environment was considered to be indicated by a significant decrease in the total distance travelled from the first to the 4$^{th}$ minute of the session. Locomotor activity was measured by evaluating the total distance travelled and the total time spent immobile during the session. Measurements of time spent immobile were only started after no detectable movement occurred for over 5 seconds. Anxiety was evaluated based on the amount of time the rats explored the centre of the arena (5 cm away from the wall).

All sessions were recorded by a video camera positioned above the arena. Videotapes were analysed using ANY-Maze® dedicated software as a tracking system. The apparatus was cleaned with 70° alcohol and dried after each session.

**CSF sampling**

Twenty-four hours after hepatectomy or sham surgery, the rats were anesthetized with isoflurane and placed on a stereotaxic apparatus to collect CSF samples (100 - 150 µL per rat) via direct puncture of the cisterna magna [54]. CSF samples were centrifuged at 1000 x *g* for 10 min, and the supernatant was stored at -80°C for subsequent evaluation of amino acids levels via high-performance liquid chromatography (HPLC).

**HPLC analysis**

The concentrations of free amino acids in CSF samples were determined via HPLC as described previously [55]. Aliquots of cell-free CSF supernatant were used to quantify amino acid (aspartate, glutamate, alanine, tyrosine, tryptophan, methionine, valine, phenylalanine, isoleucine, leucine, ornithine, glycine, serine and lysine) and glutamine levels. Analyses were performed using a reverse phase column (Supelcosil LC-18, 250 mm × 4.6 mm × 5 µm, Supelco) in a Shimadzu Instruments liquid chromatograph (50 µL loop valve injection, injection volume 40 µL) with fluorescence detection after pre-column derivatization with 100.5 µL of an O-Phthaldialdehyde (OPA) solution (5.4 mg OPA in 1 mL 0.2 M sodium borate, pH 9.5, plus 10 µL of mercaptoethanol), 25.5 µL of 4% mercaptoethanol and 20 µL of sample. The mobile phase flowed at a rate of 1.4 mL/min, and column temperature was 24 °C. Buffer A was a 0.04 mol/L sodium dihydrogen phosphate monohydrate buffer (pH 5.5) containing 80% methanol, and buffer B was a 0.01 mol/L sodium dihydrogen phosphate

monohydrate buffer (pH 5.5) containing 20% methanol. The gradient profile was modified according to the content of buffer B in the mobile phase as follows: 100% at 0.10 min, 90% at 15 min, 48% at 10 min, and 100% at 60 min. Absorbance was read at excitation and emission wavelengths of 360 nm and 455 nm, respectively, in a Shimadzu fluorescence detector. Derivatized samples were used, and concentrations are expressed in μM (as the mean±SEM). Amino acids were identified based on their retention time and were quantified based on their chromatographic peak area. An amino acid standard mixture was used for calibration.

The BCAA/AAA ratio (Fischer's ratio) was calculated as the sum of BCAAs (leucine, isoleucine and valine) divided by the sum of the AAAs (phenylalanine, tyrosine and tryptophan) [23].

**Western Blotting analysis**

Twenty-four hours after hepatectomy or sham surgery, cortical brain tissues samples were obtained immediately after euthanasia via decapitation for protein immunocontent evaluation. Total proteins were extracted following cellular lysis in ice-cold lysis buffer (4% SDS, 2 mM EDTA, 50 mM Tris-HCl (pH 6.8)) and were standardized in SDS-PAGE sample buffer (62.5 mM Tris-HCl (pH 6.8), 2% (w/v) SDS, 5% β-mercaptoethanol, 10% (v/v) glycerol, 0.002% (w/v) bromophenol blue). Samples were boiled at 95 ºC for 5 min before loading. Proteins (10 μg protein/well) were separated in a 10% acrylamide running gel and a 4% acrylamide stacking gel using an electrophoresis unit (Bio-Rad). Proteins were then transferred to a nitrocellulose membrane (GE Healthcare). Membranes were blocked with 5% (w/v) skimmed milk overnight and then incubated with primary polyclonal rabbit antibodies overnight at 4 ºC [polyclonal rabbit anti-rat GLAST1 (#GLAST11-A, 1:5000 dilution, Alpha Diagnostics), polyclonal rabbit anti-rat GLT-1 (#GLT11-A, 1:5000 dilution, Alpha Diagnostics) and polyclonal rabbit anti-rat GAPDH (#sc-9104, 1:5000 dilution, Santa Cruz Biotechnology)] followed by incubation with horseradish peroxidase-conjugated donkey anti-rabbit IgG (NA934V, 1:5000 dilution, GE Healthcare, UK) secondary antibodies for 2 h. Finally, 3 chemiluminescent bands were detected in an ImageQuant LAS4000 system (GE Healthcare) using an Immobilon™ Western chemiluminescence kit (#P90720, Millipore). Both types of labelling were quantified with ImageQuant TL software (Version 8.1, GE Healthcare).

**Statistical analysis**

Data are expressed as the means±S.E.M. A Student's t test, ANOVA followed by Newman–Keuls post-test or a Kruskal Wallis test followed by Dunn's Multiple Comparison Test were performed using GraphPad Prism v 5 (La Jolla, CA, USA). Differences were considered significant at $p<0.05$.

**Acknowledgements**

This work was supported by the following Brazilian agencies and grants: Science Without Borders, CNPq, CAPES, FAPERGS, Brazilian Institute of Neuroscience/FINEP, INCT/Excitotoxicity and Neuroprotection (573577/2008-5).

**Author Contributions**

GFCS and PAG were responsible for the design, acquisition, analysis, interpretation, drafting, and approval of the final version of the manuscript. YN, FUF, MVP, RFA, FJF, RMB and ABO were responsible for acquisition, analysis, interpretation, and approval of the final version of the manuscript. AMA and MEC were responsible for interpretation, drafting, critical revision, and approval of the final version of the manuscript. DOS was responsible for the design, interpretation, drafting, critical revision, and approval of the final version of the manuscript.

## References


1 Nusrat, S., Khan, M. S., Fazili, J. & Madhoun, M. F. Cirrhosis and its complications: evidence based treatment. *World journal of gastroenterology* **20**, 5442-5460, doi:10.3748/wjg.v20.i18.5442 (2014).

2 Vilstrup, H. *et al.* Hepatic encephalopathy in chronic liver disease: 2014 Practice Guideline by the American Association for the Study of Liver Diseases and the European Association for the Study of the Liver. *Hepatology* **60**, 715-735, doi:10.1002/hep.27210 (2014).

3 Amodio, P. *et al.* Prevalence and prognostic value of quantified electroencephalogram (EEG) alterations in cirrhotic patients. *Journal of hepatology* **35**, 37-45 (2001).

4 Poordad, F. F. Review article: the burden of hepatic encephalopathy. *Aliment Pharmacol Ther* **25 Suppl 1**, 3-9, doi:10.1111/j.1746-6342.2006.03215.x (2007).

5 Ciecko-Michalska, I., Szczepanek, M., Slowik, A. & Mach, T. Pathogenesis of hepatic encephalopathy. *Gastroenterology research and practice* **2012**, 642108, doi:10.1155/2012/642108 (2012).

6 Saab, S. Evaluation of the impact of rehospitalization in the management of hepatic encephalopathy. *International journal of general medicine* **8**, 165-173, doi:10.2147/IJGM.S81878 (2015).

7 Monfort, P., Munoz, M. D., ElAyadi, A., Kosenko, E. & Felipo, V. Effects of hyperammonemia and liver failure on glutamatergic neurotransmission. *Metabolic brain disease* **17**, 237-250 (2002).

8 Parekh, P. J. & Balart, L. A. Ammonia and Its Role in the Pathogenesis of Hepatic Encephalopathy. *Clinics in liver disease* **19**, 529-537, doi:10.1016/j.cld.2015.05.002 (2015).

9 Cittolin-Santos, G. F. *et al.* Guanosine Exerts Neuroprotective Effect in an Experimental Model of Acute Ammonia Intoxication. *Molecular neurobiology*, doi:10.1007/s12035-016-9892-4 (2016).

10 Scott, T. R., Kronsten, V. T., Hughes, R. D. & Shawcross, D. L. Pathophysiology of cerebral oedema in acute liver failure. *World journal of gastroenterology* **19**, 9240-9255, doi:10.3748/wjg.v19.i48.9240 (2013).

11 Albrecht, J. & Norenberg, M. D. Glutamine: a Trojan horse in ammonia neurotoxicity. *Hepatology* **44**, 788-794, doi:10.1002/hep.21357 (2006).

12 Record, C. O., Chase, R. A., Hughes, R. D., Murray-Lyon, I. A. & Williams, R. Glycerol therapy for cerebral oedema complicating fulminant hepatic failure. *British medical journal* **2**, 540 (1975).

13 Timmermann, L. *et al.* Neural synchronization in hepatic encephalopathy. *Metabolic brain disease* **20**, 337-346, doi:10.1007/s11011-005-7916-2 (2005).

14 Butz, M., May, E. S., Haussinger, D. & Schnitzler, A. The slowed brain: cortical oscillatory activity in hepatic encephalopathy. *Archives of biochemistry and biophysics* **536**, 197-203, doi:10.1016/j.abb.2013.04.004 (2013).

15 Olesen, S. S. *et al.* Electroencephalogram variability in patients with cirrhosis associates with the presence and severity of hepatic encephalopathy. *Journal of hepatology* **65**, 517-523, doi:10.1016/j.jhep.2016.05.004 (2016).

16 Demedts, M., Pillen, E., De Groote, J. & Van de Woestijne, K. P. Hepatic encephalopathy: comparative study of EEG abnormalities, neuropsychic disturbances and blood ammonia. *Acta neurologica Belgica* **73**, 281-288 (1973).

17 Kaplan, P. W. The EEG in metabolic encephalopathy and coma. *Journal of clinical neurophysiology : official publication of the American Electroencephalographic Society* **21**, 307-318 (2004).

18 Sutter, R., Stevens, R. D. & Kaplan, P. W. Clinical and imaging correlates of EEG patterns in hospitalized patients with encephalopathy. *Journal of neurology* **260**, 1087-1098, doi:10.1007/s00415-012-6766-1 (2013).
19 Chatrian, G. E. in *Current practice of clinical electroencephalography* (ed D.D. ; Pedley Daly, T.A.) 425-487 (1990).
20 Accolla, E. A., Kaplan, P. W., Maeder-Ingvar, M., Jukopila, S. & Rossetti, A. O. Clinical correlates of frontal intermittent rhythmic delta activity (FIRDA). *Clinical neurophysiology : official journal of the International Federation of Clinical Neurophysiology* **122**, 27-31, doi:10.1016/j.clinph.2010.06.005 (2011).
21 Gloor, P., Ball, G. & Schaul, N. Brain lesions that produce delta waves in the EEG. *Neurology* **27**, 326-333 (1977).
22 Vogels, B. A., van Steynen, B., Maas, M. A., Jorning, G. G. & Chamuleau, R. A. The effects of ammonia and portal-systemic shunting on brain metabolism, neurotransmission and intracranial hypertension in hyperammonaemia-induced encephalopathy. *Journal of hepatology* **26**, 387-395 (1997).
23 James, J. H., Ziparo, V., Jeppsson, B. & Fischer, J. E. Hyperammonaemia, plasma aminoacid imbalance, and blood-brain aminoacid transport: a unified theory of portal-systemic encephalopathy. *Lancet* **2**, 772-775 (1979).
24 Zanchin, G., Rigotti, P., Bettineschi, F., Vassanelli, P. & Battistin, L. Cerebral amino acid levels and uptake in rats after portocaval anastomosis: I. Regional studies in vitro. *Journal of neuroscience research* **4**, 291-299, doi:10.1002/jnr.490040406 (1979).
25 Zanchin, G., Rigotti, P., Dussini, N., Vassanelli, P. & Battistin, L. Cerebral amino acid levels and uptake in rats after portocaval anastomosis: II. Regional studies in vivo. *Journal of neuroscience research* **4**, 301-310, doi:10.1002/jnr.490040407 (1979).
26 Wagenmakers, A. J. Muscle amino acid metabolism at rest and during exercise: role in human physiology and metabolism. *Exercise and sport sciences reviews* **26**, 287-314 (1998).
27 Jessy, J., Mans, A. M., DeJoseph, M. R. & Hawkins, R. A. Hyperammonaemia causes many of the changes found after portacaval shunting. *The Biochemical journal* **272**, 311-317 (1990).
28 James, J. H., Escourrou, J. & Fischer, J. E. Blood-brain neutral amino acid transport activity is increased after portacaval anastomosis. *Science* **200**, 1395-1397 (1978).
29 Terblanche, J. & Hickman, R. Animal models of fulminant hepatic failure. *Digestive diseases and sciences* **36**, 770-774 (1991).
30 Detry, O. *et al.* A modified surgical model of fulminant hepatic failure in the rat. *The Journal of surgical research* **181**, 85-90, doi:10.1016/j.jss.2012.05.080 (2013).
31 Madrahimov, N., Dirsch, O., Broelsch, C. & Dahmen, U. Marginal hepatectomy in the rat: from anatomy to surgery. *Annals of surgery* **244**, 89-98, doi:10.1097/01.sla.0000218093.12408.0f (2006).
32 Eguchi, S. *et al.* Fulminant hepatic failure in rats: Survival and effect on blood chemistry and liver regeneration. *Hepatology* **24**, 1452-1459 (1996).
33 Butterworth, R. F. *et al.* Experimental models of hepatic encephalopathy: ISHEN guidelines. *Liver international : official journal of the International Association for the Study of the Liver* **29**, 783-788, doi:10.1111/j.1478-3231.2009.02034.x (2009).
34 Paniz, L. G. *et al.* Neuroprotective effects of guanosine administration on behavioral, brain activity, neurochemical and redox parameters in a rat model of chronic hepatic encephalopathy. *Metabolic brain disease* **29**, 645-654, doi:10.1007/s11011-014-9548-x (2014).

* Kieling, C. O. *et al.* The effects of anesthetic regimen in 90% hepatectomy in rats. *Acta cirurgica brasileira / Sociedade Brasileira para Desenvolvimento Pesquisa em Cirurgia* **27**, 702-706 (2012).
* Maheandiran, M. *et al.* Severe hypoglycemia in a juvenile diabetic rat model: presence and severity of seizures are associated with mortality. *PloS one* **8**, e83168, doi:10.1371/journal.pone.0083168 (2013).
* Amodio, P. & Montagnese, S. Clinical neurophysiology of hepatic encephalopathy. *Journal of clinical and experimental hepatology* **5**, S60-68, doi:10.1016/j.jceh.2014.06.007 (2015).
* Amodio, P. & Gatta, A. Neurophysiological investigation of hepatic encephalopathy. *Metab Brain Dis* **20**, 369-379, doi:10.1007/s11011-005-7921-5 (2005).
* Sutter, R. & Kaplan, P. W. Clinical and electroencephalographic correlates of acute encephalopathy. *Journal of clinical neurophysiology : official publication of the American Electroencephalographic Society* **30**, 443-453, doi:10.1097/WNP.0b013e3182a73bc2 (2013).
* Vogels, B. A., Maas, M. A., Bosma, A. & Chamuleau, R. A. Significant improvement of survival by intrasplenic hepatocyte transplantation in totally hepatectomized rats. *Cell transplantation* **5**, 369-378 (1996).
* Almeida, R. F. *et al.* Systemic administration of GMP induces anxiolytic-like behavior in rats. *Pharmacology, biochemistry, and behavior* **96**, 306-311, doi:10.1016/j.pbb.2010.05.022 (2010).
* Padilla, E. *et al.* Novelty-evoked activity in open field predicts susceptibility to helpless behavior. *Physiology & behavior* **101**, 746-754, doi:10.1016/j.physbeh.2010.08.017 (2010).
* Zimmer, E. R. *et al.* Long-term NMDAR antagonism correlates reduced astrocytic glutamate uptake with anxiety-like phenotype. *Frontiers in cellular neuroscience* **9**, 219, doi:10.3389/fncel.2015.00219 (2015).
* Dejong, C. H., van de Poll, M. C., Soeters, P. B., Jalan, R. & Olde Damink, S. W. Aromatic amino acid metabolism during liver failure. *The Journal of nutrition* **137**, 1579S-1585S; discussion 1597S-1598S (2007).
* Miyazaki, T. *et al.* Amino acid ratios in plasma and tissues in a rat model of liver cirrhosis before and after exercise. *Hepatology research : the official journal of the Japan Society of Hepatology* **27**, 230-237 (2003).
* Rossle, M. *et al.* Amino acid, ammonia and neurotransmitter concentrations in hepatic encephalopathy: serial analysis in plasma and cerebrospinal fluid during treatment with an adapted amino acid solution. *Klinische Wochenschrift* **62**, 867-875 (1984).
* Jellinger, K., Riederer, P., Rausch, W. D. & Kothbauer, P. Brain monoamines in hepatic encephalopathy and other types of metabolic coma. *Journal of neural transmission. Supplementum*, 103-120 (1978).
* Smith, A. R. *et al.* Alterations in plasma and CSF amino acids, amines and metabolites in hepatic coma. *Annals of surgery* **187**, 343-350 (1978).
* Herneth, A. M., Steindl, P., Ferenci, P., Roth, E. & Hortnagl, H. Role of tryptophan in the elevated serotonin-turnover in hepatic encephalopathy. *Journal of neural transmission* **105**, 975-986, doi:10.1007/s007020050106 (1998).
* Hermenegildo, C., Monfort, P. & Felipo, V. Activation of N-methyl-D-aspartate receptors in rat brain in vivo following acute ammonia intoxication: characterization by in vivo brain microdialysis. *Hepatology* **31**, 709-715, doi:10.1002/hep.510310322 (2000).
* Tofteng, F. & Larsen, F. S. Monitoring extracellular concentrations of lactate, glutamate, and glycerol by in vivo microdialysis in the brain during liver transplantation in acute liver failure. *Liver transplantation : official publication of*

*the American Association for the Study of Liver Diseases and the International Liver Transplantation Society* **8**, 302-305, doi:10.1053/jlts.2002.32283 (2002).

1 Butterworth, R. F. Pathogenesis of hepatic encephalopathy in cirrhosis: the concept of synergism revisited. *Metabolic brain disease*, doi:10.1007/s11011-015-9746-1 (2015).

2 Paxinos, G. & Watson, C. *The rat brain in stereotaxic coordinates*. 6th edn, (Elsevier, 2007).

3 Almeida, R. F. *et al.* Guanosine Anxiolytic-Like Effect Involves Adenosinergic and Glutamatergic Neurotransmitter Systems. *Molecular neurobiology*, doi:10.1007/s12035-015-9660-x (2016).

4 Schmidt, A. P. *et al.* The NMDA antagonist MK-801 induces hyperalgesia and increases CSF excitatory amino acids in rats: reversal by guanosine. *Pharmacology, biochemistry, and behavior* **91**, 549-553, doi:10.1016/j.pbb.2008.09.009 (2009).

## Figures

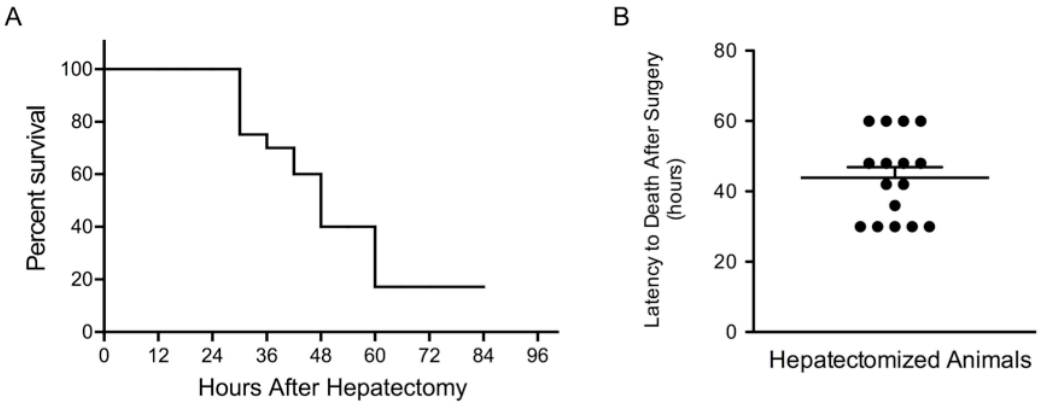


**Figure 1: Survival rate.** (A) Survival rate (in percentage) of rats submitted to subtotal hepatectomy. (B) Mean latency to death ± S.E.M. n: 20

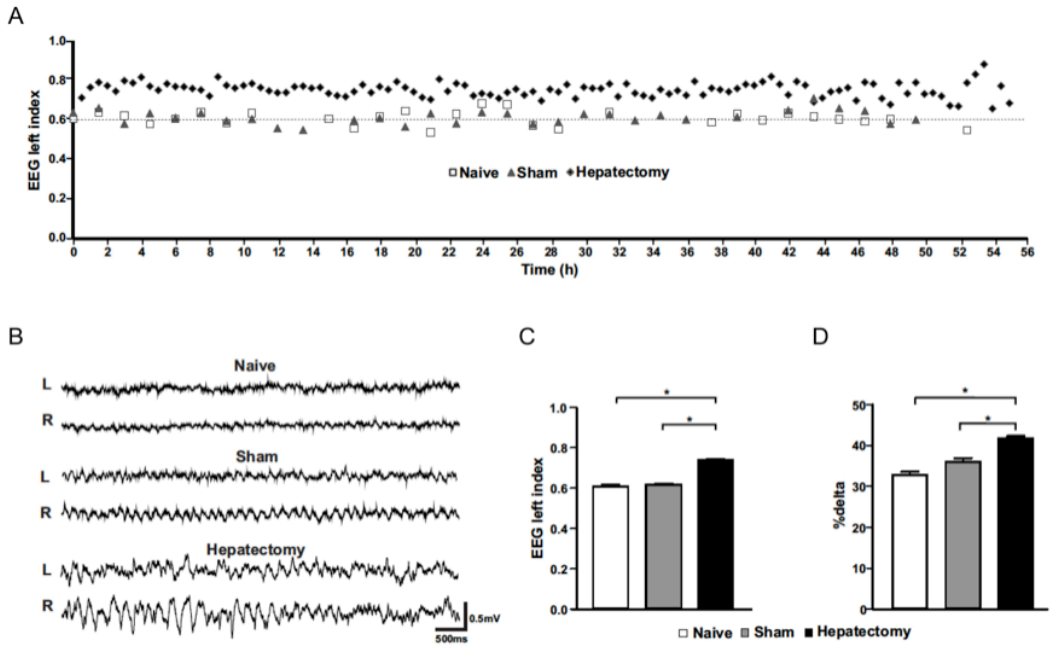


**Figure 2: EEG left index and delta oscillations.** (A) EEG left index for naïve, sham and hepatectomized animals measured every hour during a 56-h recording. The dashed line represents the normal left index value. (B) Representative EEG traces. (C) Plots of the mean ± SEM of EEG left index values (**p<0.0001, one-way ANOVA followed by Tukey's post-hoc test) (D) Percentage of delta waves (**p<0.0001, one- way ANOVA followed by Tukey's post-hoc test). n: Naïve=3, Sham=3, Hepatectomy=8

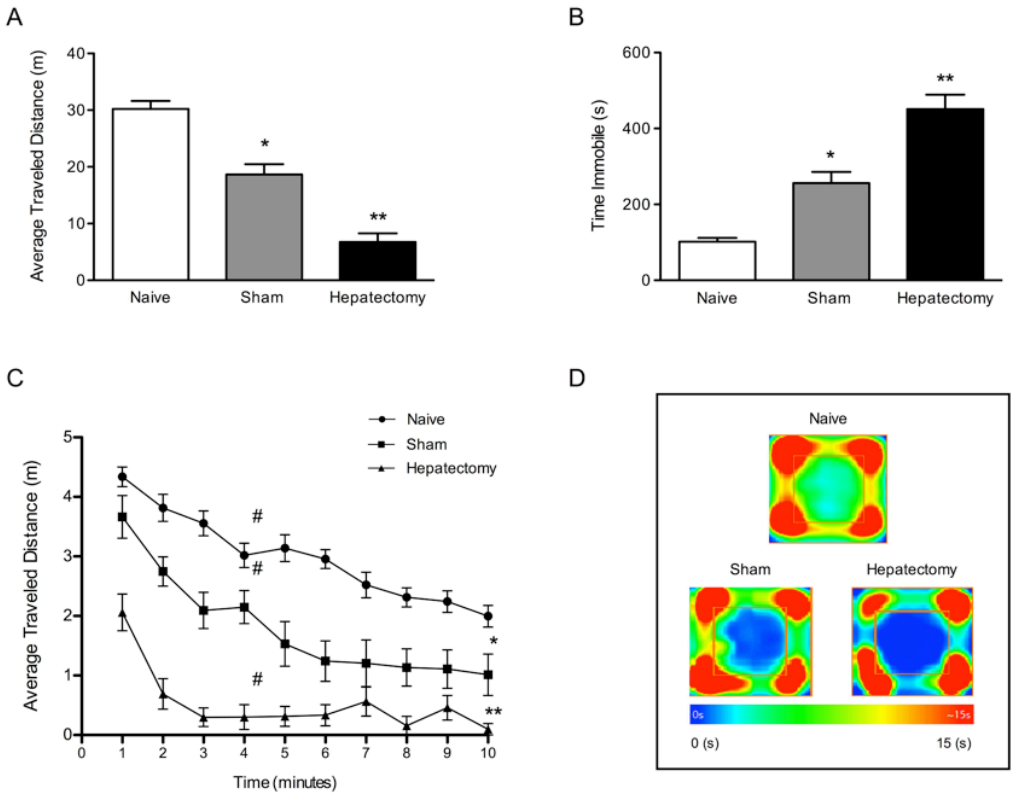


**Figure 3**: **Open Field Task** (A) Total distance travelled, (B) time immobile, (C) group heat map of animal position, and (D) distance travelled per minute. Values are the mean ± SEM. * ($p < 0.05$) and ** ($p<0.001$) indicate a significant difference from all other groups. # Indicates a difference between the 1st and 4th min within the same group (one-way ANOVA). n: Naïve=28, Sham=9, Hepatectomy=12

Distances travelled (in metres): Naïve: 30.20, Sham: 18.64, and Hepatectomy: 6.75; time immobile (in seconds): Naïve: 102, Sham: 256, and Hepatectomy: 451; and distance travelled in the 1st and 4th minutes (in metres): Naive 4.34 and 3.22, Sham 3.67 and 2.15, and Hepatectomy 2.06 and 0.54, respectively.

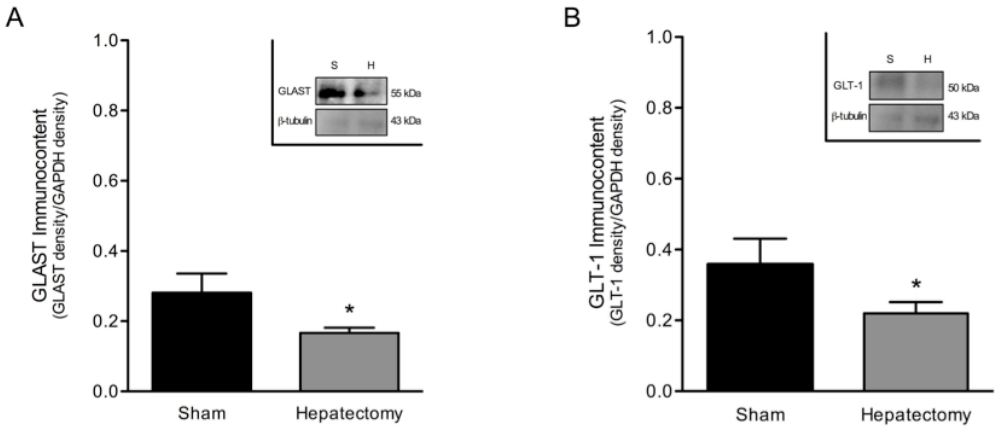


**Figure 4**: **Cortical GLAST (A) and GLT-1 (B) immunocontent.** Results are expressed as the mean ± SEM of the GLAST/GAPDH and GLT-1/GAPDH ratios. * Indicates a significant difference between groups ($p < 0.05$, t-student). n: Sham=5, Hepatectomy=5

**Table 1.** Serum Biochemical Parameters

| | Sham | Hepatectomy | Result |
|---|---|---|---|
| AST (U/L) | 29.26 ± 1.90 | 54.85 ± 3.41 | ** ↑ 87% |
| ALT (U/L) | 37.42 ± 2.38 | 63.26 ± 3.43 | ** ↑ 69% |
| GGT (U/L) | 26.21 ± 2.02 | 51.85 ± 3.38 | ** ↑ 98% |
| Total Bilirubin (mg/dL) | 0.05 ± 0.01 | 1.66 ± 0.08 | ** ↑ 3200% |
| Direct Bilirubin (mg/dL) | 0.03 ± 0.00 | 0.58 ± 0.14 | ** ↑ 1833% |
| LDH (U/L) | 371.70 ± 16.12 | 649.6 ± 35.71 | ** ↑ 75% |
| Lactate (nmol/L) | 1.67 ± 0.23 | 5.54 ± 0.42 | ** ↑ 232% |
| Glucose (mg/dL) | 52.47 ± 1.38 | 39.85 ± 1.19 | ** ↓ 232% |
| Ammonia (µmol/L) | 24.79 ± 1.73 | 49.79 ± 3.41 | ** ↑ 101% |

The results are expressed in U/L (AST, ALT, GGT e LDH), mg/dL (glucose, total and indirect bilirubin), µmol/L (ammonia) and nmol/L (lactate. Values are expressed as the mean ± S.E.M. ** Indicates a significant difference between the groups ($p < 0.0001$, t-student). N: Sham = 19 and Hepatectomy = 34.

**Table 2.** CSF amino acids

| Amino Acid (μM) | Sham | Hepatectomy | Result |
|---|---|---|---|
| Aspartic acid | 0.42 ± 0.02 | 0.46 ± ± 0.03 | - |
| Glutamic acid | 1.27 ± 0.13 | 2.46 ± 0.29 | * ↑ 93% |
| Serine | 63.45 ± 1.28 | 85.79 ± 2.64 | ** ↑ 35% |
| Histidine/Glutamine | 351.50 ± 17.65 | 1158.00 ± 99.06 | ** ↑ 230% |
| Glycine | 58.07 ± 4.16 | 117.60 ± 6.08 | ** ↑ 103% |
| Alanine | 61.40 ± 3.11 | 75.59 ± 5.84 | - |
| Tyrosine | 8.85 ± 0.48 | 68.01 ± 6.92 | ** ↑ 668% |
| Tryptophan | 2.30 ± 0.07 | 3.82 ± 0.28 | * ↑ 66% |
| Valine | 8.44 ± 0.56 | 14.96 ± 1.13 | * ↑ 77% |
| Methionine | 5.81 ± 0.12 | 16.46 ± 0.79 | ** ↑ 183% |
| Isoleucine | 1.78 ± 0.05 | 3.26 ± 0.19 | ** ↑ 83% |
| Leucine | 2.57 ± 0.11 | 4.66 ± 0.32 | * ↑ 81% |
| Phenylalanine | 4.67 ± 0.21 | 17.37 ± 1.17 | ** ↑ 272% |
| Ornitine | 2.18 ± 0.19 | 2.44 ± 0.16 | - |
| Lysine | 81.22 ± 3.45 | 156.00 ± 15.89 | * ↑ 92% |

The results are expressed in μM. All values expressed as mean ± S.E.M. * ($p < 0.05$) and ** ($p < 0.001$) indicate significant diferences between groups (t-student's test). N: Sham = 6 and Hepatectomy = 8.

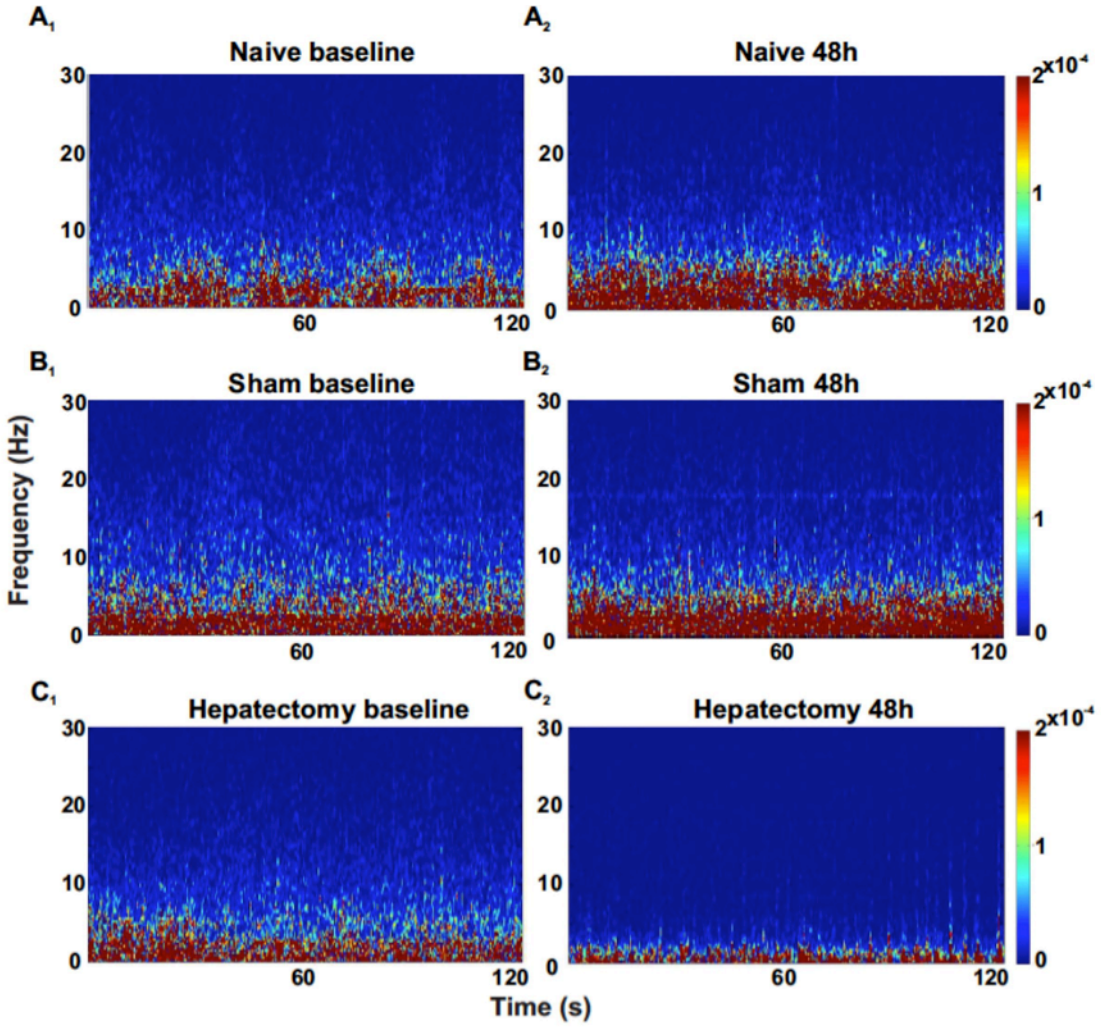


**Supplementary Figure 1: Hepatectomized animals exhibit a predominance of delta oscillations on EEGs**. (A-C) Representative spectrograms at baseline (1) and 48 h after surgery (2) for all groups. n: Naïve=3, Sham=3, Hepatectomy=8

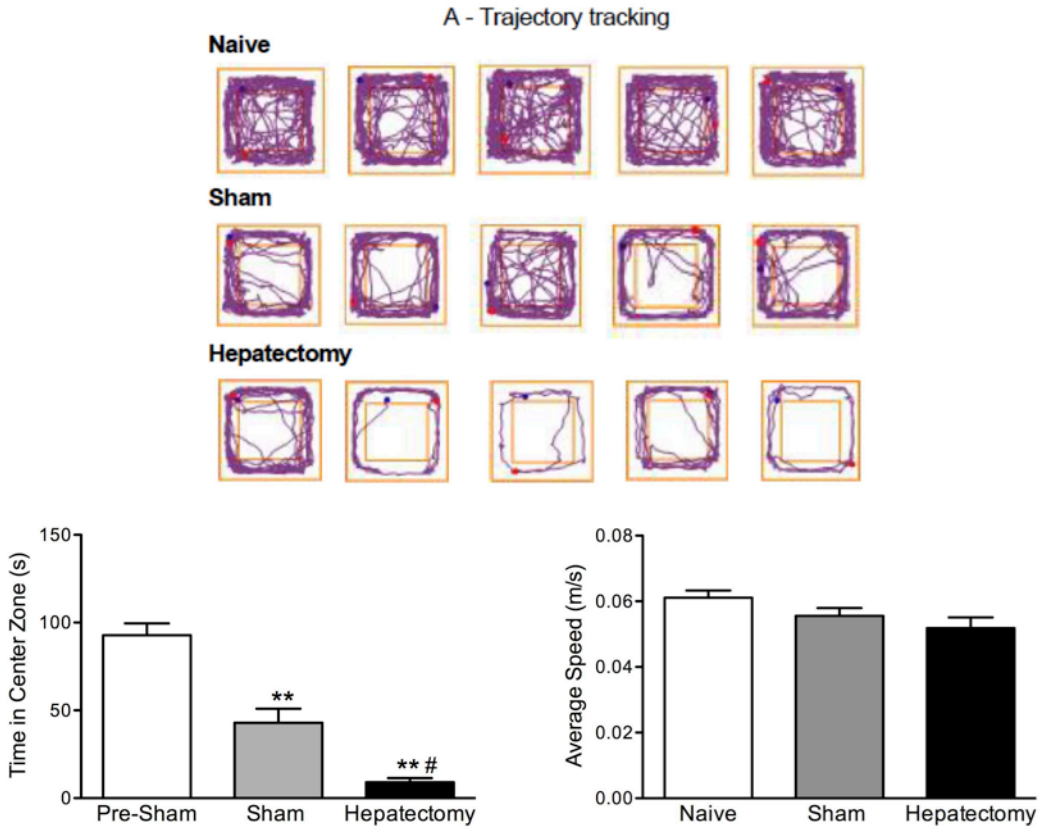


**Supplementary Figure 2: Open Field Task**. (A) Representative trajectory tracking of animals during the 10-minute OFT. (B) Time spent in the central zone and (C) average speed. Values are the mean ± SEM. ** Indicates a significant difference from the Naïve group ($p < 0.001$), and # indicates a significant difference from the sham group ($p=0.05$), (one-way ANOVA). n: Naïve=28, Sham=9, Hepatectomy=12
Time in central zone (in seconds): Naive 92, Sham 43, and Hepatectomy 9; and average speed (in metres/seconds): Naïve: 0.06, Sham 0.06, and Hepatectomy: 0.05.

# CAPÍTULO 3

## Brain metabolic alterations in a rat model of Hepatic Encephalopathy induced by Subtotal Hepatectomy

Guazzelli PA [1], Cittolin-Santos GF[1], Grings M[1], Lazzarotto GS[1,] Nonose Y [1], Guilian [1], , Souza DO [1,2], de Assis AM [1]

[1] Programa de Pós-Graduação em Ciências Biológicas: Bioquímica, ICBS, Universidade Federal do Rio Grande do Sul, Porto Alegre, RS 90035-003, Brasil;

[2] Departamento de Bioquímica, Universidade Federal do Rio Grande do Sul, Porto Alegre, RS 90035-003, Brasil;

Manuscrito em preparação: serão mostrados informações, materiais e métodos utilizados, assim como resultados parciais

* A introdução e discussão referente ao trabalho são feitas na Parte 1 e Parte 3, respectivamente.

**Abstract**

Liver disease is an important cause of morbidity and mortality associated with an important reduction in quality of life and significant economic burden for patients and medical systems. Hepatic encephalopathy (HE) is a major complication of both acute and chronic liver failure, which presents symptoms of attention, psychomotor and psychiatric alterations and in severe cases leads to brain edema, coma and death. It is known that ammonia is the main agent involved in HE's physiopathology. Recent studies have suggested that several brain alterations such as astrocytic dysfunction and energy metabolism impairment may synergistically interact and play a role in the development of the disease. Hyperammonemia is associated with higher glycolysis rates and increased brain lactate levels despite adequate oxygen supply. However, the direct effect of liver failure on brain bioenergetics is still controversial.

The purpose of the presenting study is to study brain energy metabolism in cerebral cortex of rats with hepatic encephalopathy induced via an experimental model of acute liver failure.

We used adult male Wistar rats, which were submitted either to subtotal hepatectomy (92% of liver mass) or sham operation (SO). Twenty-four hours after the surgery, the animals were euthanized and the cerebral cortex was immediately collected for analysis of the following parameters: redox status, TCA enzyme activity and substrate oxidation.

Subtotal hepatectomy also induced an increase in the levels of reactive oxygen species (ROS) while diminishing the activity of the enzymes superoxide dismutase (SOD) and glutathione peroxidase (GSH-Px). The hepatectomy group also presented higher TCA enzyme activity. Moreover, hepatectomy induced an increase in glutamate oxidation concomitant with a decrease in glucose and lactate oxidation.

Hepatic encephalopathy is an important complication of liver failure that is associated with high circulating ammonium and several brain alterations. Here, we used an effective animal model of acute liver failure induced via subtotal hepatectomy to investigate the brain bioenergetics.

**Financial Support**

This work was supported by Brazilian agencies and grants: Science Without Border, CNPq, CAPES, FAPERGS, Brazilian Institute of Neuroscience/FINEP, INCT/Excitotoxicity and Neuroprotection (573577/2008-5). The authors declare no competing financial interests.

## MATERIAIS E MÉTODOS

### Reagents

All chemicals were purchased from Sigma-Aldrich (St. Louis, MO, USA). Glucose-D, [$^{14}$C(U)] (ARC0122H) and Lactic acid,L-[1-$^{14}$C] sodium salt were purchased from American Radiolabeled Chemicals, Inc. (St. Louis, MO, USA). Glutamic acid, L-[$^{14}$C(U)] (#NEC290E250UC) and Optiphase 'Hisafe' 3 (1-437) scintillation liquid were purchased from PerkinElmer (Boston, MA, USA). Protein quantification was performed with BCA Protein Assay kit from Thermo Fisher Scientific (#23227, Rockford, IL, USA), using bovine serum albumin as standard.

### Animals

Ninety-day-old male Wistar rats, obtained from the Central Animal House of the Department of Biochemistry, ICBS, Universidade Federal do Rio Grande do Sul, Porto Alegre, RS, Brazil, were used. The animals were maintained on a 12:12 h light/dark cycle (lights on 07:00–19:00 h) in air-conditioned constant temperature (22 ± 1 °C) colony room, with free access to water and standard commercial chow (SUPRA, Porto Alegre, RS, Brazil). The experimental protocol was approved by the Ethics Committee for Animal Research of the Universidade Federal do Rio Grande do Sul, Porto Alegre, Brazil, and

followed the NIH Guide for the Care and Use of Laboratory Animals (NIH publication 85-23, revised 1996). All efforts were made to minimize the number of animals used and their suffering.

**Surgical Procedure**

Subtotal hepatectomy was performed according to a previous description of our group. Anesthesia was induced and maintained with 3% isoflurane and an oxygen flow of 0.8 L/min during the whole procedure. The animals were then positioned on a warmed operating table and a median laparoscopy was performed to expose the liver. The pedicles of the anterior lobes were ligated and the lobe was then resected. The same procedure was performed on the right lobes. Only the omental lobes (8% of the liver mass) remained functional.

The animals received intramuscular lidocaine in the abdominal wound to reduce postoperative pain and were kept in a warmed box until full recovering of the anesthesia before being returned to their home cages. Animals had free access to 20% glucose in the drinking water during the whole experiment. In addition, glucose injections (2 ml/kg i.p.) were administered 0, 6 and 12 hours after the surgery in order to avoid hypoglycemia.

The sham group was submitted to the exact same protocol, except for the pedicle ligation and liver resection.

**Tissue preparation**

Twenty-four hours after the surgery, the rats were euthanized and blood was immediately collected in heparinized tubes. The samples were then centrifuged at 2500x *g* for 10 min at 20°C to yield the serum fraction, which was used for subsequent biochemical analyses. Cerebral cortex were dissected, removed and homogenized in phosphate/saline buffer (1 g/5 ml, 20 mM, pH 7.4) or in Laemmli sample buffer [62.5 mMTris/HCl, pH 6.8, 1% (w/v) SDS, and 10% (v/v) glycerol] and stored at -80°C for neurochemical evaluation or western blotting analysis, respectively.

**Blood biochemical parameters**

Plasma gamma GT, glucose and ammonia levels were measured using commercial kits (Labtest, MG, Brazil) and a SpectraMax M5 microplate reader (Molecular Devices, CA, USA) (2).The neuron specific enolase (NSE) was analyzed using a commercial kit (eBIOSCIENCE, San Diego, CA, USA) (3).

**Determination of glutamate dehydrogenase (GDH) activity**

GDH activity was assayed according to Colon et al (6). The reaction mixture contained mitochondrial preparations (60 µg of protein), 50 mM triethanolamine buffer, pH 7.8, 2.6 mM EDTA, 105 mM ammonium acetate, 0.2 mM NADH, 10 mM α-ketoglutarate and 1.0 mM ADP. The reduction of NADH absorbance was monitored spectrophotometrically at 340 nm. GDH activity was calculated as µmol $NADH \cdot min^{-1} \cdot mg\ protein^{-1}$.

**Determination of malate dehydrogenase (MDH) activity**

MDH activity was measured according to Kitto et al (7). The incubation medium consisted of mitochondrial preparations (1 µg of protein), 10 µM

rotenone, 0.1% Triton X-100, 0.14 mM NADH, 0.3 mM oxaloacetate and 50 mM potassium phosphate, pH 7.4. MDH activity was determined following the reduction of NADH fluorescence at wavelengths of excitation and emission of 366 and 450 nm, respectively. MDH activity was calculated as nmol $NADH \cdot min^{-1} \cdot mg\ protein^{-1}$.

**Determination of α-ketoglutarate dehydrogenase (α-KGDH) complex activity**

α-KGDH complex activity was evaluated according to Lai and Cooper (8) and Tretter and Adam-Vizi (9) with some modifications. The incubation medium contained mitochondrial preparations (250 µg of protein), 1 mM $MgCl_2$, 0.2 mM thiamine pyrophosphate, 0.4 mM ADP, 10 µM rotenone, 0.2 mM EGTA, 0.12 mM coenzyme A-SH, 1 mM α-ketoglutarate, 2 mM $NAD^+$, 0.1% Triton X-100 and 50 mM potassium phosphate, pH 7.4. The reduction of $NAD^+$ was recorded at wavelengths of excitation and emission of 366 and 450 nm, respectively. α-KGDH activity was calculated as nmol $NADH \cdot min^{-1} \cdot mg\ protein^{-1}$.

**Determination of citrate synthase (CS) activity**

CS activity was measured according to Shepherd and Garland (1969) (10), by determining 5,5-dithio-bis (2-nitrobenzoic acid) (DTNB) reduction at λ = 412 nm. The incubation medium contained mitochondrial preparations (2 µg of protein), 5 mM potassium phosphate buffer, pH 7.4, 300 mM sucrose, 1 mM EGTA, 0.1 % BSA, 5 mM MOPS, 0.1 % Triton X-100, 0.1 mM DTNB, 0.1 mM acetyl-CoA and 0.2 mM oxaloacetate. CS activity was calculated as nmol $TNB\ min^{-1}\ mg\ protein^{-1}$.

**Determination of succinate dehydrogenase (SDH) activity**

SDH activity was measured according to Fischer et al. (11), by determining 2,6-dichloroindophenol (DCIP) reduction at λ = 600 nm. The incubation medium contained tissue supernatant (30 µg of protein), 40 mM potassium phosphate buffer pH 7.4, 16 mM sodium succinate, 4 mM sodium azide, 7 µM rotenone, 8 µM DCIP and 1 mM phenazinemethosulfate. SDH activity was calculated as nmol reduced DCIP / min / mg protein.

**Redox Assays**

**Reactive Oxygen Species levels**

To assess ROS levels, DCFH-DA, was used as a probe (14). An aliquot of the cerebral cortex homogenate (100 µg - 30µL) was incubated with DCFH-DA (100 µM) at 37°C for 30 min. The formation of fluorescent DCF was monitored at excitation and emission wavelengths of 488 and 525nm, respectively, using a fluorescence spectrophotometer. ROS contents were quantified using a DCF standard curve. The results are expressed as nmol DCF formed / mg protein.

**Antioxidant enzymes activities**

SOD (EC 1.15.1.1) activity was assessed by quantifying the inhibition of superoxide-dependent adrenaline auto-oxidation at 480nm, as previously described, and the results were expressed as units SOD/mg protein (15). GSH-Px (EC 1.11.1.9) activity was measured according to Wendel (16). One unit of GSH-Px activity was defined as 1µmol NADPH consumed/min, and the specific activity is expressed as units/mg protein.

**Substrates oxidation to $^{14}CO_2$**

Cerebral cortex slices (300 µm, 100-120 mg) were obtained as described above, transferred into flasks and pre-incubated in Dulbecco's buffer for 30 min. Before incubation with substrates, the reaction medium was gassed with a 95%$O_2$: 5% $CO_2$ mixture for 30 seconds. Slices were incubated in 1 mL of Dulbecco's buffer containing either: (i) 5 mM D-Glucose + 0.2 µCi D-[$^{14}$C(U)]Glucose (American Radiolabeled Chemicals, Inc., St. Louis, MO, USA); 10 µM L-Glutamic Acid + 0.2 µCi L-[$^{14}$C(U)] Glutamate (PerkinElmer Boston, MA, USA); (iii) 10 µM sodium L-Lactate + 0.2 µCi L-[U-$^{14}$C]Lactate (American Radiolabeled Chemicals, Inc., St. Louis, MO, USA). Then, flasks containing the slices were sealed with rubber caps and parafilm, and incubated at 37ºC for 1 hour in a Dubnoff metabolic shaker (60 cycles/min) as described previously (17, 18). The incubation was stopped by adding 0.2 mL 50% trichloroacetic acid (TCA) through the rubber cap into the flask, while 0.1 mL of 2 N NaOH was injected into the central wells. Thereafter, flasks were shaken for an additional 30 min at 37ºC to trap $CO_2$. Afterwards, the content of the central well was transferred to vials and assayed for $^{14}CO_2$ radioactivity in a liquid-scintillation counter. All the results are expressed as nmol of substrate oxidized per mg of tissue and the initial specific activity of the incubation medium was considered for calculations (19).

All measurements were made in 3 regions of our interest (referred as Fig. 7 A, B, and C), approximately 300 µM surrounding the cortex lesion, at 2 days and 9 days post- surgery (Fig. 7A). Evaluation of cellular fluorescence intensity was performed as previously described (20) with modifications (see supplementary data).

**Statistical analysis**

The data are expressed as mean ± S.E.M. All analyses were performed with Prism GraphPad (Version 6.01 for Windows, GraphPad Software, San Diego, CA, USA, www.graphpad.com). Differences among the groups were analyzed by *t* test, with levels of significance below *P<0.05* indicated in the following section.

## RESULTADOS

**Serum Biochemical Parameters**

The hepatectomy group presented higher levels of ammonia, lactate and GGT as well as lower levels of glucose when compared to sham operated animals. [Data not shown]

É importante citarmos que não houve nenhuma diferença entre os resultados objetivos quando comparado com o manuscrito do Capítulo 2 – “Behavioural, neurochemical and brain oscillation abnormalities in rats submitted to subtotal hepatectomy”

**Figure 1 - Redox assays**

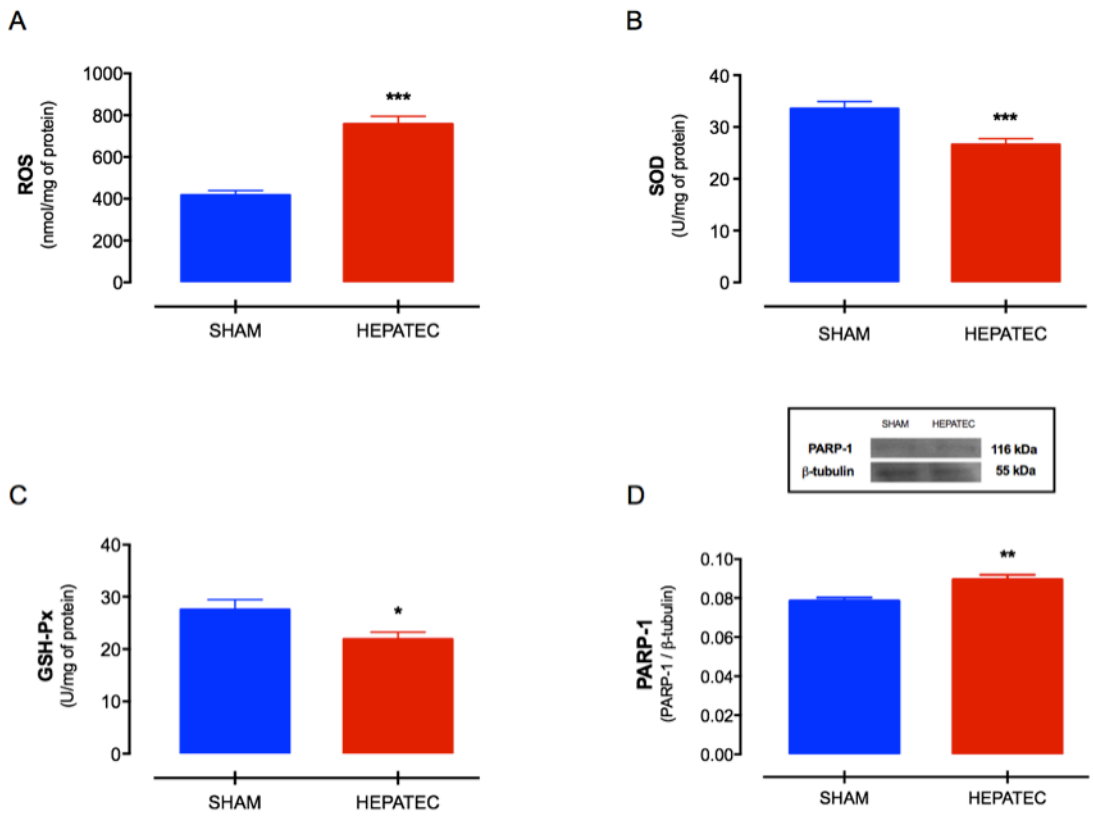


Hepatectomy group had elevated levels of ROS when compared to control (Figure 1A). In accordance, we found that operated animals presented a decrease in the activity of important antioxidant enzymes (SOD and GSH-Px) (Figure 1B and 1C). Hepatectomized animals also expressed an elevated immunocontent of PARP-1 (Figure 1D).

**n = 11-13**

**Figure 2 - TCA enzyme activity**

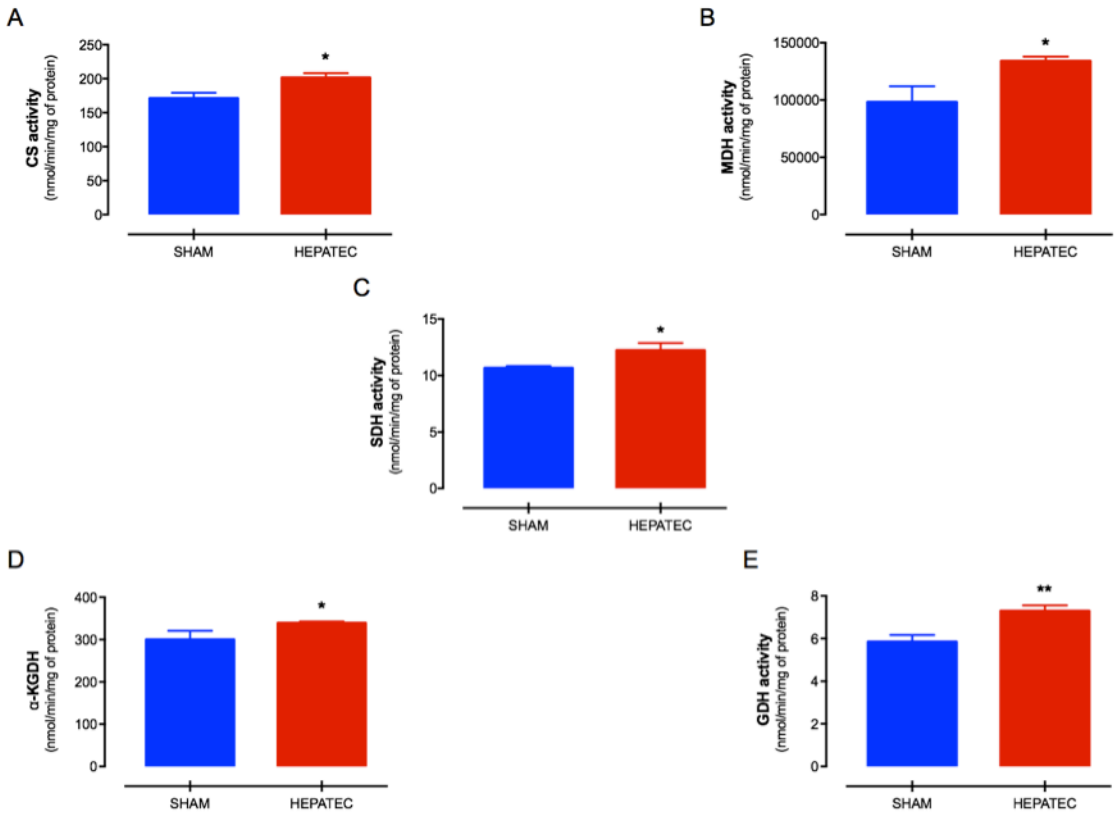


Hepatectomized animals presented increased activity in all evaluated enzymes – CS, MDH, SDH, α-KGDH and GDH- when compared to the sham group (Figure 2).

**n = 5-6**

**Figure 3 - Substrates oxidation to $^{14}CO_2$**

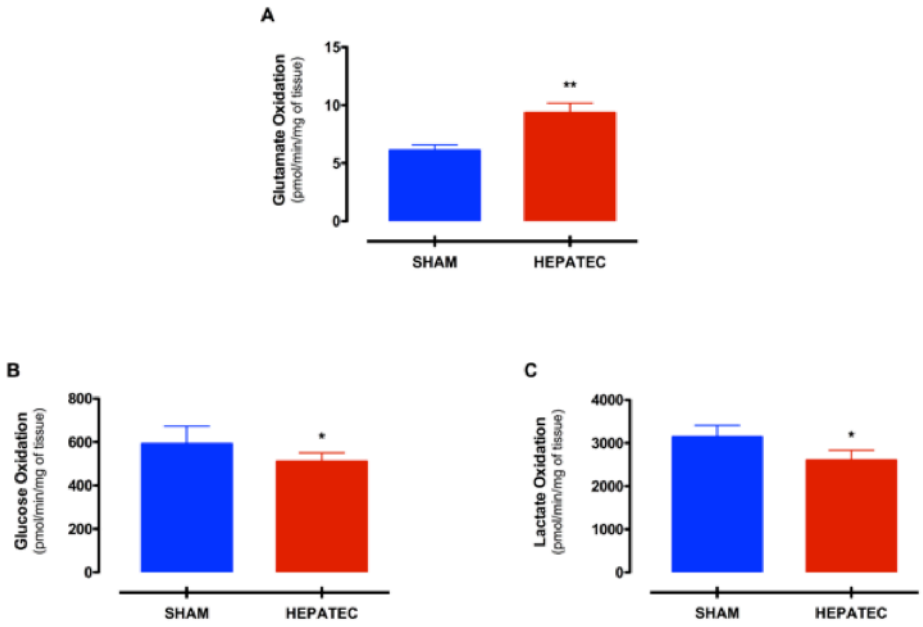


Animals submitted to hepatectomy presented elevated glutamate oxidation to $^{14}CO_2$ when compared to the sham group (Figure 3A). On the other hand, we found that the hepatectomy group had lower glucose and lactate oxidation to $^{14}CO_2$ than the control animals (Figure 3B and 3C).

**n = 8-9**

# PARTE 3

## “O RETORNO DA GUANOSINA”

## Discussão

Abordaremos a discussão dos resultados apresentados na Parte 2 da seguinte forma, por motivos de melhor entendimento: analisaremos em conjunto parte dos resultados do manuscrito referente ao Capítulo 1, alguns resultados serão, inicialmente, propositalmente deixados de lado; após isso, analisaremos em conjunto parte dos resultados dos manuscritos referentes aos Capítulos 2 e 3 (pois são oriundos do mesmo modelo experimental) e, por fim, formaremos considerações finais, sumarizando pensamentos e hipóteses.

Nesta tese, tivemos como objetivo inicial testar o efeito neuroprotetor da guanosina em um modelo de hiperamonemia aguda induzida por acetato de amônia. Após isso, padronizamos um modelo de encefalopatia hepática aguda induzida por hepatectomia subtotal e avaliamos diversas variáveis comportamentais, eletroencefalográficas e metabolismo cerebral. Tivemos como objetivo expandir o conhecimento de metabolismo cerebral em modelos animais de hiperamonemia e encefalopatia hepática.

Como falado na Parte 1, a encefalopatia hepática é uma síndrome com diversos mecanismos fisiopatológicos envolvidos, incluindo estresse oxidativo, aumento dos níveis de glutamato e excitotoxidade glutamatérgica, aumento de glutamina e alterações no metabolismo energético e de aminoácidos (Swain M, Butterworth RF, Blei AT, 1992; Ciećko-Michalska I, et al, 2012). Pensando nisso, desenvolvemos nosso estudo baseado em dois modelos animais com características complementares. É sabido que a amônia é a principal substância no desenvolvimento de EH e, por isso, em

nosso primeiro estudo, utilizamos um modelo de hiperamonemia aguda em roedores, já consagrado por Hermenegildo C. e colaboradores (2010). Ao utilizar um modelo de hiperamonemia induzida por injeção i.p. de acetato de amônia, reduzimos a fisiopatogênese da encefalopatia a um fator causal isolado – o aumento da amônia -, embora múltiplas variáveis estejam sempre envolvidas. Em nosso segundo modelo animal, causamos de fato um quadro de encefalopatia hepática através de hepatectomia subtotal (Madrahimov N, et al, 2006; Detry O, et al, 2013). Nesse modelo realizamos 92% de hepatectomia, causando o rápido desenvolvimento de encefalopatia hepática e, dessa forma, lidamos com uma variedade de diferentes mecanismos fisiopatológicos envolvidos simultaneamente. O objetivo de abordarmos dois modelos animais é, ao mesmo tempo em que conseguimos pesquisar especificamente o efeito da hiperamonemia em roedores, não nos privamos de tentar validar experimentos similares em um modelo de hepatectomia subtotal, que se aproxima mais fielmente à EH em humanos e, consequentemente, nos permite aproximar mais fielmente do potencial uso de guanosina como tratamento para hiperamonemia e encefalopatia hepática na prática clínica (Detry O, et al, 2013; Hermenegildo C, Monfort P, Felipo V., 2000).

Em nosso primeiro modelo (Capítulo 1), observamos leve diminuição da glicemia. Uma vez que os animais que recebiam acetato de amônia apresentavam convulsões, atribuímos a hipoglicemia com o efeito direto do aumento de utilização de glicose como substrato energético pelo músculo ao realizarem intensa contração muscular. Também, como há um aumento na glicólise cerebral em estados de hiperamonemia, esperamos que o nível

glicemia seja afetado. De qualquer forma, é importante fazermos duas considerações em relação às alterações glicêmicas encontradas: I) não houve diminuição na glicemia a ponto de provocar alterações neurológicas ou hipoglicemia importante (Maheandiran, M. et al, 2013); II) o grupo pré-tratado com guanosina não apresentou normalização na glicemia, dessa forma provavelmente a glicemia não esta ligada ao efeito neuroprotetor da guanosina.

Atribuímos o aumento plasmático das enzimas hepáticas observadas em nosso estudo como oriundo da metabolização da amônia. Essas alterações, no entanto, não fecham critérios para insuficiência hepática aguda, além da histologia hepática se manter inalterada (Figura suplementar). Porém, sabemos que 20 minutos pode não ser tempo suficiente para detectarmos alterações séricas e histológicas mais pronunciadas. Desta forma, não nos permitiremos realizar conclusões definitivas sobre isso.

Assim como era esperado, de acordo com o modelo apresentado por Hermenegildo C, Monfort P e Felipo V. (2000), os animais que receberam injeções com acetato de amônia apresentaram alterações no *status* neurológico e aumento liquórico de amônia e glutamato. Adicionalmente aos resultados observados nos experimentos de Hermenegildo C. (2000), mostramos que esses animais apresentam: 1) aumento liquóricos de alanina; 2) diminuição na captação cerebral de glutamato e na atividade da enzima glutamina sintetase; 3) alterações na atividade da enzima SOD e glutationa peroxidase. Todas estas alterações foram revertidas com o uso da

guanosina. É interessante notar que 10 minutos após a injeção de acetato de amônia, já havia alterações nos níveis de glutamato no líquor, sem haver nenhuma alteração nas atividades de SOD ou glutationa peroxidase, permitindo-nos concluir que alterações no sistema glutamatérgico antecedem alterações no estresse oxidativo.

As alterações observadas no EEG após os animais serem injetados com acetato de amônia são semelhantes às observadas em pacientes com EH (Amodio P, et al, 2001). Ainda, 10 a 20 minutos após os animais receberem acetato de amônia foi observado um elevado *left-index* na análise feita a partir dos resultados do EEG, corroborando as alterações observadas clinicamente (pré-coma, coma e morte) – quanto mais elevado a quantificação na escala do *left-index*, mais alterado está o padrão eletrofisiológico e mais próximo ao coma o animal se encontra. É importante frisarmos que os animais que foram pré-tratados com guanosina apresentaram os mesmos níveis de alteração neurológica que os animais que receberam injeção placebo 10 a 20 minutos após receberem acetato de amônia. A diferença entre os dois grupos foi que, posteriormente, o grupo tratado com guanosina apresentou rápida melhora no *status* neurológico, com retorno à normalidade.

Com esses resultados, podemos chegar à conclusão de que a guanosina não agiu sistemicamente, pois não alterou níveis de amônia encontrados no sistema nervoso central. Assim como também não reverteu alterações glicemia, AST e ALT. Fica claro que a guanosina não preveniu os efeitos da amônia, como a droga MK-801 o faz (Hermenegildo C, Monfort P,

Felipo V, 2000), uma vez que houve alterações eletroencefalográficas similares ao grupo controle no período 10 a 20 minutos após receberem acetato de amônia. Por isso, concluímos que a guanosina teve efeito predominantemente por aumentar a captação de glutamato, uma vez que mostrou aumentar a velocidade de recuperação dos animais observada clinicamente (30% menor o tempo de coma) e no EEG (rápida melhora do *left-index).* Ainda mais importante, o tratamento com guanosina levou à diminuição da letalidade em aproximadamente 50%, reforçando a grande importância do sistema purinérgico frente à excitotoxicidade glutamatérgica (Schmidt AP, Lara DR, Souza DO. 2007).

Em nosso modelo cirúrgico, induzimos EH através de hepatectomia subtotal, removendo 92% do fígado em uma única operação cirúrgica. Essa cirurgia provoca uma alta letalidade nos animais – letalidade de 80%, 60 horas pós-cirurgia (Detry O. et al 2012). Foram encontradas: 1) alterações plasmáticas características do modelo experimental de hepatectomia; 2) alterações comportamentais, como diminuída atividade locomotora e sinais de ansiedade; 3) alterações liquóricas com aumento de aminoácidos, incluindo alanina, glutamato e glutamina; 4) reduzido imunoconteúdo cortical de transportadores glutamatérgicos GLT-1 e GLAST; 5) aumento dos níveis de estresse oxidativo; 6) aumento da oxidação de glutamato no SNC e diminuída oxidação de lactato e glicose; 7) aumento da atividade das enzimas envolvidas no CAT; 8) alterações no EEG compatíveis com EH.

As alterações do *left-index* no EEG iniciaram rapidamente, ao redor de 30 minutos após hepatectomia, e permanecem presentes durante todo o

registro. Em animais hepatectomizados, há predominância de ondas mais lentas e aumento de ondas delta, o que é compatível com o quadro de EH (Amodio P, et al, 2001; Sutter, R. & Kaplan, P. W.,2013). As alterações vistas no EEG são complementadas com o padrão comportamental observadas na tarefa de campo aberto. Animais hepatectomizados apresentaram diminuição da locomoção e aumento do tempo na periferia da caixa. Essas alterações também são compatíveis com o quadro de EH (Almeida RF, et al, 2010; Padilla E, et al 2010). É importante notarmos que as alterações observadas no EEG nesse modelo são menos graves (*left-index* 0.7) quando comparadas às observadas no modelo de hiperamonemia (*left-index* 0.9) (Paniz LG, et al, 2014). Também, como observado no modelo de hiperamonemia induzida por acetato de amônia, as alterações glicêmicas não são graves a ponto de provocarem alterações neurológicas (Maheandiran, M. et al, 2013).

Encontramos um aumento na atividade das enzimas do CAT e também na atividade de a-CGDH, o que vai ao encontro da teoria de que a hiperamonemia provoca um “estado hipermetabólico” (Johansen ML, et al, 2007). Ainda, foi observado um aumento muito importante na oxidação de glutamato. Isso ocorre quando há aumento do glutamato extracelular e, consequentemente, aumento de sua captação na fenda sináptica. Dessa forma, a oxidação do glutamato gera ATP, supre o gasto energético provocado por sua captação e ainda poupa o uso de glicose. (Dienel, Gerald A, 2013).

Embora haja uma diminuição global da oxidação de lactato no SNC, acreditamos que o lactato ainda seja utilizado como substrato preferencial

pelos neurônios (Pellerin L, Magistretti PJ, 2012; Schurr, A, 2006), os quais representam uma parcela metabólica do SNC. Também, houve pequena diminuição na oxidação de glicose. Atribuímos essa alteração ao aumento da oxidação de glutamato, o que poupa parcialmente a oxidação de glicose.

Embora não tenhamos analisado os níveis de lactato no SNC, esperamos um aumento de lactato devido a elevados níveis de amônia e aumento consequente de glicólise em modelos de hiperamonemia (Ott P, Vilstrup H., 2014). Observamos que houve aumento de 132% nos níveis séricos de lactato. Elevados níveis arteriais de lactato levam ao aumento de lactato no SNC por dois mecanismos distintos: 1) existe elevada permeabilidade da BHE em EH ao lactato (Dalsgaard et al., 2004; Smith et al., 2003); 2) existem receptores MCT1, transportadores de lactato, expressados pelas células endoteliais na BHE, que tem sua atividade aumentada (Gerhart et al., 1997).

O aumento generalizado dos níveis liquóricos dos aminoácidos observado após hepatectomia corrobora com a proteólise esperada em EH proposta por Ott P, e colaboradores (2005). É interessante que encontramos níveis liquóricos elevados de alanina em animais que receberam injeção de acetato de amônia (e não foram tratados com guanosina), porém níveis normais de alanina em animais hepatectomizados. Em modelos de hiperamonemia, é esperado o aumento de alanina em consequência de aumento na transaminação de glutamina e também devido a um aumento do piruvato oriundo de maior glicólise. O aumento de glicólise é causado tanto por efeito direto da amônia (Muntz and Hurwitz, 1951; Abrahams and

Younathan, 1971; Ratnakumari and Murthy, 1993), quanto por estimulação por excesso de glutamato extracelular e sua captação (Dienel, Gerald A., 2013). Interpretamos que, uma vez que animais hepatectomizados apresentaram grande ativação das enzimas do CAT, os níveis de alfa-cetoglutarato devam estar normais. Dessa forma, a enzima glutamina transaminase não favorece tanto formação de alfa-cetoglutarato e alanina, mantendo níveis de alanina dentro da normalidade (Swain M, Butterworth RF, Blei AT, 1992). Por outro lado, animais que receberam acetato de amônia tem um aumento mais abrupto de amônia cerebral. Possivelmente, isso provoca inibição da enzima a-CGDH e maior formação de glutamato e glutamina, favorecendo a formação de alanina.

Animais hepatectomizados apresentaram níveis normais de aspartato. Interpretamos esse achado como consequência da utilização desse aminoácido no aspartato-malato *shuttle,* funcionando como substrato energético para o CAT. Mesmo em estado de proteólise e insuficiência hepática aguda, o aspartato não atravessa a BHE (Strauss et al., 2001). Considerando a aumentada utilização no CAT e impermeabilidade da BHE ao aspartato, níveis normais ou diminuídos desse aminoácido são esperados **(**Swain et al., 1992; Strauss et al., 2001).

Encontramos elevados níveis de isoleucina, leucina e valina. A leucina pode ser metabolizada a acetil-CoA e succinil-CoA, enquanto a leucina e valina podem prover succinil-CoA. Dessa forma, o aumento destes aminoácidos tem papel importante na reposição de cadeias carbonadas para o CAT (Ott P, Clemmesen O, Larsen FS, 2005). Ao contrário do aspartato,

isoleucina e leucina são os únicos aminoácidos que são transportados através da BHE em pacientes com insuficiência hepática aguda (Strauss et al., 2001). Por isso, embora sejam consumidos ao proverem cadeias carbonadas ao CAT, mantém níveis elevados no SNC, diferentemente do aspartato. Contudo, mesmo com o aumento dos níveis dos aminoácidos de cadeia ramificada (isoleucina, leucina e valina), sua proporção sobre a quantidade total de aminoácidos no SNC diminuiu. Diversos estudos sugerem que uma diminuição nessa razão - chamada de *Fischer's Ratio* (aminoácidos ramificados / quantidade total de aminoácidos), está implicada na patogênese da EH (Dejong, C. H, et al, 2007; Miyazaki T, et al, 2003).

É interessante que ambos modelos apresentaram resultados complementares que, se analisados conjuntamente, demonstram um *continuum* de alterações, como se fossem espectros de uma mesma doença. Em um modelo, analisamos o efeito da hiperamonemia 10 e 20 minutos após receberem acetato de amônia; no outro modelo, 24 horas após hepatectomia. Não há alteração alguma em marcadores de estresse oxidativo 10 minutos após acetato de amônia, mas, 20 minutos após, já observamos diminuição da atividade da SOD e aumento da glutationa peroxidase. Consideramos esse resultado como a fase inicial do estresse oxidativo. Já 24 horas após hepatectomia, os animais apresentavam tanto diminuição na atividade da SOD e da glutationa peroxidase, além de aumento de radicais livres totais, representando uma maior alteração nos marcadores de estresse oxidativo. Também, há aumento de imunoconteúdo cortical de PARP-1, o que representa uma modulação no SNC em uma tentativa de diminuição de estresse oxidativo.

Há aumento liquórico de glutamato 10 e 20 minutos após os animais serem injetados com acetato de amônia; porém, não observamos alterações nos níveis de glutamina, a qual é um dos principais causadores de edema cerebral em EH aguda **(**Desjardins P, et al, 2012**)**. Em contraste, 24 horas após hepatectomia, além do aumento de glutamato liquórico, observamos o aumento de glutamina. O rápido aumento de glutamato extracelular após injeção de acetato de amônia é explicado pelo efeito despolarizante da amônia sobre a membrana neuronal, provocando a exocitose de glutamato (Hermenegildo C, Monfort P, Felipo V., 2000). Já o aumento de glutamina se dá principalmente pelo aumento de sua síntese a partir de glutamato e amônia, podendo 20 minutos não ser suficientes para a passagem da glutamina intracelular para o meio extracelular. Por outro lado, 24 horas após hepatectomia, já observamos aumento de glutamina. Embora os níveis liquóricos de glutamato permaneçam elevados no espaço extracelular 24, horas após hepatectomia, acreditamos que exista um consumo na quantidade total de glutamato cerebral (Butterworth, 1997; Cooper and Plum, 1987). Por fim, o aumento do glutamato extracelular após hepatectomia também é causado por diminuição de imunoconteúdo dos transportadores glutamatérgicos GLAST e GLT-1 (Lehmann C, Bette S, Engele J. 2009).

Já havia sido mostrado por Lucas Paniz e colaboradores (2014) que a guanosina apresentou efeito neuroprotetor em um modelo de EH crônico. Também demonstramos diminuição de letalidade com a administração de guanosina em um modelo de hiperamonemia aguda. Após analisarmos as alterações fisiopatológicas no SNC induzidas por hepatectomia subtotal, acreditamos que a guanosina apresente potencial neuroprotetor frente à

modelos mais complexos de hiperamonemia e encefalopatia hepática. Embora com diversos outros mecanismos envolvidos, o aumento de glutamato extracelular e do estresse oxidativo estão entre os principais colaboradores para o desenvolvimento de EH. Foi demonstrado que a guanosina apresenta capacidade de aumentar a captação astrocitária de glutamato (Schmidt, A. P., & Souza, D. O, 2005; Schmidt, A. P., & Souza, D. O, 2010**)** e de diminuir o estresse oxidativo (Petronilho F., et al, 2012).

Exposta esta análise, reforçamos a importância do estudo do sistema purinérgico, especialmente da guanosina, frente a modelos de excitotoxicidade glutamatérgica, e, principalmente, em modelos de EH. Acreditamos que a guanosina possa vir a ser usada como adjuvante no tratamento de encefalopatia hepática em humanos.

## Perspectivas

“A conclusão deste estudo responde algumas perguntas, mas também, como é característico da ciência, traz outras tantas interrogações. “ foi a frase que o Lucas Paniz utilizou no inicio da conclusão de sua tese em 2014. Da mesma forma, uma vez que nosso trabalho não está acabado, nosso grupo tem como objetivo continuar pesquisando na linha de modelos animais de hiperamonemia e encefalopatia hepática. Em curto prazo, planejamos continuar utilizando os mesmos modelos animais que foram apresentados nessa tese.

Já estamos estudando os efeitos da guanosina em nosso modelo animal de hepatectomia subtotal. Continuamos a tentar compreender com mais detalhamento o metabolismo cerebral, metabolismo de aminoácidos, respiração celular e efeitos na reatividade astrocitária frente à hiperamonemia. Objetivamente, procuramos entender o mecanismo específico pelo qual a guanosina promove neuroproteção.

Nosso grupo, cada vez mais, adquire expertise no assunto. Mais pessoas talentosas e dedicadas se juntam e, com isso, damos seguimento ao estudo. Ao fazer a retrospectiva desses 48 meses, percebo que avançamos muito enquanto grupo pesquisando sobre hiperamonemia. No entanto, ao fazer isso, criamos ainda mais perguntas, que pretendemos continuar a buscar respostas.

# ANEXO

## COVER SUBMETIDO PARA REVISTA MOLECULAR NEUROBIOLOGY

### Historia por trás dessa gravura:

Após submetermos o Manuscrito “Guanosine exerts neuroprotective effect in an experimental model of acute ammonia intoxication” para o periódico Molecular Neurobiology, recebemos o aceite para publicação em 22 dias juntamente com o pedido para enviarmos uma proposta de capa.

A gravura é uma modificação de uma pintura original datada de 1932, “*Finding Calm in the Storm*”, ou “Encontrando paz durante a tempestade”. Essa imagem nos apresenta um barco em um vasto oceano no meio de uma tempestade, porém o barco se encontra estável. É relacionada ao papel da Guanosina em nosso modelo de Hiperamonemia Aguda do mesmo trabalho, no qual, ela apresenta efeitos neuroprotetores em meio a uma tempestade de amônia. Juntamente com meu tio Otávio, nos inspiramos em *cartoons* dos anos 80 para desenhar o cérebro.

**Estudos na *University California of San Francisco***

Experiência,

Em 2014, aproveitando um edital da CAPES do programa Ciências sem Fronteiras, o professor Diogo contatou seu antigo amigo e colega de laboratório, professor Neurologista Raymond A. Swanson. Discutimos a possibilidade de eu permanecer um ano estudando no laboratório de neurociência da *University California of San* Francisco, em San Francisco, Califórnia, nos Estados Unidos. Desenvolvemos um projeto e em Outubro de 2014 recebi o aceite, iniciando meus estudos na América do Norte.

Trabalhei com camundongos transgênicos para EAAC-1 em modelos de estresse oxidativo e doença de *Parkinson*, assim como modelos de trauma cerebral. Aprendi a trabalhar com imunofluorescência e microscopia confocal, estudos com glutationa, comportamento animal, entre outras técnicas.

Morei um ano em uma cidade maravilhosa e conheci pessoas que se tornaram minhas amigas mesmo distantes. Foi uma experiência excepcional, que acabou por me deixar com o sentimento de saudades.

Também, mantemos contato com o professor Swanson, ainda com trabalhos em desenvolvimento, os quais não foram citados nessa tese.

**Manuscrito Anexo 1**

# Assessment at the Single-Cell Level Identifies Neuronal Glutathione Depletion as Both a Cause and Effect of Ischemia-Reperfusion Oxidative Stress

Seok Joon Won, Ji-Eun Kim, Giordano Fabricio Cittolin-Santos,

Raymond A. Swanson

**Manuscrito publicado no periódico THE JOURNAL OF NEUROSCIENCE**

**Submetido: 25, Novembro de 2014**

**Aceito: 31 de Março de 2015**

Neurobiology of Disease

# Assessment at the Single-Cell Level Identifies Neuronal Glutathione Depletion As Both a Cause and Effect of Ischemia-Reperfusion Oxidative Stress

**Seok Joon Won,[1,2] Ji-Eun Kim,[1,2] Giordano Fabricio Cittolin-Santos,[1,2] and Raymond A. Swanson[1]**

Departments of [1]Neurology, University of California San Francisco, and [2]Neurology Service, San Francisco Veterans Affairs Medical Center (SFVAMC), San Francisco, California 94121

**Oxidative stress contributes to neuronal death in brain ischemia-reperfusion. Tissue levels of the endogenous antioxidant glutathione (GSH) are depleted during ischemia-reperfusion, but it is unknown whether this depletion is a cause or an effect of oxidative stress, and whether it occurs in neurons or other cell types. We used immunohistochemical methods to evaluate glutathione, superoxide, and oxidative stress in mouse hippocampal neurons after transient forebrain ischemia. GSH levels in CA1 pyramidal neurons were normally high relative to surrounding neuropil, and exhibited a time-dependent decrease during the first few hours of reperfusion. Colabeling for superoxide in the neurons showed a concurrent increase in detectable superoxide over this interval. To identify cause–effect relationships between these changes, we independently manipulated superoxide production and GSH metabolism during reperfusion. Mice in which NADPH oxidase activity was blocked to prevent superoxide production showed preservation of neuronal GSH content, thus demonstrating that neuronal GSH depletion is result of oxidative stress. Conversely, mice in which neuronal GSH levels were maintained by *N*-acetyl cysteine treatment during reperfusion showed less neuronal superoxide signal, oxidative stress, and neuronal death. At 3 d following ischemia, GSH content in reactive astrocytes and microglia was increased in the hippocampal CA1 relative to surviving neurons. Results of these studies demonstrate that neuronal GSH depletion is both a result and a cause of neuronal oxidative stress after ischemia-reperfusion, and that postischemic restoration of neuronal GSH levels can be neuroprotective.**

*Key words:* **glutathione; hyperglycemia; ischemia; *N*-acetyl cysteine; neuron; oxidative stress**

## Introduction

Ischemia-reperfusion leads to the production of superoxide and nitric oxide by neurons and other cell types (Chan, 2001; Brennan-Minnella et al., 2015). These oxidants form peroxynitrite and other highly reactive oxygen species (ROS) that rapidly damage lipids, proteins, and DNA. DNA damage in turn triggers the poly(ADP-ribose) polymerase cell death pathway (parthanatosis), which is the primary cause of acute neuronal death in ischemia-reperfusion injury (Moroni, 2008; Andrabi et al., 2011; Baxter et al., 2014).

Glutathione (GSH) plays a crucial role in cell defense against oxidative stress (Dringen, 2000; Maher, 2006). GSH scavenges superoxide and other ROS both directly and, more rapidly, in enzyme-catalyzed reactions. One such reaction class reduces peroxides, as exemplified by the glutathione peroxidase reaction: $2GSH + H_2O_2 \rightarrow GSSG + 2H_2O$. A second class of reactions includes glutaredoxin-mediated repair of proteins that have been oxidatively modified at cysteine residues. These reactions also ultimately generate GSSG from GSH. The GSSG (glutathione disulfide) formed in these processes can either be exported from cells or recycled to GSH in the glutathione reductase reaction: $GSSG + NADPH \rightarrow 2GSH + NADP^+$. GSSG has intrinsic cytotoxicity, and consequently cells export GSSG when formation exceeds capacity for recycling to GSH (Homolya et al., 2003). GSH moieties lost through GSSG export must be replaced by *de novo* GSH synthesis, for which cysteine availability is usually the rate liming factor (Jones, 2008). GSH depletion has also been shown to impair mitochondrial ATP production (Vesce et al., 2005) and promote mitochondrially driven apoptosis (Muyderman et al., 2007).

The obligatory role of GSH in these anti-oxidant and repair processes suggests that intracellular GSH levels could be an important factor affecting neuronal survival during ischemia-reperfusion, but there are several gaps to our understanding in this area. It is not known whether ischemia-reperfusion reduces GSH levels specifically in neurons, if so by what mechanism, or if this reduction significantly contributes to neuronal demise. There is also uncertainty as to the relative GSH concentrations in neurons compared with astrocytes. Studies of pure neuronal and astrocyte cultures suggest that neurons contain far less GSH than astrocytes (Makar et al., 1994; Dringen et al., 1999); however, this

Received Nov. 25, 2014; revised March 17, 2015; accepted March 31, 2015.

Author contributions: S.J.W. and R.A.S. designed research; S.J.W. and J.-E.K. performed research; S.J.W. contributed unpublished reagents/analytic tools; S.J.W., J.-E.K., and G.F.C.S. analyzed data; S.J.W. and R.A.S. wrote the paper.

This work was supported by the NIH (NS081149 to R.A.S.) and the US Department of Veterans Affairs.

The authors declare no competing financial interests.

Correspondence should be addressed to Dr Seok Joon Won, Department of Neurology (127), 4150 Clement Street, UCSF, VAMC, San Francisco, CA 94121. E-mail: Seokjoon.won@va.gov.

J. Kim's present address: Department of Anatomy and Neurobiology, Institute of Epilepsy Research, College of Medicine, Hallym University, Chuncheon 200-702, South Korea.

DOI:10.1523/JNEUROSCI.4826-14.2015

 0270-6474/15/357143-10$15.00/0

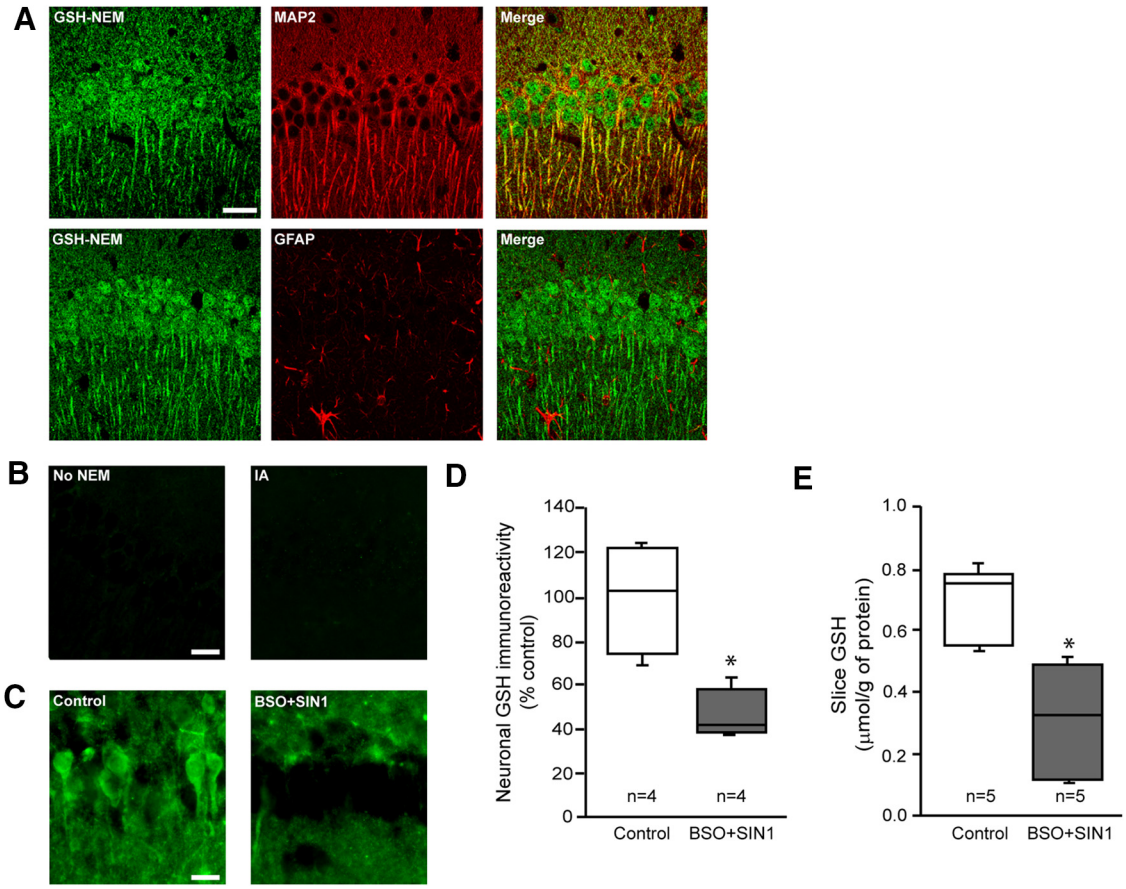


**Figure 1.** Immunohistochemical quantification of neuronal GSH content. ***A***, Confocal images of mouse hippocampal sections treated with NEM to generate NEM-GSH adducts and immunostained with antibody for GSH-NEM (green). Sections were counterstained (red) with either anti-MAP2 to identify neuronal processes or GFAP to identify astrocyte processes. Specificity was validated by lack of GSH-NEM signal in sections not treated with NEM, and in sections pretreated with iodoacetamide to render sulhydryl groups unreactive with NEM (***B***). Scale bar, 20 $\mu$m. ***C***, In *ex vivo* brain slices, neuronal GSH-NEM signal was reduced after incubation with 1 mM BSO plus 500 $\mu$M SIN1 for 6 h. Scale bar, 20 $\mu$m. ***D***, Immunohistochemical quantification of neuronal GSH in *ex vivo* brain slices. ***E***, Biochemical quantification of GSH in the same *ex vivo* brain slices (*$p < 0.05$).

may be a cell culture artifact because cultured astrocytes display a reactive phenotype in which the GSH biosynthetic pathway is upregulated (Shih et al., 2003), and neuron levels of GSH are artificially depressed when cultured in the absence of astrocytes (Dringen et al., 1999; Dringen, 2000).

To resolve these issues, we used an immunohistochemical method to evaluate GSH content in individual neurons. Results of these studies show that GSH levels in hippocampal pyramidal neurons are normally greater than astrocyte GSH levels, and that neuronal GSH levels fall in a time-dependent manner after ischemia-reperfusion. Blocking superoxide production during reperfusion preserves neuronal GSH levels, and supporting neuronal GSH levels with *N*-acetyl cysteine reduces oxidative stress and neuronal death.

## Materials and Methods

Studies were approved by the SFVAMC animal studies committee. Mice were male, C57BL/6, 3–5 months of age. Wild-type (WT) mice were obtained from Simonsen Laboratories. p47$^{phox-/-}$ Mice were obtained from The Jackson Laboratory, and subsequently back-crossed to WT C57BL/6 mice for >10 generations. Reagents were obtained from Sigma-Aldrich except where otherwise noted.

*Transient forebrain ischemia.* Ischemia was induced by transient occlusion of both common carotid arteries, as described previously (Barone et al., 1993; Won et al., 2010). Mice were fasted overnight and anesthetized with 2% isoflurane in a 70% $N_2O$/30% $O_2$ mixture. Body temperature was maintained at 37 ± 0.3°C with a homeothermic blanket and heating lamp (Harvard Apparatus). The common carotid arteries were exposed through a midline neck skin incision and occluded for 12 min with small aneurysm clips. Artery occlusion and reperfusion was confirmed in each case by visual inspection. Anesthetics were discontinued after skin closure. When mice showed spontaneous respiration, they were returned to a recovery chamber maintained at 37°C until ambulatory. Sham-operated animals received neck incisions without artery occlusion.

Where used, *N*-acetyl cysteine (NAC), apocynin, or their corresponding vehicles were administered as 10 $\mu$l/g intraperitoneal injections at the time of reperfusion. NAC was dissolved in physiological saline, and apocynin was dissolved in 1% dimethylsulfoxide. For studies using hyperglycemia, mice were given intraperitoneal injection of 50% glucose in saline, (2.5 $\mu$l/g body weight) immediately before reperfusion as described previously (Suh et al., 2008). The corresponding normoglycemic mice received equal volumes of saline only. Blood glucose was measured from tail vein samples 15 min before ischemia onset and 30 min after reperfusion using ACCU-CHEK glucometer (Roche).

*Immunohistochemistry.* Mice were anesthetized and transcardially perfused with cold saline followed by 4% formaldehyde solution. Brains were removed and postfixed in 4% formaldehyde overnight. Brains used for 4-hydroxynonenal (4HNE) and nitrotyrosine (NT) immunostaining were embedded in paraffin for collection of 7 $\mu$m coronal sections. The sections were deparaffinized with xylene, rehydrated, and then boiled in 10 mM sodium citrate, pH 7.0, for 10 min to achieve antigen retrieval (Shi et al., 1991). Brains used for other outcome measures were cryoprotected in sucrose and cryostat sectioned at either 25 $\mu$m thickness for Fluoro-Jade B staining, or 40 $\mu$m thickness for all other measures.

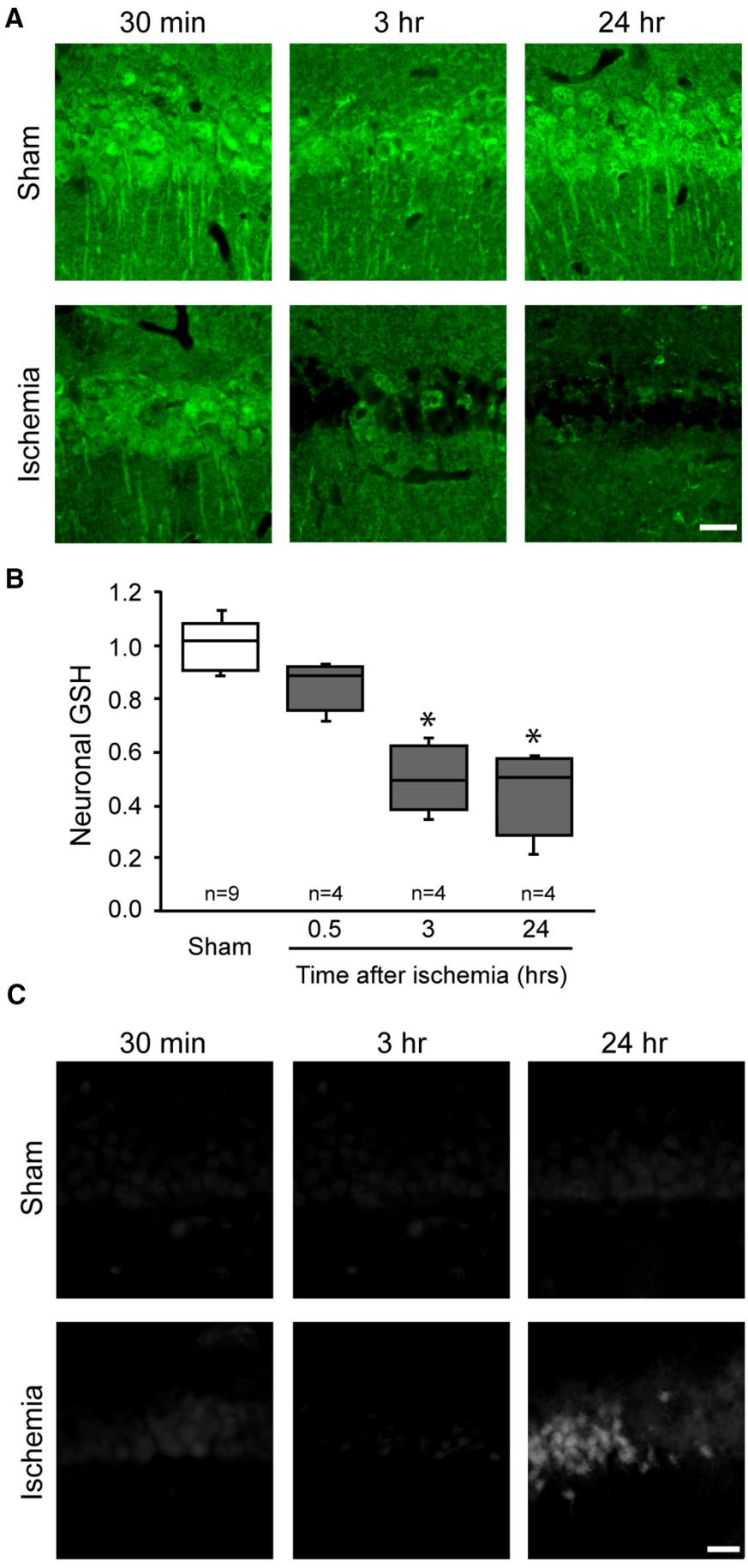


GSH was detected in sections that were preincubated with 10 mM *N*-ethylmaleimide (NEM) for 4 h at 4°C, using a mouse antibody to GSH-NEM (clone 8.1GSH, Millipore) as described previously (Miller et al., 2009; Escartin et al., 2011). The sections were subsequently incubated with rabbit antibodies to 4HNE (Abcam), NT (Millipore), MAP2 (Millipore), GFAP (Millipore), or Iba1 (Waco). Antibody binding was visualized using AlexaFluor 488-conjugated goat anti-mouse IgG or AlexaFluor 594-conjugated goat anti-rabbit IgG (Invitrogen).

For detection of superoxide-derived ROS, 3 mg/kg dihydroethidium (Invitrogen) dissolved in 1% dimethylsulfoxide was intraperitoneally injected 15 min before artery occlusion and brains were harvested at the designated time points following reperfusion. Cryostat sections were photographed with a fluorescent microscope using excitation at 510–550 nm and emission >580 nm to detect oxidized ethidium species (Eth) (Murakami et al., 1998; Won et al., 2010).

Quantification of fluorescent labeling was performed using four evenly spaced sections collected through the hippocampus of each mouse. Each section was photographed with a fluorescence microscope using uniform conditions. Antibody or Eth fluorescence intensity was measured in the bilateral CA1 pyramidal layer of each of section, and the values obtained in the four sections were averaged for each brain. To assess colocalization of glutathione and superoxide formation at the single-cell level, brain sections from dihydroethidium-injected mice were immunostained with anti-GS-NEM and photographed with a confocal fluorescence microscope. Eth and anti-GS-NEM fluorescence were measured in each neuronal soma of hippocampal CA1, with >70 cells analyzed in each section.

*Neuron death.* Degenerating neurons were evaluated by Fluoro-Jade B staining as described previously (Schmued and Hopkins, 2000; Won et al., 2010), using five evenly spaced sections through the hippocampus. In brief, 25 μm sections mounted on slides were immersed in a basic alcohol solution followed by 0.06% potassium permanganate for 15 min, placed in 0.0004% Fluoro-Jade B (Millipore) for 20 min. The number of degenerating neurons in CA1 pyramidal layer was counted bilaterally and averaged over the five sections from each brain.

*Acute brain-slice cultures.* Mouse brains were vibratome sectioned into 300 μm coronal slices. The slices were placed in ice-cold artificial CSF (130 mM NaCl, 3.5 mM KCl, 1.25 mM

←

**Figure 2.** Transient forebrain ischemic injury produces a delayed depletion of GSH in hippocampal CA1 pyramidal neurons. ***A***, Hippocampal brain sections harvested at the designated times after ischemia-reperfusion or sham surgery and immunostained for GSH. Scale bar, 20 μm. ***B***, Quantification of neuronal GSH immunoreactivity (*$p < 0.05$ vs sham). ***C***, Neuronal death as detected with Fluoro-Jade B under conditions as in ***A***. Scale bar, 20 μm.

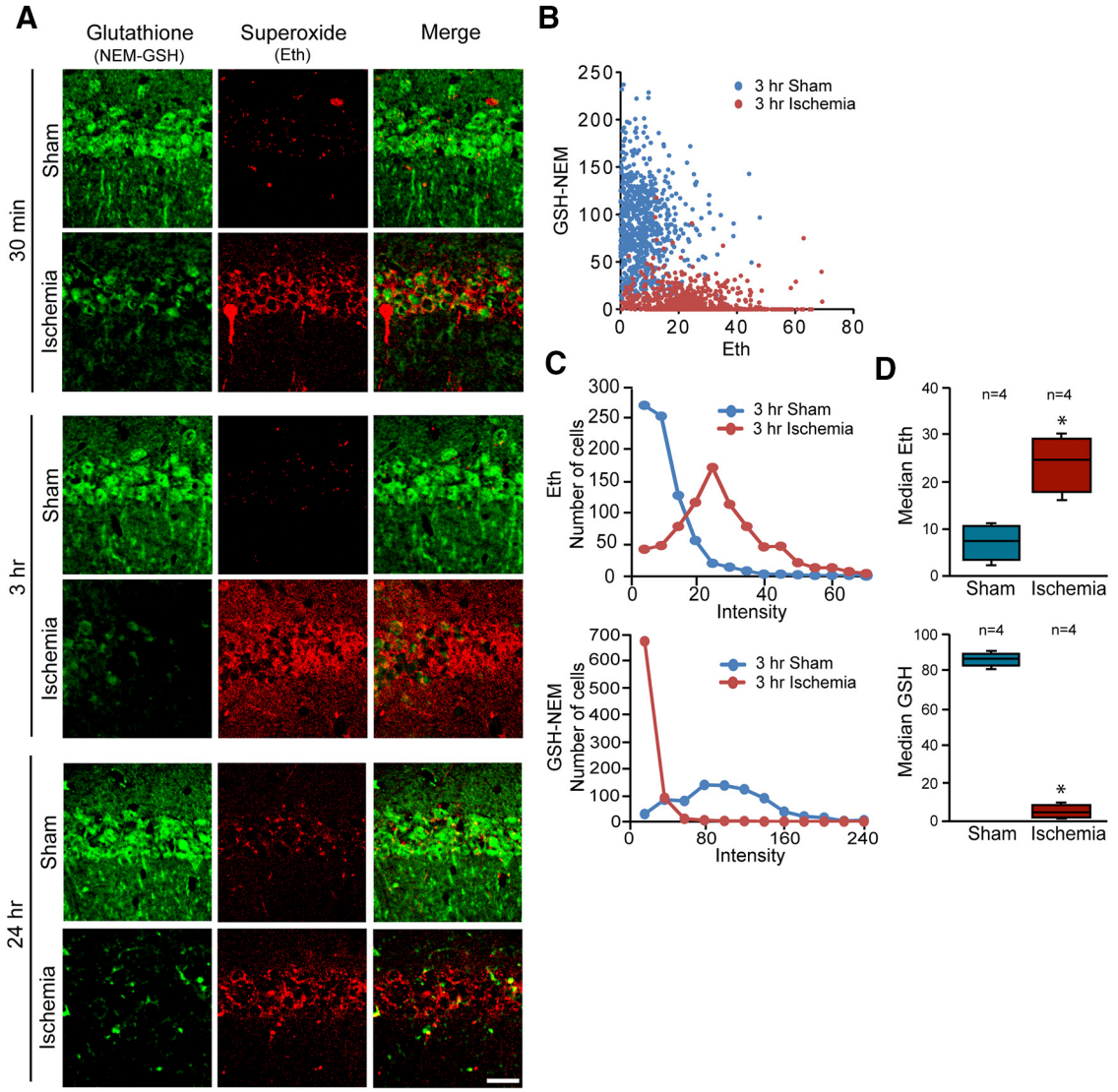


**Figure 3.** Inverse relationship between superoxide and GSH levels in postischemic hippocampal neurons. ***A***, Confocal images showing glutathione (GSH-NEM, green) and superoxide (Eth, red) in neurons of hippocampal sections harvested after ischemia-reperfusion or sham surgery. Scale bar, 20 $\mu$m. ***B***, Scatterplot shows relative levels of GSH and superoxide measured in individual neurons harvested 3 h after ischemia or sham surgery (sham $n = 4{,}744$ cells; ischemia $n = 4{,}783$ cells). ***C***, Histograms show the distribution of data plotted in ***B***. ***D***, Box-and-whisker plots show the median values from $n = 4$ animals in each treatment group (*$p < 0.05$).

$NaH_2PO_4$, 2 mM $MgSO_4$, 2 mM $CaCl_2$, 20 mM $NaHCO_3$ and 10 mM glucose, pH7.2) while equilibrated with 95% oxygen and 5% $CO_2$. After 30 min, the incubation temperature was raised to 30°C and one-half of the slices were treated with 0.5 mM 3-morpholinosydnonimine (SIN-1) plus 1 mM buthionine sulfoxamine (BSO) to reduce glutathione content (SIN-1 generates peroxynitrite, which avidly reacts with GSH, and BSO prevents *de novo* GSH synthesis; Griffith and Meister, 1979; Zhang et al., 1997). After 6 h, slices were either frozen for biochemical GSH determination or fixed in 4% formaldehyde for GSH-NEM immunohistochemistry.

*GSH assay.* Brain slices were sonicated with 0.5 ml of 5% sulfosalicylic acid and centrifuged at 10,000 × *g* for 10 min at 4°C. The supernatant was mixed with 1 mM dithiobis-2-nitrobenzoic acid and 1 mM EDTA in 100 mM sodium phosphate buffer, pH 7.5, and 1 mM NADPH and 200 U/ml of glutathione reductase were added (Baker et al., 1990). GSH standards were treated identically, and optical absorbance of samples and standards was measured at 405 nm. Values were normalized to protein content as determined with a BCA protein assay kit (Thermo Scientific).

*Statistical analyses.* Quantified data are presented as box-and-whisker plots, with the boxes showing the median and the upper and lower quartiles, and the whiskers showing the highest and lowest values in each the dataset. Statistical significance was assessed with the Mann–Whitney *U* test for two-group comparisons, and with the Kruskal–Wallis nonparametric one-way ANOVA test followed by Dunn's test for multiple group comparisons. *P* values $<0.05$ were considered significant. The number of mice in each experimental group is displayed in each figure.

## Results

### Ischemia reduces neuronal GSH content

To evaluate cell-type-specific changes in glutathione content, we adapted an immunohistochemical approach that uses antibody to GSH-NEM adducts. This method specifically identifies GSH in NEM-treated tissues, and thereby overcomes the more limited specificity of antibodies directed to native GSH (Miller et al., 2009). Hippocampal sections evaluated using this approach showed a strong GSH signal in the CA1 pyramidal neuron soma, with lesser signal in the adjacent neuropil and astrocyte cell bodies (Fig. 1*A*). The CA1 pyramidal layer was chosen for analysis of neuronal GSH changes because this region is relatively poor in astrocyte processes (Ouyang et al., 2007). This was confirmed here by staining for the astrocyte

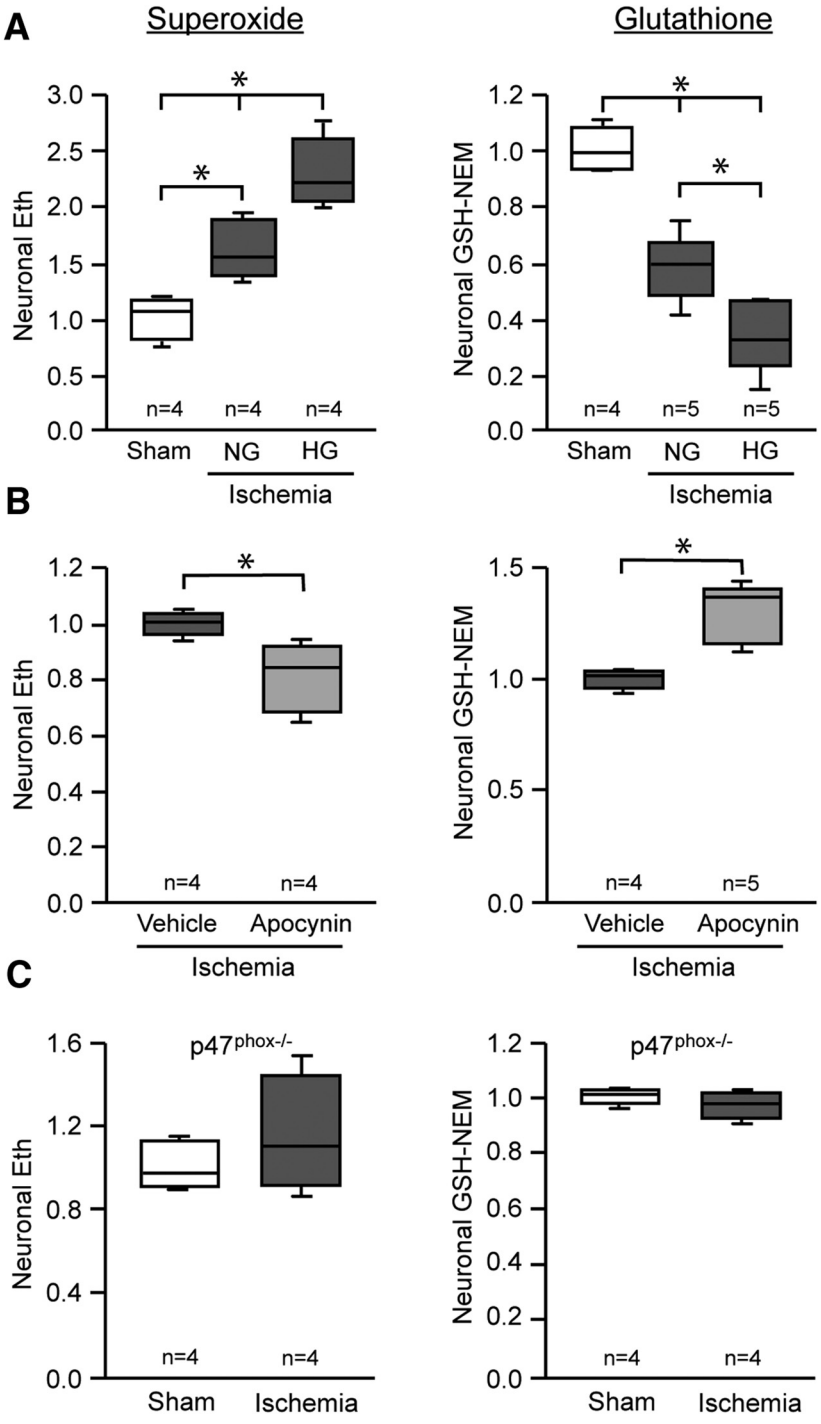


**Figure 4.** Neuronal GSH levels are influenced by postischemic superoxide production. Neuronal superoxide and GSH levels were assessed in hippocampal CA1 pyramidal neurons fixed 3 h after ischemia-reperfusion or sham surgery. ***A***, Superoxide levels were increased by normoglycemic ischemia-reperfusion (NG), and further increased in mice rendered hyperglycemic during reperfusion (HG; $*p < 0.05$ vs sham). Neuronal GSH exhibited reciprocal changes. Blood glucose levels were $4.61 \pm 0.82$ mmol/L in normoglycemic mice and $14.89 \pm 2.93$ mmol/L in the hyperglycemic mice. ***B***, Apocynin (15 mg/kg) reduced superoxide production in postischemic neurons, and prevented GSH depletion ($*p < 0.05$). ***C***, Ischemia-reperfusion did not increase superoxide levels in $p47^{phox-/-}$ mice, and neurons in these mice showed no significant fall in GSH levels.

marker, GFAP (Fig. 1*B*; see also Fig. 7*A*). GSH-NEM staining was absent in sections that had not been treated with NEM, and in sections treated with iodoacetamide to render sulfhydryl groups unreactive to NEM (Fig. 1*B*). To further evaluate the specificity of this histochemical approach, we compared the GSH-NEM signal to biochemical measurements of GSH in acutely isolated hippocampal slices. In one-half of the slices GSH levels were lowered by 6 h incubations in medium containing 3-morpholinosydnonimine and L-buthionine sulfoxamine. Slices treated this way showed a ~50% reduction in total slice GSH-NEM signal, and a comparable reduction in biochemically measured slice GSH content (Fig. 1*C–E*).

We then used the GSH-NEM method to evaluate changes in the GSH content of hippocampal CA1 pyramidal neurons at serial time points after transient forebrain ischemia. GSH levels were not detectably altered at 30 min after reperfusion, but were significantly decreased at 3 h and nearly absent at 24 h after reperfusion (Fig. 2*A*,*B*). To determine whether these decreases were simply indicative of neuronal death, degenerating neurons were identified by Fluoro-Jade B staining in adjacent sections. The Fluoro-Jade B staining showed only scattered dead neurons at 24 h and no signal at the earlier time points (Fig. 2*C*), consistent with delayed neuronal death in this stroke model (Barone et al., 1993; Bennett et al., 1996; Lee et al., 2004; Won et al., 2010).

### Reduced neuronal GSH content is accompanied by increased superoxide levels

Superoxide and certain superoxide-derived ROS produced during ischemia-reperfusion can be detected by evaluating oxidation of dihydroethidium to fluorescent oxidized Eth (Murakami et al., 1998; Peshavariya et al., 2007; Won et al., 2010). We prepared confocal images from sections double-labeled for Eth formation and GSH-NEM to evaluate the relationships between superoxide and GSH levels in individual neurons. Eth formation in hippocampal sections harvested at serial time points after ischemia-reperfusion showed increased signal in the CA1 pyramidal neurons at 0.5, 3, and 24 h after reperfusion (Fig. 3*A*). Focusing on the 3 h time-point, preceding neuronal death, the colabeling showed a corresponding reduction in neuronal GSH levels (Fig. 3*A–D*).

### Superoxide production causes neuronal GSH depletion after ischemia

GSH is consumed in the process of scavenging superoxide and superoxide-derived reactive oxygen species. As a consequence, the reciprocal changes in GSH and superoxide levels in postischemic neurons could result either from increased GSH consumption in neurons with increased superoxide formation, or from reduced superoxide-scavenging capacity in neurons with reduced GSH content. To test these possibilities, we first evaluated the effects of increased and decreased superoxide production on neuronal GSH levels. Superoxide formation

was increased by rendering mice hyperglycemic during reperfusion (Muranyi and Li, 2006; Kamada et al., 2007; Suh et al., 2008; Won et al., 2011). The hyperglycemia-induced increase in superoxide production produced a corresponding decrease in neuronal GSH content (Fig. 4*A*). Next, we suppressed superoxide formation by treating mice with the NADPH oxidase inhibitor apocynin (Stolk et al., 1994; Suh et al., 2008). The reduced superoxide signal in neurons of these mice was accompanied by a corresponding increase in neuronal GSH content (Fig. 4*B*). We also evaluated this relationship in p47$^{phox-/-}$ mice, which cannot assemble a functional NADPH oxidase-2 complex (Bedard and Krause, 2007). Ischemia-reperfusion in these mice produced no significant increase in neuronal superoxide signal, and no reduction in neuronal GSH content (Fig. 4*C*). Together, these findings support the idea that accelerated superoxide production is the primary cause of GSH depletion in postischemic neurons. The absence of ischemia-induced neuronal Eth formation in mice lacking NADPH oxidase-2 activity also confirms that this signal is attributable to superoxide or superoxide-derived ROS.

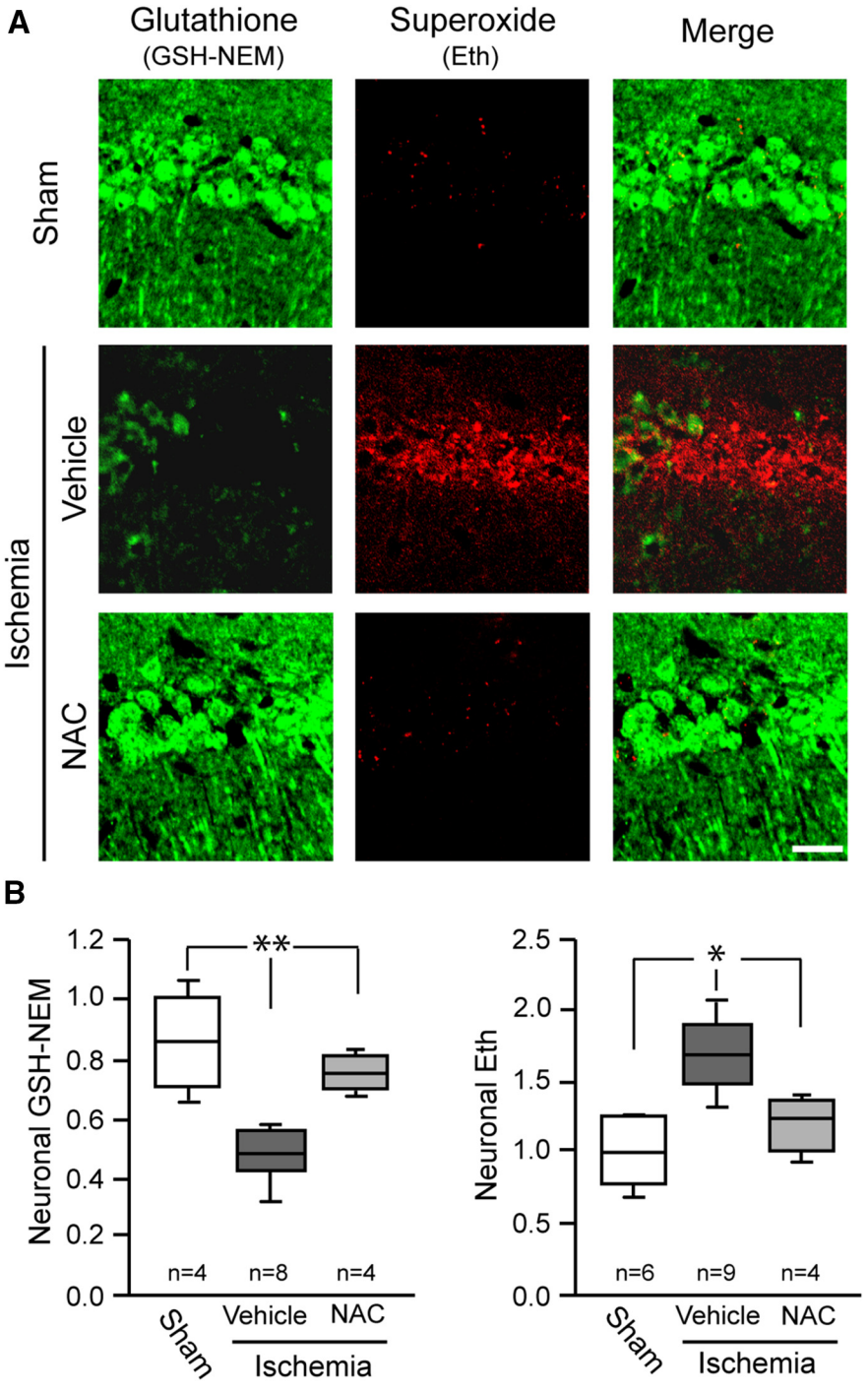


**Figure 5.** *N*-acetyl cysteine administered after ischemia-reperfusion restores neuronal GSH and reduces detectable superoxide. ***A***, Representative photomicrographs showing relative levels of GSH and superoxide detection in hippocampal CA1 neurons. NAC or saline vehicle was administered at reperfusion, and tissues were harvested 3 h later. Scale bar, 20 $\mu$m. ***B***, Quantified results (*$p < 0.05$, **$p < 0.01$ vs ischemia/vehicle).

### Increased GSH content suppresses superoxide levels after ischemia

The above findings do not exclude the alternative possibility, that elevated superoxide levels result from decreased neuronal GSH content. We evaluated this possibility by treating mice with NAC immediately after reperfusion. NAC serves as a source of cysteine, the rate-limiting step for *de novo* GSH synthesis (Aoyama et al., 2008; Samuni et al., 2013). Mice treated with NAC after ischemia had normal neuronal GSH levels and less Eth formation than vehicle-treated mice (Fig. 5), suggesting that the normalized GSH content prevents elevated superoxide levels during reperfusion. This suggestion was supported by measures of 4-hydroxynonenal and nitrotyrosine, which are oxidative modifications of lipids and proteins that are produced in part by superoxide (Reiter et al., 2000; Awasthi et al., 2004). Both 4-hydroxynonenal and nitrotyrosine were formed in CA1 neurons after ischemia-reperfusion (Fig. 6*A*), and their formation was attenuated in mice treated with NAC (Fig. 6*A*,*B*). NAC administration also reduced CA1 neuronal death, as measured by Fluoro-Jade B in brains harvested 3 d after ischemia-reperfusion (Fig. 6*C*,*D*). Together, these findings results indicate that neuronal GSH levels contribute to the ability of neurons to scavenge superoxide and suppress oxidative damage after ischemia-reperfusion.

### GSH content is increased in glia at 3 d after ischemia-reperfusion

Although our findings show a fall in neuronal GSH content over the first few hours after ischemia-reperfusion, prior studies using biochemical GSH determinations have identified an increase in bulk tissue GSH content at later time points (days) after ischemia-reperfusion (Uemura et al., 1991; Ningaraj and Rao, 1998; Namba et al., 2001). To determine whether the later increase in GSH content might be in non-neuronal cells, we performed double-labeling for GSH-NEM with astrocyte and

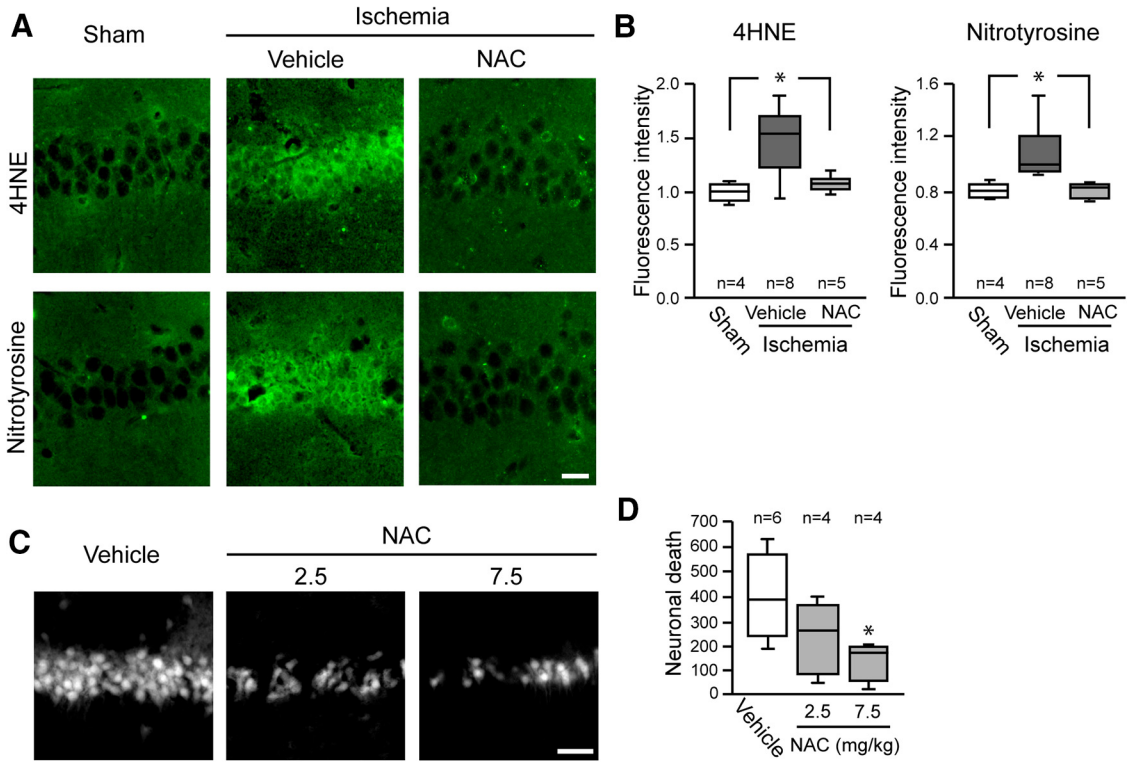


**Figure 6.** *N*-acetyl cysteine administered after ischemia-reperfusion attenuates oxidative stress and cell death. ***A***, Hippocampal sections immunostained for 4HNE and NT. Mice received 7.5 mg/kg NAC or saline vehicle at reperfusion, and tissues were harvested 3 h later. Scale bar, 20 $\mu$m. ***B***, Quantification of 4HNE and NT immunofluorescence. ***C***, Fluoro-Jade B staining identifies degenerating hippocampal CA1 neurons in mouse brain 3 d after ischemia-reperfusion. Scale bar, 50 $\mu$m. ***D***, Quantified cell death (*$p < 0.05$ vs ischemia/vehicle).

microglial markers in brains harvested 3 d after ischemia reperfusion. These studies showed reduced GSH signal in the CA1 pyramidal layer, corresponding to a reduced number of surviving neurons. However, these studies also showed increased GSH content in both astrocytes and microglia in the underling stratum radiatum (Fig. 7). High-power views (Fig. 7*C*,*D*) suggested an increase in GSH concentration in the glial processes, in addition to increased numbers of cells and processes.

## Discussion

These findings demonstrate that ischemia-reperfusion causes both a fall in GSH and an increase in superoxide levels in pyramidal CA1 neurons. Pharmacological or genetic blockade of superoxide production preserved neuronal GSH content, whereas conversely, *N*-acetyl cysteine treatment supported GSH levels and reduced superoxide levels, oxidative stress, and neuronal death. These results indicate that GSH depletion is both a result and a cause of neuronal oxidative stress after ischemia-reperfusion, and that restoration of neuronal GSH levels during reperfusion can be neuroprotective.

It can be difficult to reliably distinguish between GSH and other thiols by histochemical methods. Initial studies of brain tissue using mercury orange as a label found a relatively low GSH signal in neuronal somata (Slivka et al., 1987), but this agent was later found to react with protein sulfhydryls in addition to GSH (Thomas et al., 1995). Studies using monochlorobimane to detect GSH also suggested a relative paucity of GSH in neurons (Bragin et al., 2010). However, the reaction between monochlorobimane and GSH requires glutathione *S*-transferase. The GSH-bimane signal is therefore influenced by cell-type differences in this enzyme, as well as by differing rates of GSH-bimane excretion (Ublacker et al., 1991). In contrast to these histochemical methods, immunostaining with antibodies to GSH showed abundant labeling in neuronal soma and processes (Ong et al., 2000), inline with the present results. Nonenzymatic GSH labeling with fluorescently labeled C5-maleimide also shows strongest signal in neurons (Aoyama et al., 2006; Escartin et al., 2011). The NEM-GSH antibody method used here uses antibodies to *N*-ethylmaleimide-glutathione adducts to further improve specificity for GSH (Miller et al., 2009).

In the present studies, comparisons of GSH-NEM staining with biochemical GSH measures in acute hippocampal slices confirmed that the GSH-NEM method provides a quantitative measure of brain tissue GSH content. The GSH-NEM approach has limitations, however, as with other immunohistochemical methods a linear relationship between neuronal GSH content and the GSH-NEM signal cannot be assumed to hold over the full range of signal detected. Additionally, the inability to discriminate between neuronal and non-neuronal processes in the neuropil restricted our analysis to neuronal cell bodies, and it is possible that these do not uniformly reflect GSH metabolism in the neuronal processes.

When used in studies of ischemia-reperfusion, GSH-NEM staining showed GSH depletion in hippocampal pyramidal neurons over the first few hours of ischemia-reperfusion. This depletion occurs long before neuronal death, as evidenced both by Fluoro-Jade B staining (Fig. 2*C*) and by prior work showing delayed CA1 neuronal death in this transient ischemia model (Barone et al., 1993; Bennett et al., 1996; Lee et al., 2004; Won et al., 2010). Biochemical measurements of GSH in brain tissue homogenates have shown a decrease in bulk tissue GSH content over this same time period (Uemura et al., 1991; Shivakumar et al., 1995), and a subsequent normalization or supranormaliza-

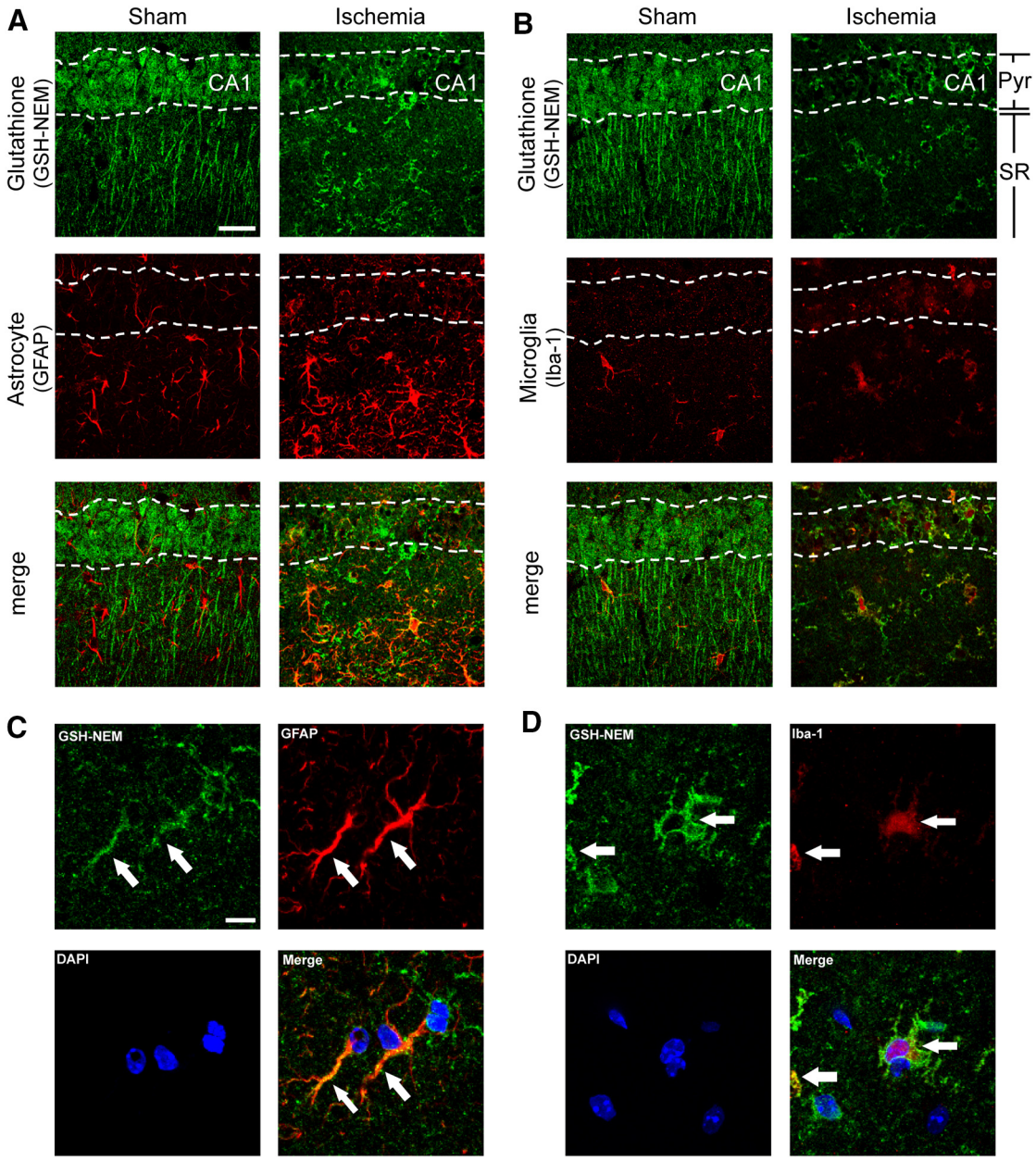


**Figure 7.** GSH content is increased in glia at 3 d after ischemia-reperfusion. Confocal images show fewer pyramidal neurons in the postischemic CA1 region, but increased numbers of astrocytes (***A***) and microglial (***B***) in both the CA1 pyramidal cell layer and underlying stratum radiatum. Colabeling for GSH shows increased signal in astrocytes (GFAP) and microglia (Iba-1) in the postischemic CA1. Pyr, Pyramidal layer; SR, stratum radiatum. Scale bar, 20 $\mu$m. ***C***, ***D***, High-magnification images with glial processes marked with arrows and cell nuclei stained with DAPI (blue). Scale bar, 10 $\mu$m. Images are representative of $n = 4$ sham and ischemic mice.

tion after 72 h (Ningaraj and Rao, 1998; Namba et al., 2001). Our studies using GSH-NEM staining together with cell-type-specific markers indicates that this later recovery of GSH levels is attributable to GSH accumulation in reactive astrocytes and microglia, rather than to a rebound increase in surviving neurons. The mechanism and functional effects of this delayed GSH accumulation are not known, but may be attributable to increased NRF2 signaling in reactive astrocytes (Hamby and Sofroniew, 2010).

Although Eth formation is specific for superoxide under cell-free conditions, the presence of metals and peroxidases in cells allows $H_2O_2$ and other peroxides to oxidize dihydroethidium to Eth species (Fernandes et al., 2007). Elevated Eth signal is generally considered an indicator of increased ROS production, but in the present studies, the high Eth signal observed in neurons with low GSH content more likely reflects impaired superoxide scavenging. Superoxide is scavenged in part by direct reaction with GSH, and superoxide-derived peroxides and protein oxidation products are reduced primarily by enzymatic processes coupled to GSH (Dringen, 2000; Maher, 2006).

The mechanism by which ischemia-reperfusion causes GSH depletion has not been identified, but our results suggest that superoxide production is a major factor. We found that neuronal GSH depletion was attenuated when superoxide production by NADPH oxidase-2 was blocked, and increased in when superoxide production was accelerated by hyperglycemia (Fig. 4*A*). GSH is oxidized to GSSG in the process of scavenging superoxide and superoxide-derived peroxides, and exported from cells when

GSSG formation outstrips its reduction back to GSH (Homolya et al., 2003).

GSH that is lost in the form of exported GSSG must be replaced by *de novo* synthesis from cysteine, glycine, and glutamate, of which cysteine availability is the rate-limiting factor. NAC is membrane-permeable form of cysteine that can be de-acetylated and used for GSH synthesis by neurons (Berman et al., 2011; Samuni et al., 2013). Prior studies have shown that NAC administered before brain ischemia can be neuroprotective (Knuckey et al., 1995; Carroll et al., 1998; Cuzzocrea et al., 2000). Our results additionally show that NAC administered during reperfusion following ischemia can restore or maintain intracellular GSH content in neurons, and thereby limit oxidative neuronal damage and death. It is possible that the effects of NAC are due in part to direct actions of this thiol with superoxide or other ROS; however, this is likely a minor factor because the reaction between NAC and superoxide is slow (Samuni et al., 2013), and because unlike GSH, NAC cannot serve as a substrate for either the reduction of peroxides by glutathione peroxidase or the repair of oxidized proteins by glutaredoxins. Accordingly, prior studies show that the antioxidant effects of NAC during acute oxidative stress are negated if *de novo* GSH synthesis is prevented with buthionine sulfoximine (Wong and Corcoran, 1987; Yang et al., 2003; Aoyama et al., 2006). This control was not feasible in the present ischemia studies because inhibitors of GSH synthesis downregulate NMDA receptor activity and thus also affect superoxide production (Ryu et al., 2003; Brennan et al., 2009).

The observation that both GSH depletion and neuronal demise were attenuated in mice treated with NAC during reperfusion after ischemia also suggests that this approach could have therapeutic potential. NAC is inexpensive and safe, and it is already approved by the US Federal Drug Administration for other indications (Miller and Rumack, 1983). Our findings suggest that administration of NAC to stroke patients during the initial period of reperfusion could improve outcomes, but the "therapeutic window of opportunity" remains to be established.

## References


Andrabi SA, Kang HC, Haince JF, Lee YI, Zhang J, Chi Z, West AB, Koehler RC, Poirier GG, Dawson TM, Dawson VL (2011) Iduna protects the brain from glutamate excitotoxicity and stroke by interfering with poly(ADP-ribose) polymer-induced cell death. Nat Med 17:692–699. CrossRef Medline

Aoyama K, Suh SW, Hamby AM, Liu J, Chan WY, Chen Y, Swanson RA (2006) Neuronal glutathione deficiency and age-dependent neurodegeneration in the EAAC1 deficient mouse. Nat Neurosci 9:119–126. CrossRef Medline

Aoyama K, Watabe M, Nakaki T (2008) Regulation of neuronal glutathione synthesis. J Pharmacol Sci 108:227–238. CrossRef Medline

Awasthi YC, Yang Y, Tiwari NK, Patrick B, Sharma A, Li J, Awasthi S (2004) Regulation of 4-hydroxynonenal-mediated signaling by glutathione S-transferases. Free Radic Biol Med 37:607–619. CrossRef Medline

Baker MA, Cerniglia GJ, Zaman A (1990) Microtiter plate assay for the measurement of glutathione and glutathione disulfide in large numbers of biological samples. Anal Biochem 190:360–365. CrossRef Medline

Barone FC, Knudsen DJ, Nelson AH, Feuerstein GZ, Willette RN (1993) Mouse strain differences in susceptibility to cerebral ischemia are related to cerebral vascular anatomy. J Cereb Blood Flow Metab 13:683–692. CrossRef Medline

Baxter P, Chen Y, Xu Y, Swanson RA (2014) Mitochondrial dysfunction induced by nuclear poly(ADP-ribose) polymerase-1: a treatable cause of cell death in stroke. Transl Stroke Res 5:136–144. CrossRef Medline

Bedard K, Krause KH (2007) The NOX family of ROS-generating NADPH oxidases: physiology and pathophysiology. Physiol Rev 87:245–313. CrossRef Medline

Bennett MV, Pellegrini-Giampietro DE, Gorter JA, Aronica E, Connor JA, Zukin RS (1996) The GluR2 hypothesis: Ca(++)-permeable AMPA receptors in delayed neurodegeneration. Cold Spring Harb Symp Quant Biol 61:373–384. CrossRef Medline

Berman AE, Chan WY, Brennan AM, Reyes RC, Adler BL, Suh SW, Kauppinen TM, Edling Y, Swanson RA (2011) *N*-acetylcysteine prevents loss of dopaminergic neurons in the EAAC1 $^{-/-}$ mouse. Ann Neurol 69:509–520. CrossRef Medline

Bragin DE, Zhou B, Ramamoorthy P, Müller WS, Connor JA, Shi H (2010) Differential changes of glutathione levels in astrocytes and neurons in ischemic brains by two-photon imaging. J Cereb Blood Flow Metab 30:734–738. CrossRef Medline

Brennan AM, Suh SW, Won SJ, Narasimhan P, Kauppinen TM, Lee H, Edling Y, Chan PH, Swanson RA (2009) NADPH oxidase is the primary source of superoxide induced by NMDA receptor activation. Nat Neurosci 12:857–863. CrossRef Medline

Brennan-Minnella AM, Won SJ, Swanson RA (2015) NADPH oxidase-2: linking glucose, acidosis, and excitotoxicity in stroke. Antioxid Redox Signal 22:161–174. CrossRef Medline

Carroll JE, Howard EF, Hess DC, Wakade CG, Chen Q, Cheng C (1998) Nuclear factor-kappa B activation during cerebral reperfusion: effect of attenuation with *N*-acetylcysteine treatment. Brain Res Mol Brain Res 56:186–191. CrossRef Medline

Chan PH (2001) Reactive oxygen radicals in signaling and damage in the ischemic brain. J Cereb Blood Flow Metab 21:2–14. CrossRef Medline

Cuzzocrea S, Mazzon E, Costantino G, Serraino I, Dugo L, Calabrò G, Cucinotta G, De Sarro A, Caputi AP (2000) Beneficial effects of *N*-acetylcysteine on ischaemic brain injury. Br J Pharmacol 130:1219–1226. CrossRef Medline

Dringen R (2000) Metabolism and functions of glutathione in brain. Prog Neurobiol 62:649–671. CrossRef Medline

Dringen R, Pfeiffer B, Hamprecht B (1999) Synthesis of the antioxidant glutathione in neurons: supply by astrocytes of CysGly as precursor for neuronal glutathione. J Neurosci 19:562–569. Medline

Escartin C, Won SJ, Malgorn C, Auregan G, Berman AE, Chen PC, Déglon N, Johnson JA, Suh SW, Swanson RA (2011) Nuclear factor erythroid 2-related factor 2 facilitates neuronal glutathione synthesis by upregulating neuronal excitatory amino acid transporter 3 expression. J Neurosci 31:7392–7401. CrossRef Medline

Fernandes DC, Wosniak J Jr, Pescatore LA, Bertoline MA, Liberman M, Laurindo FR, Santos CX (2007) Analysis of DHE-derived oxidation products by HPLC in the assessment of superoxide production and NADPH oxidase activity in vascular systems. Am J Physiol Cell Physiol 292:C413–C422. CrossRef Medline

Griffith OW, Meister A (1979) Potent and specific inhibition of glutathione synthesis by buthionine sulfoximine (*S-n*-butyl homocysteine sulfoximine). J Biol Chem 254:7558–7560. Medline

Hamby ME, Sofroniew MV (2010) Reactive astrocytes as therapeutic targets for CNS disorders. Neurotherapeutics 7:494–506. CrossRef Medline

Homolya L, Váradi A, Sarkadi B (2003) Multidrug resistance-associated proteins: export pumps for conjugates with glutathione, glucuronate or sulfate. BioFactors 17:103–114. CrossRef Medline

Jones DP (2008) Radical-free biology of oxidative stress. Am J Physiol Cell Physiol 295:C849–C868. CrossRef Medline

Kamada H, Yu F, Nito C, Chan PH (2007) Influence of hyperglycemia on oxidative stress and matrix metalloproteinase-9 activation after focal cerebral ischemia/reperfusion in rats: relation to blood–brain barrier dysfunction. Stroke 38:1044–1049. CrossRef Medline

Knuckey NW, Palm D, Primiano M, Epstein MH, Johanson CE (1995) *N*-acetylcysteine enhances hippocampal neuronal survival after transient forebrain ischemia in rats. Stroke 26:305–310; discussion 311. CrossRef Medline

Lee SR, Tsuji K, Lo EH (2004) Role of matrix metalloproteinases in delayed neuronal damage after transient global cerebral ischemia. J Neurosci 24:671–678. CrossRef Medline

Maher P (2006) Redox control of neural function: background, mechanisms, and significance. Antioxid Redox Signal 8:1941–1970. CrossRef Medline

Makar TK, Nedergaard M, Preuss A, Gelbard AS, Perumal AS, Cooper AJ (1994) Vitamin E, ascorbate, glutathione, glutathione disulfide, and enzymes of glutathione metabolism in cultures of chick astrocytes and neurons: evidence that astrocytes play an important role in antioxidative processes in the brain. J Neurochem 62:45–53. CrossRef Medline

Miller LF, Rumack BH (1983) Clinical safety of high oral doses of acetylcysteine. Semin Oncol 10:76–85. Medline

Miller VM, Lawrence DA, Mondal TK, Seegal RF (2009) Reduced glutathione is highly expressed in white matter and neurons in the unperturbed mouse brain: implications for oxidative stress associated with neurodegeneration. Brain Res 1276:22–30. CrossRef Medline

Moroni F (2008) Poly(ADP-ribose)polymerase 1 (PARP-1) and postischemic brain damage. Curr Opin Pharmacol 8:96–103. CrossRef Medline

Murakami K, Kondo T, Kawase M, Li Y, Sato S, Chen SF, Chan PH (1998) Mitochondrial susceptibility to oxidative stress exacerbates cerebral infarction that follows permanent focal cerebral ischemia in mutant mice with manganese superoxide dismutase deficiency. J Neurosci 18:205–213. Medline

Muranyi M, Li PA (2006) Hyperglycemia increases superoxide production in the CA1 pyramidal neurons after global cerebral ischemia. Neurosci Lett 393:119–121. CrossRef Medline

Muyderman H, Wadey AL, Nilsson M, Sims NR (2007) Mitochondrial glutathione protects against cell death induced by oxidative and nitrative stress in astrocytes. J Neurochem 102:1369–1382. CrossRef Medline

Namba K, Takeda Y, Sunami K, Hirakawa M (2001) Temporal profiles of the levels of endogenous antioxidants after four-vessel occlusion in rats. J Neurosurg Anesthesiol 13:131–137. CrossRef Medline

Ningaraj NS, Rao MK (1998) Disulfiram augments oxidative stress in rat brain following bilateral carotid artery occlusion. J Biomed Sci 5:226–230. CrossRef Medline

Ong WY, Hu CY, Hjelle OP, Ottersen OP, Halliwell B (2000) Changes in glutathione in the hippocampus of rats injected with kainate: depletion in neurons and upregulation in glia. Exp Brain Res 132:510–516. CrossRef Medline

Ouyang YB, Voloboueva LA, Xu LJ, Giffard RG (2007) Selective dysfunction of hippocampal CA1 astrocytes contributes to delayed neuronal damage after transient forebrain ischemia. J Neurosci 27:4253–4260. CrossRef Medline

Peshavariya HM, Dusting GJ, Selemidis S (2007) Analysis of dihydroethidium fluorescence for the detection of intracellular and extracellular superoxide produced by NADPH oxidase. Free Radic Res 41:699–712. CrossRef Medline

Reiter CD, Teng RJ, Beckman JS (2000) Superoxide reacts with nitric oxide to nitrate tyrosine at physiological pH via peroxynitrite. J Biol Chem 275:32460–32466. CrossRef Medline

Ryu BR, Lee YA, Won SJ, Noh JH, Chang SY, Chung JM, Choi JS, Joo CK, Yoon SH, Gwag BJ (2003) The novel neuroprotective action of sulfasalazine through blockade of NMDA receptors. J Pharmacol Exp Ther 305:48–56. CrossRef Medline

Samuni Y, Goldstein S, Dean OM, Berk M (2013) The chemistry and biological activities of *N*-acetylcysteine. Biochim Biophys Acta 1830:4117–4129. CrossRef Medline

Schmued LC, Hopkins KJ (2000) Fluoro-jade B: a high affinity fluorescent marker for the localization of neuronal degeneration. Brain Res 874:123–130. CrossRef Medline

Shi SR, Key ME, Kalra KL (1991) Antigen retrieval in formalin-fixed, paraffin-embedded tissues: an enhancement method for immunohistochemical staining based on microwave oven heating of tissue sections. J Histochem Cytochem 39:741–748. CrossRef Medline

Shih AY, Johnson DA, Wong G, Kraft AD, Jiang L, Erb H, Johnson JA, Murphy TH (2003) Coordinate regulation of glutathione biosynthesis and release by Nrf2-expressing glia potently protects neurons from oxidative stress. J Neurosci 23:3394–3406. Medline

Shivakumar BR, Kolluri SV, Ravindranath V (1995) Glutathione and protein thiol homeostasis in brain during reperfusion after cerebral ischemia. J Pharmacol Exp Ther 274:1167–1173. Medline

Slivka A, Mytilineou C, Cohen G (1987) Histochemical evaluation of glutathione in brain. Brain Res 409:275–284. CrossRef Medline

Stolk J, Hiltermann TJ, Dijkman JH, Verhoeven AJ (1994) Characteristics of the inhibition of NADPH oxidase activation in neutrophils by apocynin, a methoxy-substituted catechol. Am J Respir Cell Mol Biol 11:95–102. CrossRef Medline

Suh SW, Shin BS, Ma H, Van Hoecke M, Brennan AM, Yenari MA, Swanson RA (2008) Glucose and NADPH oxidase drive neuronal superoxide formation in stroke. Ann Neurol 64:654–663. CrossRef Medline

Thomas M, Nicklee T, Hedley DW (1995) Differential effects of depleting agents on cytoplasmic and nuclear non-protein sulphydryls: a fluorescence image cytometry study. Br J Cancer 72:45–50. CrossRef Medline

Ublacker GA, Johnson JA, Siegel FL, Mulcahy RT (1991) Influence of glutathione S-transferases on cellular glutathione determination by flow cytometry using monochlorobimane. Cancer Res 51:1783–1788. Medline

Uemura Y, Miller JM, Matson WR, Beal MF (1991) Neurochemical analysis of focal ischemia in rats. Stroke 22:1548–1553. CrossRef Medline

Vesce S, Jekabsons MB, Johnson-Cadwell LI, Nicholls DG (2005) Acute glutathione depletion restricts mitochondrial ATP export in cerebellar granule neurons. J Biol Chem 280:38720–38728. CrossRef Medline

Won SJ, Yoo BH, Brennan AM, Shin BS, Kauppinen TM, Berman AE, Swanson RA, Suh SW (2010) EAAC1 gene deletion alters zinc homeostasis and exacerbates neuronal injury after transient cerebral ischemia. J Neurosci 30:15409–15418. CrossRef Medline

Won SJ, Tang XN, Suh SW, Yenari MA, Swanson RA (2011) Hyperglycemia promotes tissue plasminogen activator-induced hemorrhage by increasing superoxide production. Ann Neurol 70:583–590. CrossRef Medline

Wong BK, Corcoran GB (1987) Effects of esterase inhibitors and buthionine sulfoximine on the prevention of acetaminophen hepatotoxicity by *N*-acetylcysteine. Res Commun Chem Pathol Pharmacol 55:397–408. Medline

Yang B, Keshelava N, Anderson CP, Reynolds CP (2003) Antagonism of buthionine sulfoximine cytotoxicity for human neuroblastoma cell lines by hypoxia is reversed by the bioreductive agent tirapazamine. Cancer Res 63:1520–1526. Medline

Zhang H, Squadrito GL, Uppu RM, Lemercier JN, Cueto R, Pryor WA (1997) Inhibition of peroxynitrite-mediated oxidation of glutathione by carbon dioxide. Arch Biochem Biophys 339:183–189. CrossRef Medline

**Manuscrito Anexo 2**

# Neuronal Glutathione Content and Antioxidant Capacity can be Normalized *In Situ* by N-acetyl Cysteine Concentrations Attained in Human Cerebrospinal Fluid

Reno C. Reyes, Giordano Fabricio Cittolin-Santos, Ji-Eun Kim, Seok Joon Won, Angela M. Brennan-Minnella, Maya Katz, Graham A. Glass, Raymond A. Swanson

*Reno C. Reyes and Giordano Fabricio Cittolin-Santos contribuiram igualmente para esse trabalho

**Manuscrito publicado no periódico NEUROTHERAPEUTICS**

**Submetido: Setembro de 2015**

**Aceito: 16 de Novembro de 2015**

Neurotherapeutics (2016) 13:217–225
DOI 10.1007/s13311-015-0404-4

ORIGINAL ARTICLE

# Neuronal Glutathione Content and Antioxidant Capacity can be Normalized *In Situ* by *N*-acetyl Cysteine Concentrations Attained in Human Cerebrospinal Fluid

**Reno C. Reyes[1,2] · Giordano Fabricio Cittolin-Santos[1,2,3,4] · Ji-Eun Kim[1,2] · Seok Joon Won[1,2] · Angela M. Brennan-Minnella[1,2] · Maya Katz[1,2] · Graham A. Glass[1,2] · Raymond A. Swanson[1,2]**

Published online: 16 November 2015


**Abstract** *N*-acetyl cysteine (NAC) supports the synthesis of glutathione (GSH), an essential substrate for fast, enzymatically catalyzed oxidant scavenging and protein repair processes. NAC is entering clinical trials for adrenoleukodystrophy, Parkinson's disease, schizophrenia, and other disorders in which oxidative stress may contribute to disease progression. However, these trials are hampered by uncertainty about the dose of NAC required to achieve biological effects in human brain. Here we describe an approach to this issue in which mice are used to establish the levels of NAC in cerebrospinal fluid (CSF) required to affect brain neurons. NAC dosing in humans can then be calibrated to achieve these NAC levels in human CSF. The mice were treated with NAC over a range of doses, followed by assessments of neuronal GSH levels and neuronal antioxidant capacity in *ex vivo* brain slices. Neuronal GSH levels and antioxidant capacity were augmented at NAC doses that produced peak CSF NAC concentrations of ≥50 nM. Oral NAC administration to humans produced CSF concentrations of up to 10 μM, thus demonstrating that oral NAC administration can surpass the levels required for biological activity in brain. Variations of this approach may similarly facilitate and rationalize drug dosing for other agents targeting central nervous system disorders.

**Key Words** Cysteine · Parkinson's disease · oxidative stress · human · cerebrospinal fluid · target engagement

## Introduction

Oxidative stress contributes the pathogenesis of Parkinson's disease (PD) and other neurodegenerative disorders. The neuronal populations that are most affected in PD accumulate oxidized lipids, proteins, and DNA [1]. These markers of oxidative damage are accompanied by reduced levels of the major cellular antioxidant, glutathione (GSH), which is used by cells to both scavenge reactive oxygen species (ROS) and repair oxidized protein residues [2]. A causal role for oxidative stress and GSH depletion in PD is supported by both clinical and animal studies [1, 3–5]. In particular, factors that cause global impairments in neuronal GSH metabolism cause cytotoxicity preferentially in the neuronal populations most affected in PD [6–8].

Clinical trials have evaluated several agents targeting oxidative damage in PD, including coenzyme Q10, α-tocopherol, selegiline, and rasagaline; but disappointingly none of these trials have demonstrated an unequivocal slowing of disease progression [9, 10]. These negative results are difficult to interpret, however, because it is unknown whether the agents succeeded in having a significant effect on neuronal oxidative stress at the doses employed. This critical knowledge gap

Reno C. Reyes and Giordano Fabricio Cittolin-Santos contributed equally to this work.

**Electronic supplementary material** The online version of this article (doi:10.1007/s13311-015-0404-4) contains supplementary material, which is available to authorized users.

✉ Raymond A. Swanson
raymond.swanson@ucsf.edu

[1] Neurology Service, San Francisco Veterans Affairs Medical Center, 4150 Clement St., San Francisco, CA 94121, USA

[2] The Department of Neurology, University of California, San Francisco Medical Center, San Francisco, CA, USA

[3] Programa de Pós Graduação em Ciências Biológicas: Bioquímica, UFRGS, Porto Alegre, Brazil

[4] Science Without Borders, CNPq, Brasilia, Brazil

stems both from difficulties in measuring antioxidant effects *in vivo* and uncertainties about drug penetration across the human blood–brain barrier.

*N*-Acetyl cysteine (NAC) is a synthetic compound that enters cells by a presumably passive mechanism, where it is cleaved to generate intracellular cysteine [11]. Cysteine availability is normally the rate-liming factor in GSH synthesis [12], and consequently NAC can be used to promote GSH synthesis under conditions in which GSH consumption exceeds supply. NAC is currently approved by the US Food and Drug Administration for the treatment of acetaminophen toxicity and contrast nephropathy, and it has been identified as promising agent for treatment of PD [3, 13–15]. There is also a growing interest in the use of NAC to treat other neurological and psychiatric disorders in which oxidative stress has been implicated, including adrenoleukodystrophy, Alzheimer disease, schizophrenia, and compulsive disorders [15, 16]. However, there has been uncertainty as to the extent that NAC can cross the human blood–brain barrier [17], with resulting uncertainty about doses required for a rational clinical trial.

Here we present an approach for addressing these issues. The approach uses *ex vivo* assessments of neuronal GSH levels and antioxidant capacity in mice to identify the cerebrospinal fluid (CSF) concentrations of NAC required to have biological activity in neurons. Dosing in humans can then be tailored to reach or exceed these levels in human CSF.

## Materials and Methods

Reagents were obtained from Sigma-Aldrich (St. Louis, MO, USA) except where otherwise noted. Animal studies were approved by the San Francisco Veterans Affairs Medical Center animal studies committee. Sprague–Dawley rats, aged 3–6 months, were obtained from Simonsen Laboratories (Gilroy, CA, USA). Mice were either wild-type 3–6-month-old C57BL/6 strain (Jackson Laboratories, West Grove, PA, USA) or SLC1A1$^{-/-}$ mice that had been back-crossed to the C57BL/6 strain. The SLCA1$^{-/-}$ colony was maintained as homozygous with breeders back-crossed with C57BL/6 mice every 6 generations, to avoid genetic drift [6, 18]. SLC1A1 is more commonly known as excitatory amino acid transporter 3 or excitatory amino acid carrier 1 (EAAC1), and will be termed EAAC1 throughout this report.

### Drug Administration

L-Buthionine-(S,R)-sulfoximine (BSO) was administered 5 h prior to brain harvest at a dose of 1.3 g/kg body weight by intraperitoneal (i.p.) injection. NAC was administered either i.p. or by oral gavage 5 h prior to brain harvest, at doses ranging from 0.1 to 75.0 mg/kg. The drugs were dissolved in 0.9 % sodium chloride solution and administered in approximately 3.0-ml volumes in rats or 0.3-ml volumes in mice. Vehicle-treated animals received equal volumes of 0.9 % sodium chloride only.

### Mouse Brain Harvest

Mice were decapitated under isoflurane/nitrous oxide anesthesia and brains were quickly removed. The rostral third of each brain was immediately frozen in dry ice and stored at –70 °C for biochemical measurement of brain GSH content; the caudal third of each brain was fixed in phosphate buffered 4 % formaldehyde for GSH immunohistochemistry; and the middle third of each brain was sectioned in a vibratome for *ex vivo* assessment of functional antioxidant capacity (Fig. 1). In some studies slices were also taken through the upper midbrain to include neurons of the substantia nigra.

### *Ex Vivo* Brain Slice Studies

The middle third of each brain was sectioned using a vibratome while maintained at approximately 0 °C by immersion in a solution containing 250 mM sucrose, 11 mM glucose, 2.5 mM KCl, 1.0 mM $NaH_2PO_4$, 2.0 mM $MgSO_4$, and 2.0 mM $CaCl_2$ [19]. Three or 4 slices of 275-μm thickness were obtained. Each slice

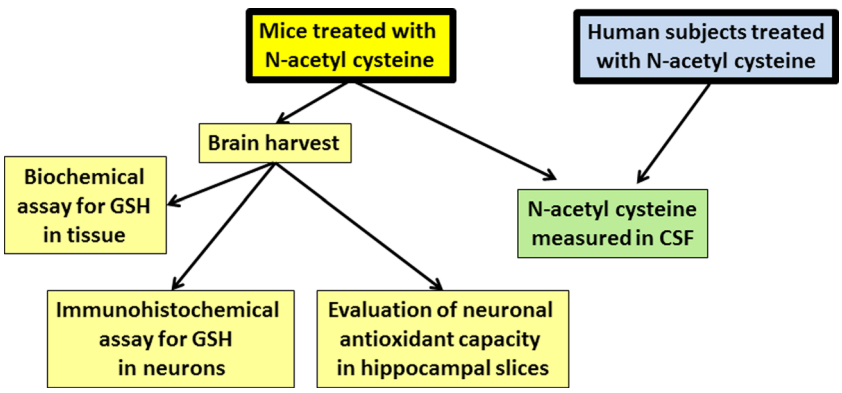


**Fig. 1** Outline of experimental procedures. GSH = glutathione; CSF = cerebrospinal fluid

was divided in the midline and one half was placed in artificial CSF (ACSF) and the other half placed in ACSF containing 0–2.0 mM 3-morpholinosydonimide (SIN-1; Sigma-Aldrich, St. Louis, MO, USA), which forms superoxide, nitric oxide, and peroxynitrite in oxygenated solutions [20]. The ACSF contained 126 mM NaCl, 2.5 mM KCl, 1.2 mM $MgCl_2$, 2.4 mM $CaCl_2$, 1.2 mM $NaH_2PO_4$, 21.4 mM $NaHCO_3$, and 25 mM glucose, and was continuously bubbled with 95 % $O_2$/5 % $CO_2$. The sections were incubated in these solutions at room temperature (22 °C) for 30 min, then fixed overnight in phosphate buffered 4 % formaldehyde.

### Immunostaining

The fixed, 275-μm-thick slices were incubated with antibodies to either nitrotyrosine (06-284; Millipore, Darmstadt, Germany) or 4-hydroxynonenal (HNE 11-S; Alpha Diagnostics, San Antonio, TX, USA), as described [21]. In each case the sections were also incubated with antibody to microtubule-associated protein 2 (MAB3418; Millipore) for identification of neuronal cell bodies. Using a confocal microscope, photomicrographs were taken of 4 randomly selected regions of the pyramidal cell layer in each hippocampal section. The images were taken at a tissue depth of 20 μm and with an optical thickness of 1 μm. Image acquisition parameters were the same in each experiment and set so that signal saturation did not occur. Control sections in which primary or secondary antibodies were omitted showed no signal under these acquisition conditions. The fluorescence signal intensity was measured in neuronal soma identified by the microtubule-associated protein 2 signal. All measurements were normalized to the mean values obtained in $EAAC1^{-/-}$ sections that had been incubated with SIN-1, immunostained, and photographed in parallel.

Immunostaining for GSH was performed on 40-μm cryostat sections prepared from formaldehyde-fixed brain tissue blocks. The sections were treated with 10 mM *N*-ethylmaleimide (NEM) for 4 h at 4 °C prior to incubation with antibody to GSH–NEM (clone 8.1GSH; Millipore), as described previously [21, 22]. Antibody binding was visualized using Alexa Fluor 488-conjugated goat antimouse IgG. Quantification of fluorescent labeling was performed in 4 evenly spaced sections collected through the hippocampus of each mouse and photographed under uniform conditions. Fluorescence intensity was measured in the neuronal soma of hippocampal of the CA1 pyramidal layer bilaterally in each section, and the values obtained in the 4 sections were averaged for each brain. All measurements were normalized to the mean values obtained in $EAAC1^{-/-}$ brains that were immunostained and photographed in parallel.

### GSH Biochemical Assay

Brain tissue was sonicated with 5 % sulfosalicylic acid (200 mg/ml) and centrifuged at 10,000 × *g* for 10 min at 4 °C. The supernatant was mixed with 1 mM dithiobis-2-nitrobenzoic acid and 1 mM ethylenediaminetetraacetic acid in 100 mM sodium phosphate buffer (pH 7.5), and 1 mM nicotinamide adenine dinucleotide phosphate and 200 U/ml GSH reductase were added [23]. Optical absorbance of samples and standards was measured at 405 nm and subtracted by values measured in the absence of GSH reductase.

### Mouse and Rat CSF Collection

Animals were anesthetized with isoflurane/nitrous oxide and placed in a stereotaxic frame with the neck flexed forward. The skin and muscles were retracted to expose the cisterna magna. For rats, 100–150 μl CSF was removed from the cisterna magna by syringe puncture. For mice, the dura of the cisterna magna was carefully punctured with a capillary tube to draw up 6–7 μl of fluid per mouse. The animals were euthanized while still under anesthesia.

### Human CSF Collection

These studies were approved by the institutional review board at the University of California, San Francisco, and the San Francisco Veterans Affairs Center. As detailed elsewhere [24], patients with PD were enrolled in the study between January 2012 and December 2013. Study inclusion criteria included age >40 years, a diagnosis of PD within 10 years, and adherence to a stable dopaminergic medication regimen for at least 2 weeks. Exclusion criteria included significant cognitive impairment, inability to sign informed consent, increased bleeding risk, or mass lesion on brain imaging. A Food and Drug Administration-approved solution form of NAC was obtained from McKesson (San Francisco, CA, USA). The capsule form was obtained from Professional Compounding Centers of America (Houston, TX, USA), a United States Pharmocopeia-certified pharmaceutical distributor, and was compounded by the University of California San Francisco Medical Center pharmacy. Patients took 4 oral doses of NAC, administered every 12 h over 48 h. Four dosing strategies were compared: 1) NAC solution at 7 mg/kg; 2) NAC capsules at 35 mg/kg; 2) NAC solution at 70 mg/kg; and 4) NAC capsules at 70 mg/kg. CSF was obtained by lumbar puncture in each participant prior to the first dose, and again 90 min after the fourth dose.

### NAC Measurements

Rat, mouse, or human CSF was immediately aliquoted into samples for separate analyses of total NAC and reduced NAC.

Samples for total NAC determinations were treated for 30 min with 2 mM Tris (2-carboxyethyl)phosphine hydrochloride to convert NAC disulfides to reduced NAC. All samples were then derivitized with 100 μM *N*-(9-acridinyl)maleimide, stabilized with 40 mM formic acid, and stored at –80 °C. Standards of NAC were prepared in water and treated exactly as the samples. A separate set of internal standards was prepared by spiking NAC into CSF collected from untreated humans and mice, to exclude the possibility that factors present in CSF might affect the NAC quantification. Samples and standards were analyzed in parallel by liquid chromatography–tandem mass spectrometry (Integrated Analytical Solutions, Berkeley, CA, USA) as previously described [24].

### Data Analysis

All data quantification was performed by individuals who were blinded to experimental conditions, and the mouse GSH determinations and antioxidant study results were confirmed by independent observers in 2 different laboratories. NAC measurements are means±SEM. All other data are presented as medians±interquartile range, with the "*n*" denoting the number of animals or human subjects in each experimental group. Group values were compared with the nonparametric Kruskal–Wallis test followed by Dunnett's test for comparison of multiple groups to a single control group.

## Results

We first determined the dose of NAC required to influence neuronal GSH synthesis and antioxidant capacity in mice. Hippocampal sections, in which GSH was quantified by the GSH–NEM immunohistochemical method [21, 22], showed a strong GSH signal in the soma and processes of pyramidal neurons, with less of a signal in the adjacent neuropil and glia (Fig. 2A). NAC administered to normal mice did not produce a detectable increase in neuronal GSH (Fig. 2B). This result is not unexpected as GSH synthesis is limited by product inhibition at normal intracellular GSH concentrations [11, 25]. For this reason we turned to the EAAC1$^{-/-}$ mouse, which has a neuron-specific reduction in cysteine and GSH levels [26]. Immunostaining for GSH confirmed reduced levels in EAAC1$^{-/-}$ neurons, and NAC administered 5 h prior to brain harvest raised these levels (Fig. 2B), as previously described [6]. Evaluation of NAC over a range of doses showed that doses of 7.5 mg/kg were sufficient to raise GHS levels in EAAC1$^{-/-}$ neurons to values comparable with those of wild-type neurons. There was no large difference in results obtained by oral or i.p. drug administration. The effect of NAC delivered by either route was negated in mice that had been co-treated with BSO, which inhibits the enzymatic step at which cysteine is incorporated into GSH [25]. Biochemical

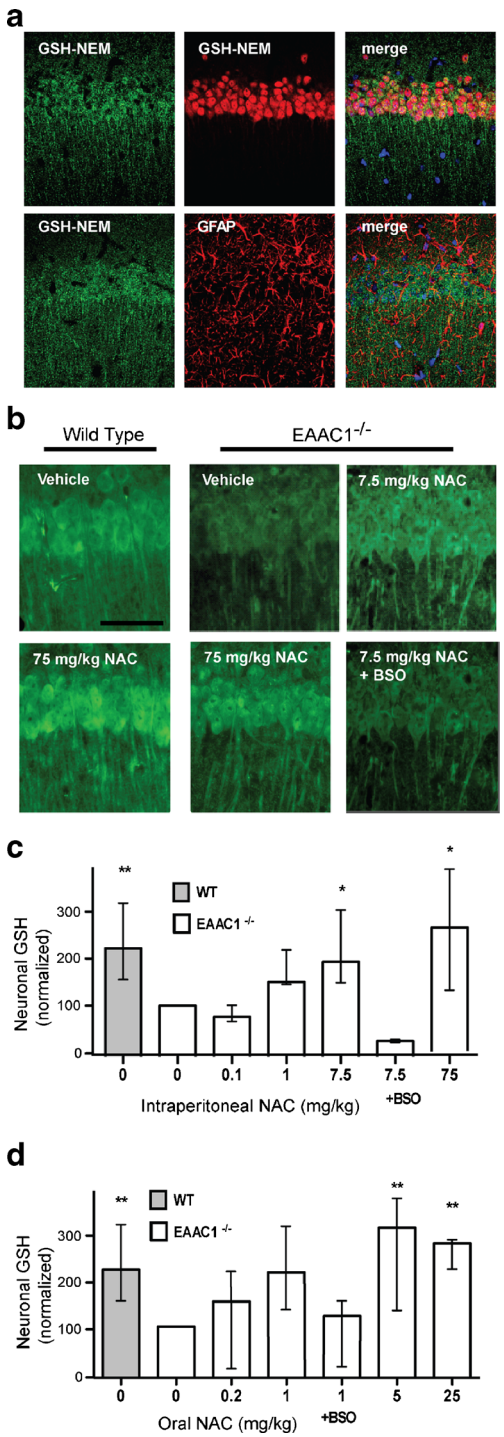


**Fig. 2** *N*-Acetyl cysteine (NAC) raises glutathione content in EAAC1$^{-/-}$ neurons. (**A**) Immuonstaining for glutathione–*N*-ethylmaleimide (GSH–NEM) adducts in hippocampal sections treated with NEM. Co-labeling with the neuronal nuclear marker NeuN and the astrocyte marker glial fibrillary acidic protein (GFAP) show the signal to be primarily localized to neurons. (**B**) Neuronal GSH in mice treated with NAC 5 h prior to brain harvest. The increase induced by 7.5 mg/kg NAC was blocked by co-treatment with buthionine sulfoximine (BSO). (**C**, **D**) Quantified measures neuronal GSH content after intraperitoneal and oral treatment with NAC. Results in each of 7 experiments were normalized to values obtained in untreated (0 NAC) EAAC1$^{-/-}$ mice. $n$=3–5 mice in each condition; *$p$<0.05; **$p$<0.01 *vs* EAAC1$^{-/-}$, 0 NAC. WT = wild-type

determinations of GSH showed no significant reduction in overall brain GSH content in mice treated with BSO alone for the 5-h interval (not shown), consistent with the slow rate of *de novo* GSH synthesis in normal brain [27].

We next established a method for evaluating the functional antioxidant capacity of mouse neurons *in situ*. In this method, acutely prepared brain slices are incubated in artificial CSF containing the peroxynitrite-generating compound SIN-1 and subsequently analyzed for the formation of 3-nitrotyrosine. EAAC1$^{-/-}$ slices incubated with SIN-1 exhibited nitrotyrosine formation in neurons, and this was attenuated in slices from mice that had been treated with NAC prior to brain harvest (Fig. 3A, B). This effect of NAC was also negated by co-treatment with BSO, indicating that NAC acts primarily by supporting GSH production rather than as a free radical scavenger per se. Measures of the lipid peroxidation product 4-hydroxynonenal as a second, independent marker of oxidative stress showed the same pattern: the neuronal 4-hydroxynonenal signal induced by SIN-1 was attenuated in treated with NAC, and the effect of NAC was negated by BSO (Fig. 3A, C). Nitrotyrosine formation also could be induced in wild-type hippocampal slices when incubated with higher SIN-1 concentrations, confirming this effect was not unique to EAAC1$^{-/-}$ cells (Fig. 4A). Likewise, neurons in cerebral cortex and likewise showed nitrotyrosine formation after incubation with SIN-1 (Fig. 4B), but for technical reasons this was easier to quantify in the hippocampal pyramidal layer.

Using this approach, we then evaluated neuronal antioxidant capacity in mice that had been treated with NAC over a range of doses. Results showed that dosing with as little as 1 mg/kg NAC i.p. was able to reduce significantly SIN-1-induced nitrotyrosine formation in EAAC1$^{-/-}$ neurons

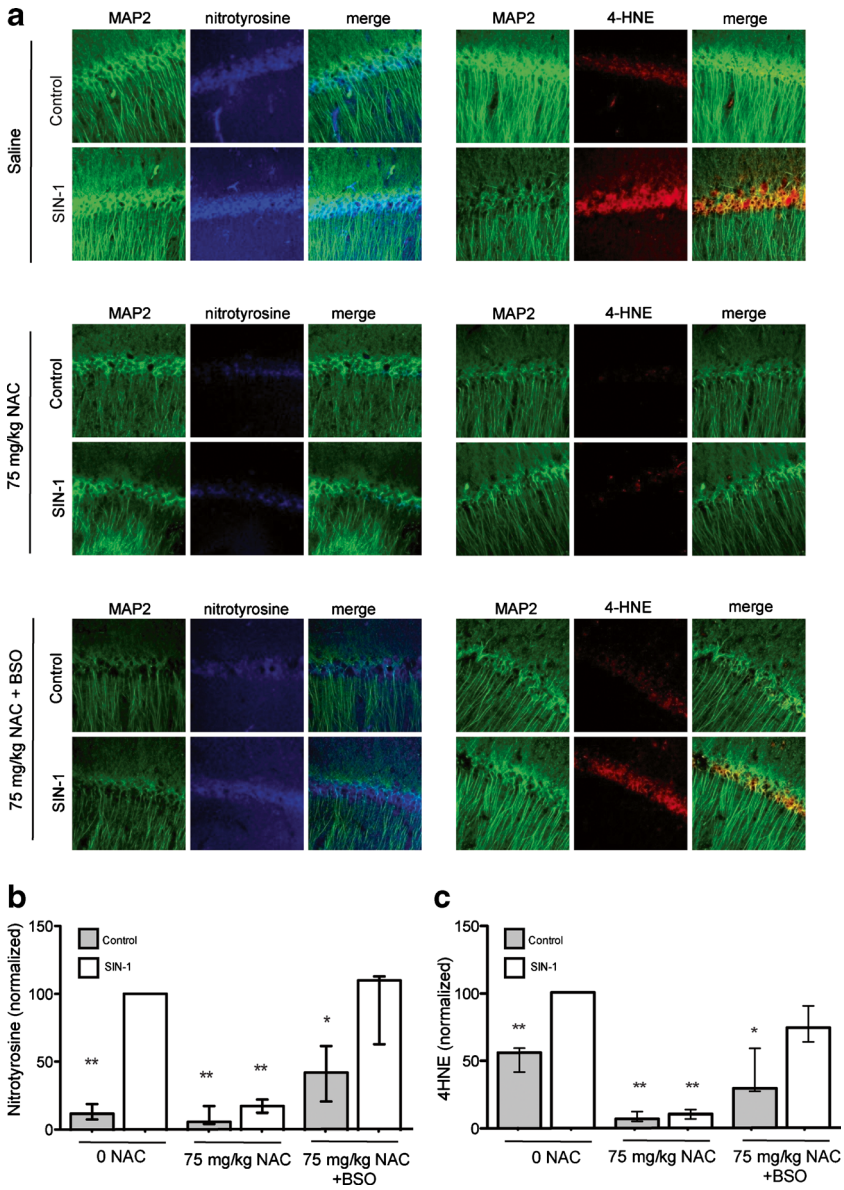


**Fig. 3** *N*-Acetyl cysteine (NAC) administered to mice restores antioxidant capacity in glutathione (GSH)-deficient neurons. (A) EAAC1$^{-/-}$ hippocampal neurons formed nitrotyrosine (blue) and 4-hydroxynonenal (4-HNE; red) during exposure to 3-morpholinosydonimide (SIN-1). Neuronal cell bodies and processes are labeled with microtubule-associated protein 2 (MAP2; green). Nitrotyrosine and 4-HNE formation were attenuated in neurons of mice treated with NAC, and the effect of NAC was blocked in mice co-treated with buthionine sulfoximine (BSO). (**B**, **C**) Quantified data, pooled from 6 experiments. Results in each experiment were normalized to values measured in EAAC1$^{-/-}$, 0 NAC mice. $n$=4 mice in each condition; $^{**}p<0.01$ *vs* EAAC1$^{-/-}$, 0 NAC

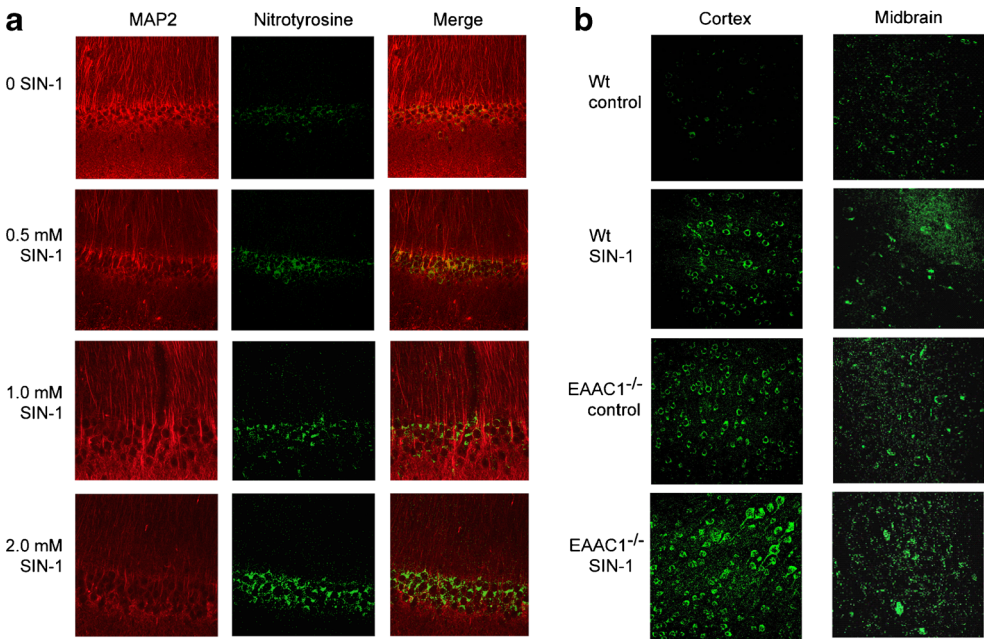


**Fig. 4** 3-Morpholinosydonimide (SIN-1)-induced nitrotyrosine formation. (**A**) Effects of increasing SIN-1 concentrations on nitrotyrosine formation in wild-type (Wt) hippocampal neurons. (**B**) SIN-1 (1 mM) also induced nitrotyrosine formation in cortical and midbrain neurons. Images are representative of sections from at least 2 mice in each condition. MAP2 = microtubule-associated protein 2

(Fig. 5A). NAC administered by oral gavage showed comparable potency (Fig. 5B).

We next measured the concentrations of NAC present in mouse CSF under these conditions. We chose a dose, 25 mg/kg, that was substantially higher than required for maximal effects on both neuronal GSH repletion and antioxidant capacity, in order to ensure that the corresponding CSF NAC measurements would identify the concentrations at which NAC has biological activity in neurons. We measured both native (reduced) NAC and total NAC (NAC present in both its reduced form and in reversible disulfide linkages with other thiols), and found that the vast majority of NAC was present in its reduced form at all doses and time points examined (Fig. 6). The peak (20 min) NAC concentration after 25 mg/kg i.p. dosing was 126±15 nM. Oral dosing produced a lower peak level but longer duration of elevation. Experiments performed using rats gave a very similar pattern but with somewhat higher CSF concentrations achieved with a lower (15 mg/kg) NAC dose (Fig. 6D).

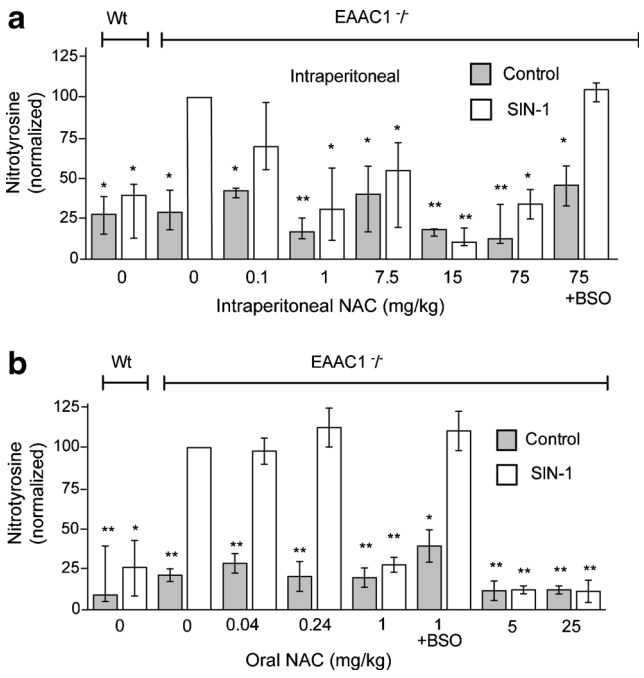


**Fig. 5** Dose–response effects of *N*-acetyl cysteine (NAC) on neuronal antioxidant capacity. Mice were treated with NAC at the indicated doses by (**A**) intraperitoneal injection or (**B**) oral gavage 5 h prior to slice harvest, and co-treated with buthionine sulfoximine (BSO) where indicated. Results in each of 12 experiments were normalized to values obtained in 3-morpholinosydonimide (SIN-1)-treated, EAAC1$^{-/-}$, 0 NAC mice. $n$=3–5 mice in each condition; *$p$<0.05; **$p$<0.01 *vs* SIN-1-treated, EAAC1$^{-/-}$, 0 NAC. Wt = wild-type

Last, we administered NAC to humans with PD at several doses and formulations to determine if the CSF levels of NAC shown to have biological activity in mouse brain could be achieved in human CSF. CSF was obtained by lumbar puncture in each subject prior to the first dose, and again 90 min after the fourth dose. Thirteen patients were enrolled, and 12 completed the study procedures [24]. Oral NAC administration produced a dose-dependent increase in CSF NAC concentrations, with the highest dose producing a peak total NAC concentration of 10.1 ±0.8 μM (Fig. 6E), a concentration > 80 times higher than the CSF NAC concentration found to have robust biological activity in mouse neurons (Fig. 6A–C). The liquid and capsule forms of NAC had comparable effects on human CSF NAC levels. As in the mouse and rat, most of the NAC in human CSF was found in its reduced (free thiol) form. The highest dose used in the human studies was 70 mg/kg twice daily, a value chosen

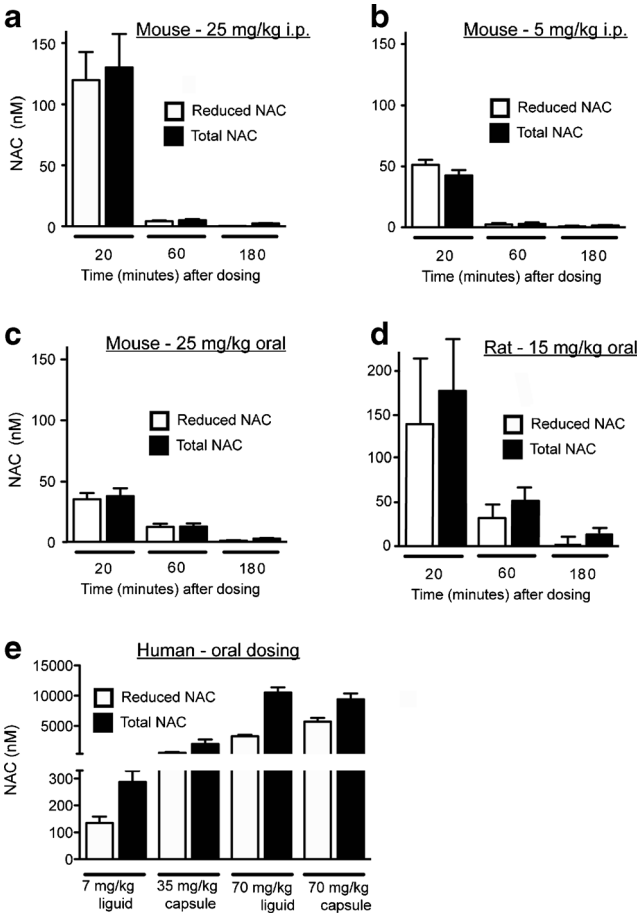


**Fig. 6** Total and reduced *N*-acetyl cysteine (NAC) levels measured in cerebrospinal fluid (CSF) in mice, rats, and humans. (**A**, **B**) NAC in EAAC1$^{-/-}$ mouse CSF at time points after 25 mg/kg or 5 mg/kg intraperitoneally (i.p.). (**C**) NAC in EAAC1$^{-/-}$ mouse CSF after 25 mg/kg orally. (**D**) NAC in rat CSF at time points after 15 mg/kg orally. (**E**) NAC in human CSF, 90 min after the designated oral dose. Data are mean±SEM. Data from human subjects are re-plotted from [24]

because it is at the upper end of published clinical trials [15, 16]. The dose of 35 mg/kg also produced CSF levels that were far higher than the comparable 25 mg/kg oral dose in mice, whereas values measured in rat CSF were intermediate between those in mice and humans (Fig. 6).

## Discussion

It is often difficult to validate drug target engagement in clinical studies of neurodegenerative disorders. The therapeutic goal of NAC in PD is to normalize neuronal GSH levels and thereby restore neuronal antioxidant capacity [13, 14]. Here we employed a strategy in which we first used an animal model to identify the CSF concentration of the drug required to have a biological effect in neurons, and then enrolled human subjects to identify the dose required to achieve this drug concentration in human CSF. Our findings show that NAC is able to both normalize neuronal GSH content and functional antioxidant capacity at doses producing peak CSF levels of 50 nM or higher in mice, and that NAC concentrations in human CSF far exceed these levels when administered at well-tolerated oral doses.

A novel aspect of this study was the use of *ex vivo* acute brain slice cultures for quantitative assessment of neuronal antioxidant capacity. This approach allowed us to administer pharmacological treatment to intact mice, and then subsequently analyze the capacity of the mouse brain neurons to counter an exogenous oxidative stress under controlled conditions. SIN-1 generates superoxide and NO, which, in turn, form the highly ROS peroxynitrite. The oxidation of tyrosine to nitrotyrosine provides a marker of peroxynitrite chemical activity in cells [28], and the formation of this product in cells exposed to peroxynitrite thus provides an index of cellular antioxidant capacity. 4-Hydroxynonenal similarly serves as a measure of functional antioxidant capacity, as it is generated by the interaction of superoxide (or superoxide metabolites) and cell lipids [29].

There are several mechanism by which neuronal GSH depletion could contribute to neuronal loss or injury in PD, including impaired mitochondrial respiratory function, accelerated apoptosis, and impaired scavenging of ROS [30–33] . Superoxide, NO, and peroxynitrite are all scavenged by GSH-dependent mechanisms [3, 34]. GSH is also a substrate for glutaredoxin-mediated repair of proteins that have been oxidatively modified, a process that may be of particular importance in disorders such as PD that are associated with toxic protein aggregates. These enzyme-catalyzed reactions ultimately generate GSH disulfide (GSSG) from GSH. GSSG can either be recycled to GSH in the GSH reductase reaction, or exported from cells. GSSG has intrinsic cytotoxicity; consequently, cells export GSSG when formation exceeds capacity for recycling to GSH [35], and the GSH moieties lost through GSSG export or other means must be replaced by *de novo* GSH synthesis.

Cysteine availability is usually the rate-liming factor for GSH synthesis [12], and consequently the ability of NAC to support GSH synthesis and antioxidant capacity provides indicators of intracellular biological activity. Here we used a previously validated immunohistochemical method for quantifying GSH levels specifically in neurons because biochemical determinations do not distinguish between neuronal GSH and GSH present in astrocytes or other cell types [21, 22]. We found that NAC doses required to normalize antioxidant function were generally lower than required to normalize neuronal GSH content, presumably because GSH content need not be fully restored to improve oxidant scavenging. In addition to providing a substrate for GSH synthesis, NAC can itself react with ROS at its cysteine residue. This property raises the possibility that observed effects of NAC could be attributable to direct antioxidant effects rather than, or in addition to, its role

in supporting GSH synthesis. However, the rate of direct NAC reaction with ROS is orders of magnitude slower than the rates of GSH-coupled enzymatic scavenging [3, 11, 36]. Accordingly, the results presented here show that NAC at the doses employed failed to increase neuronal antioxidant capacity when GSH synthesis was prevented by BSO.

It may be surprising that NAC was able to affect neuronal GSH content significantly at submicromolar CSF levels, given that the normal intracellular GSH concentration is about 1 mM. However, intracellular cysteine levels are much lower, about 25 μM in normal cells [37], and presumably far lower than this in cells with cysteine-responsive GSH depletion. Moreover, CSF concentrations do not indicate the rate of NAC flux from plasma to the neuronal intracellular space. There is a dynamic flux of NAC down its concentration gradients, plasma > CSF > intracellular space, that is maintained, in part, by deacetylation of NAC to cysteine in the intracellular space. NAC can also act more indirectly to increase cysteine availability by displacing cysteine from protein binding sites and labile disulfides (e.g., NAC + Cys–Cys ⟷ NAC–Cys + Cys) [38, 39], and NAC that is present in reversible linkages such as these may subsequently be liberated to regenerate free NAC or cysteine.

In the mouse studies, CSF NAC levels fell to negligible values within 1 h of NAC administration, but the effect of NAC on neuronal GSH levels and antioxidant capacity were robustly evident when assessed 5 h after dosing. These findings suggest a rapid NAC uptake and intracellular GSH synthesis, followed by a much slower decline in neuronal GSH content. This is consistent with a normally slow loss of GSH in brain [27], and with our present finding that BSO had no significant effect on GSH levels over a 5-h observation interval. These results also suggest that beneficial effects of NAC in the CNS can be achieved with spaced rather than continuous dosing.

We have proposed here that the NAC concentrations measured in mouse CSF under conditions in which NAC has demonstrated effects on mouse neurons can be used to provide a target human CSF concentration for guiding human dosing. A useful feature of this approach is that species differences in NAC absorption, liver metabolism, and CSF transport all become moot, as the only measure of consequence is the CSF NAC level. However, this approach does involve certain assumptions: that neuronal metabolism of NAC to cysteine and GSH is comparable in humans and mouse; that the relationships between NAC concentrations in CSF and brain extracellular fluid are comparable in human and mouse; that NAC can enter human and mouse neurons at comparable rates; and that this rate is not significantly altered with chronic NAC treatment. Moreover, the studies presented do not provide an indication of how frequently dosing must occur to maintain normal GSH levels, as this is likely dependent on the underlying cause of GSH depletion. Given these assumptions and limitations, it may be prudent in human clinical studies to use a dosing strategy that raises NAC in human CSF to levels that are several fold higher than those required for effects in the mouse. The findings of our human CSF studies indicate this is feasible.

Despite the use of NAC in numerous clinical studies, there has been uncertainty about doses required to achieve biological effect in brain. The present findings indicate that NAC can normalize GSH levels and antioxidant capacity in mouse brain, and that the CSF concentration of NAC associated with this effect can easily be achieved in humans with oral dosing. These findings should help remove a significant barrier to the use of NAC in fully powered, randomized clinical trials. Variations of this approach, pairing measures of drug efficacy in *ex vivo* brain slices with CSF drug level measurements, may be useful in rational drug dosing for other agents targeting central nervous system disorders.

**Acknowledgments** We thank Drs. Caroline Tanner (University of California San Francisco) and Dean Jones (Emory University) for many helpful discussions. This study was supported by the Michael J. Fox Foundation, the San Luis Obispo County Community Foundation, the Singing Field Foundation, and the Department of Veterans Affairs.

**Required Author Forms** Disclosure forms provided by the authors are available with the online version of this article.

## References

1. Dias V, Junn E, Mouradian MM. The role of oxidative stress in Parkinson's disease. J Parkinsons Dis 2013;3:461-491.
2. Dasuri K, Zhang L, Keller JN. Oxidative stress, neurodegeneration, and the balance of protein degradation and protein synthesis. Free Radic Biol Med 2013;62:170-185.
3. Smeyne M, Smeyne RJ. Glutathione metabolism and Parkinson's disease. Free Radic Biol Med 2013;62:13-25.
4. Perry TL, Godin DV, Hansen S. Parkinson's disease: a disorder due to nigral glutathione deficiency? Neurosci Lett 1982;33:305-310.
5. Chade AR, Kasten M, Tanner CM. Nongenetic causes of Parkinson's disease. J Neural Transm Suppl 2006:70:147-151.
6. Berman AE, Chan WY, Brennan AM, et al. N-acetylcysteine prevents loss of dopaminergic neurons in the EAAC1$^{-/-}$ mouse. Ann Neurol 2011;69:509-520.
7. Chinta SJ, Kumar MJ, Hsu M, et al. Inducible alterations of glutathione levels in adult dopaminergic midbrain neurons result in nigrostriatal degeneration. J Neurosci 2007;27:13997-14006.
8. Wullner U, Loschmann PA, Schulz JB, et al. Glutathione depletion potentiates MPTP and MPP+ toxicity in nigral dopaminergic neurones. Neuroreport 1996;7:921-923.
9. LeWitt PA, Taylor DC. Protection against Parkinson's disease progression: clinical experience. Neurotherapeutics 2008;5:210-225.
10. Olanow CW, Rascol O, Hauser R, et al. A double-blind, delayed-start trial of rasagiline in Parkinson's disease. N Engl J Med 2009;361:1268-1278.
11. Rushworth GF, Megson IL. Existing and potential therapeutic uses for N-acetylcysteine: the need for conversion to intracellular glutathione for antioxidant benefits. Pharmacol Ther 2014;141:150-159.
12. Jones DP. Radical-free biology of oxidative stress. Am J Physiol Cell Physiol 2008;295:C849-C868.

13. Martinez-Banaclocha MA. N-acetyl-cysteine in the treatment of Parkinson's disease. What are we waiting for? Med Hypotheses 2012;79:8-12.
14. Zeevalk GD, Razmpour R, Bernard LP. Glutathione and Parkinson's disease: is this the elephant in the room? Biomed Pharmacother 2008;62:236-249.
15. Holmay MJ, Terpstra M, Coles LD, et al. N-Acetylcysteine boosts brain and blood glutathione in Gaucher and Parkinson diseases. Clin Neuropharmacol 2013;36:103-106.
16. Deepmala, Slattery J, Kumar N, et al. Clinical trials of N-acetylcysteine in psychiatry and neurology: a systematic review. Neurosci Biobehav Rev 2015;55:294-321.
17. Sunitha K, Hemshekhar M, Thushara RM, et al. N-Acetylcysteine amide: a derivative to fulfill the promises of N-Acetylcysteine. Free Radic Res 2013;47:357-367.
18. Banbury Conference. Mutant mice and neuroscience: recommendations concerning genetic background. Banbury Conference on genetic background in mice. Neuron 1997;19:755-759.
19. Brennan AM, Connor JA, Shuttleworth CW. NAD(P)H fluorescence transients after synaptic activity in brain slices: predominant role of mitochondrial function. J Cereb Blood Flow Metab 2006;26:1389-1406.
20. Darley-Usmar VM, Hogg N, O'Leary VJ, Wilson MT, Moncada S. The simultaneous generation of superoxide and nitric oxide can initiate lipid peroxidation in human low density lipoprotein. Free Radic Res Commun 1992;17:9-20.
21. Won SJ, Kim JE, Cittolin-Santos GF, Swanson RA. Assessment at the single-cell level identifies neuronal glutathione depletion as both a cause and effect of ischemia-reperfusion oxidative stress. J Neurosci 2015;35:7143-7152.
22. Miller VM, Lawrence DA, Mondal TK, Seegal RF. Reduced glutathione is highly expressed in white matter and neurons in the unperturbed mouse brain—implications for oxidative stress associated with neurodegeneration. Brain Res 2009;1276:22-30.
23. Baker MA, Cerniglia GJ, Zaman A. Microtiter plate assay for the measurement of glutathione and glutathione disulfide in large numbers of biological samples. Anal Biochem 1990;190:360-365.
24. Katz M, Won SJ, Park Y, et al. Cerebrospinal fluid concentrations of N-acetylcysteine after oral administration in Parkinson's disease. Parkinsonism Relat Disord 2015;21:500-503.
25. Griffith OW. Biologic and pharmacologic regulation of mammalian glutathione synthesis. Free Radic Biol Med 1999;27:922-935.
26. Aoyama K, Suh SW, Hamby AM, et al. Neuronal glutathione deficiency and age-dependent neurodegeneration in the EAAC1 deficient mouse. Nat Neurosci 2006;9:119-126.
27. Gokce G, Ozsarlak-Sozer G, Oktay G, et al. Glutathione depletion by buthionine sulfoximine induces oxidative damage to DNA in organs of rabbits in vivo. Biochemistry 2009;48:4980-4987.
28. Beckman JS, Koppenol WH. Nitric oxide, superoxide, and peroxynitrite: the good, the bad, and ugly. Am J Physiol 1996;271:C1424-C1437.
29. Esterbauer H, Schaur RJ, Zollner H. Chemistry and biochemistry of 4-hydroxynonenal, malonaldehyde and related aldehydes. Free Radic Biol Med 1991;11:81-128.
30. Banaclocha MM. Therapeutic potential of N-acetylcysteine in age-related mitochondrial neurodegenerative diseases. Med Hypotheses 2001;56:472-477.
31. Chinta SJ, Andersen JK. Reversible inhibition of mitochondrial complex I activity following chronic dopaminergic glutathione depletion in vitro: implications for Parkinson's disease. Free Radic Biol Med 2006;41:1442-1448.
32. Hauser DN, Hastings TG. Mitochondrial dysfunction and oxidative stress in Parkinson's disease and monogenic parkinsonism. Neurobiol Dis 2013;51:35-42.
33. Muyderman H, Wadey AL, Nilsson M, Sims NR. Mitochondrial glutathione protects against cell death induced by oxidative and nitrative stress in astrocytes. J Neurochem 2007;102:1369-1382.
34. Dringen R. Metabolism and functions of glutathione in brain. Prog Neurobiol 2000;62:649-671.
35. Homolya L, Varadi A, Sarkadi B. Multidrug resistance-associated proteins: export pumps for conjugates with glutathione, glucuronate or sulfate. Biofactors 2003;17:103-114.
36. Aruoma OI, Halliwell B, Hoey BM, Butler J. The antioxidant action of N-acetylcysteine: its reaction with hydrogen peroxide, hydroxyl radical, superoxide, and hypochlorous acid. Free Radic Biol Med 1989;6:593-597.
37. Stipanuk MH, Londono M, Lee JI, Hu M, Yu AF. Enzymes and metabolites of cysteine metabolism in nonhepatic tissues of rats show little response to changes in dietary protein or sulfur amino acid levels. J Nutr 2002;132:3369-3378.
38. Radtke KK, Coles LD, Mishra U, Orchard PJ, Holmay M, Cloyd JC. Interaction of N-acetylcysteine and cysteine in human plasma. J Pharm Sci 2012;101:4653-4659.
39. Zhou J, Coles LD, Kartha RV, et al. Intravenous administration of stable-labeled N-acetylcysteine demonstrates an indirect mechanism for boosting glutathione and improving redox status. J Pharm Sci 2015;104:2619-2626.

Referências,

Abrahams, S.L., Younathan, E.S., Modulation of the kinetic properties of phosphofructokinase by ammonium ions. J. Biol. Chem (1971). 246, 2464–2467.

Almeida RF, Cereser VH Jr, Faraco RB, Böhmer AE, Souza DO, Ganzella M. Systemic administration of GMP induces anxiolytic-like behavior in rats. Pharmacol Biochem Behav. 2010 Sep;96(3):306-11.

Amodio P, Del Piccolo F, Petteno E, Mapelli D, Angeli P, Iemmolo R, Muraca M, Musto C et al, Prevalence and prognostic value of quantified electroencephalogram (EEG) alterations in cirrhotic patients, (2001) J Hepatol 35(1):37–45

Amodio P, Marchetti P, Del Piccolo F, de Tourtchaninoff M, Varghese P, Zuliani C, Campo G, Gatta A, Guérit JM. Spectral versus visual EEG analysis in mild hepatic encephalopathy. Clin Neurophysiol. (1999) Aug;110(8):1334-44.

Als-Nielsen B, Gluud LL, Gluud C. Non-absorbable disaccharides for hepatic encephalopathy: systematic review of randomised trials. BMJ 2004;328:1046.

Bass NM, Mullen KD, Sanyal A, Poordad F, Neff G, Leevy CB, et al. Rifaximin treatment in hepatic encephalopathy. N Engl J Med (2010); 362:1071-1081.

Borkakoty A, Kumar P, Taneja S. Hepatic Encephalopathy. N Engl J Med. 2017 Jan 12;376(2):186. PubMed PMID: 28079344.

Bower, W.A., Johns, M., Margolis, H.S., Williams, I.T., Bell, B.P., 2007. Population- based surveillance for acute liver failure. Am. J. Gastroenterol. 102 (11), 2459– 2463.

Butterworth R. F., Gigue`re J. F., Michaud J., Lavoie J., and Layrargues G. P., "Ammonia: key factor in the pathogenesis of hepatic encephalopathy," (1987) *Neurochemical Pathology*, vol. 6, no. 1-2, pp. 1–12.

Butterworth, R.F., 1997. Hepatic encephalopathy and brain edema in acute hepatic failure: does glutamate play a role? Hepatology 25, 1032–1034.

Ciećko-Michalska I, Szczepanek M, Słowik A, and Mach T, "Pathogenesis of Hepatic Encephalopathy," (2012) Gastroenterology Research and Practice, vol. 2012, Article ID 642108, 7 pages.

Cooper, A.J., Plum, F.,. Biochemistry and physiology of brain ammonia. Physiol. Rev. (1987) 67, 440–519.

Dalsgaard, M.K., Quistorff, B., Danielsen, E.R., Selmer, C., Vogelsang, T., Secher, N.H., (2004). A reduced cerebral metabolic ratio in exercise reflects metabolism and

D'Amico G, Morabito A, Pagliaro L, Marubini E. Survival and prog- nostic indicators in compensated and decompensated cirrhosis. Dig Dis Sci (1986) ;31:468-475.

Felipo V. Hepatic encephalopathy: effects of liver failure on brain function. Nat Rev Neurosci. 2013 Dec;14(12):851-8. doi: 10.1038/nrn3587. Review. PubMed PMID: 24149188.

Dejong, C. H., van de Poll, M. C., Soeters, P. B., Jalan, R. & Olde Damink, S. W. Aromatic amino acid metabolism during liver failure. The Journal of nutrition (2007). 137, 1579S-1585S; discussion 1597S-1598S

Desjardins P, Du T, Jiang W, Peng L, Butterworth RF. Pathogenesis of hepatic encephalopathy and brain edema in acute liver failure: role of glutamine redefined. Neurochem Int. 2012 Jun;60(7):690-6.

Detry O, Gaspar Y, Cheramy-Bien JP, Drion P, Meurisse M, Defraigne JO. A modified surgical model of fulminant hepatic failure in the rat. J Surg Res. (2013) May 1;181(1):85-90. doi: 10.1016/j.jss.2012.05.080.

Dienel, Gerald A. “Astrocytic Energetics during Excitatory Neurotransmission: What Are Contributions of Glutamate Oxidation and Glycolysis?” *Neurochemistry international* 63.4 (2013): 244–258.

Flamm SL. Rifaximin treatment for reduction of risk of overt hepatic encephalopathy recurrence. *Therapeutic Advances in Gastroenterology*. (2011);4(3):199-206.

Gerhart, D.Z., Enerson, B.E., Zhdankina, O.Y., Leino, R.L., Drewes, L.R. Expres- sion of monocarboxylate transporter MCT1 by brain endothelium and glia in adult and suckling rats. Am. J. Physiol. (1997) 273, E207–E213.

Giuliani P, Ballerini P, Ciccarelli R, Buccella S, Romano S, D'Alimonte I, Poli A, Beraudi A, Peña E, Jiang S, Rathbone MP, Caciagli F, Di Iorio P. Tissue distribution and metabolism of guanosine in rats following intraperitoneal injection. J Biol Regul Homeost Agents. 2012 Jan-Mar;26(1):51-65. Erratum in: J Biol Regul Homeost Agents. 2012 Apr-Jun;26(2):3 p following 311. D' Alimonte, I [corrected to D'Alimonte, I].

Gluud LL, Dam G, Les I, Córdoba J, Marchesini G, Borre M, Aagaard NK, Vilstrup H. Branched-chain amino acids for people with hepatic encephalopathy. Cochrane Database Syst Rev. 2015 Feb 25;(2):CD001939. doi: 10.1002/14651858.CD001939.pub2. Review. Update in: Cochrane Database Syst Rev. (2015);(9):CD001939.

Gluud LL, Dam G, Borre M, Les I, Cordoba J, Marchesini G, et al. Lactulose, rifaximin or branched chain amino acids for hepatic encephalopathy: what is the evidence? Metab Brain Dis (2013);28:221-225.

Gluud LL, Dam G, Borre M, Les I, Cordoba J, Marchesini G, et al. Oral branched chain amino acids have a beneficial effect on manifes tations of hepatic encephalopathy in a systematic review with metaanalyses of randomized controlled trials. J Nutr (2013);143:1263-1268.

Hermenegildo C, Monfort P, Felipo V. Activation of N-methyl-D-aspartate receptors in rat brain in vivo following acute ammonia intoxication: characterization by in vivo brain microdialysis. Hepatology. (2000) Mar;31(3):709-15.

Ipata PL, Camici M, Micheli V, Tozz MG. Metabolic network of nucleosides in the brain. Curr Top Med Chem. (2011);11(8):909-22. Review.

James, J. H., Ziparo, V., Jeppsson, B. & Fischer, J. E. Hyperammonaemia, plasma aminoacid imbalance, and blood-brain aminoacid transport: a unified theory of portal-systemic encephalopathy. Lancet 2, 772-775 (1979).

Johansen ML, Bak LK, Schousboe A, Iversen P, Sorensen M, Keiding S, Vilstrup H, Gjedde A, Ott P, Waagepetersen HS (2007) The meta- bolic role of isoleucine in detoxification of ammonia in cultured mouse neurons and astrocytes. Neurochem Int 50(7–8):1042–1051.

Larson, A.M., Polson, J., Fontana, R.J., Davern, T.J., Lalani, E., Hynan, L.S., et al., 2005. Acetaminophen-induced acute liver failure: results of a United States multicenter, prospective study. Hepatology 42 (6), 1364–1372.

Lee WM, Squires RH Jr, Nyberg SL, Doo E, Hoofnagle JH. Acute liver failure: summary of a workshop. Hepatology 2008;47:1401-1415

Lehmann C, Bette S, Engele J. High extracellular glutamate modulates expression of glutamate transporters and glutamine synthetase in cultured astrocytes. Brain Res. 2009 Nov 10;1297:1-8.

Leke R, Bak L, Iversen P, Sorensen M, Keiding S, Vilstrup H, Ott P, Portela LV, Schousboe A, Waagepetersen HS, Synthesis of neurotransmitter GABA via the neuronal tricarboxylic acid cycle is elevated in rats with liver cirrhosis consistent with a high GABAergic tone in chronic hepatic encephalopathy. J neurochem (2011a) 117:824-832

Lockwood AH, Yap EW, Wong W-H. Cerebral ammonia metabolism in patients with severe liver disease and minimal hepatic encephalopathy. (1991). J Cereb Blood Flow Metab 11:337-341

Kircheis G, Nilius R, Held C, Berndt H, Buchner M, Gortelmeyer R, et al. Therapeutic efficacy of L-ornithine-L-aspartate infusions in patients with cirrhosis and hepatic encephalopathy: results of a placebo-controlled, double-blind study. HEPATOLOGY 1997;25:1351- 1360.

Kim WR, Brown RS, Jr., Terrault NA, El-Serag H. Burden of liver dis- ease in the United States: summary of a workshop. HEPATOLOGY (2002_; 36:227-242.

Madrahimov N, Dirsch O, Broelsch C, Dahmen U. Marginal hepatectomy in the rat: from anatomy to surgery. Ann Surg. (2006 Jul;244(1):89-98. PubMed PMID: 16794393;

Maheandiran, M. et al. Severe hypoglycemia in a juvenile diabetic rat model: presence and severity of seizures are associated with mortality. PloS one 8, e83168, doi:10.1371/journal.pone.0083168 (2013).

Mpabanzi L, Jalan R. Neurological complications of acute liver failure: pathophysiological basis of current management and emerging therapies. Neurochem Int. (2012) Jun;60(7):736-42.

Miyazaki T, Matsuzaki Y, Karube M, Bouscarel B, Miyakawa S, Tanaka N. Amino acid ratios in plasma and tissues in a rat model of liver cirrhosis before and after exercise. Hepatol Res. (2003) Nov;27(3):230-237.

Muntz, J.A., Hurwitz, J., Effect of potassium and ammonium ions upon glycolysis catalyzed by an extract of rat brain. Arch. Biochem. Biophys. (1951) 32, 124–
136.

Ott P, Clemmesen O, Larsen FS. Cerebral metabolic disturbances in the brain during acute liver failure: from hyperammonemia to energy failure and proteolysis. Neurochem Int. (2005) Jul;47(1-2):13-8. Review.

Ott P, Larsen FS. Blood-brain barrier permeability to ammonia in liver failure: a critical reappraisal. Neurochem Int. (2004) Mar;44(4):185-98. Review.

Ott P, Vilstrup H. Cerebral effects of ammonia in liver disease: current hypotheses. Metab Brain Dis. (2014) Dec;29(4):901-11.

Padilla E, Shumake J, Barrett DW, Holmes G, Sheridan EC, Gonzalez-Lima F. Novelty-evoked activity in open field predicts susceptibility to helpless behavior. *Physiology & behavior*. (2010); 101(5): 746-754.

Paniz LG, Calcagnotto ME, Pandolfo P, Machado DG, Santos GF, Hansel G, Almeida RF, Bruch RS, Brum LM, Torres FV, de Assis AM, Rico EP, Souza DO. Neuroprotective effects of guanosine administration on behavioral, brain activity, neurochemical and redox parameters in a rat model of chronic hepatic encephalopathy. Metab Brain Dis. 2014 Sep;29(3):645-54.

Patidar KR, Bajaj JS. Antibiotics for the treatment of hepatic encephalopathy. Metab Brain Dis (2013) ;28:307-312.

Patil, D. H., Westaby, D., Mahida, Y. R., Palmer, K. R., Rees, R., Clark, M. L., Silk, D. B. (1987). Comparative modes of action of lactitol and lactulose in the treatment of hepatic encephalopathy. *Gut*, *28*(3), 255–259.

Pellerin L, Magistretti PJ. Sweet sixteen for ANLS. J Cereb Blood Flow Metab. 2012 Jul;32(7):1152-66. doi: 10.1038/jcbfm.2011.149. Review.

Petronilho F, Périco S, Vuolo F, Mina F, Constantino L, Comim C, Quevedo J, et al. (2012) Protective effects of Guanosine against sepsis-induced damage in rat brain and cognitive impairment. Brain Behav and Immun. 26: 904–910.

Rama Rao KV, Norenberg MD. Brain energy metabolism and mitochondrial dysfunction in acute and chronic hepatic encephalopathy. Neurochem Int. (2012) Jun;60(7):697-706. doi: 10.1016/j.neuint.2011.09.007. Review.

Ratnakumari L, Murthy CR. In vitro and in vivo effects of ammonia on glucose metabolism in the astrocytes of rat cerebral cortex. Neurosci Lett. 1992 Dec 14;148(1-2):85-8.

Saunders JB, Walters JRF, Davies P, Paton A. A 20-year prospective study of cirrhosis. BMJ (1981) ;282:263-266.

Schousboe A, Waagepetersen HS, Leke R, Bak LK. Effects of hyperammonemia on brain energy metabolism: controversial findings in vivo and in vitro. Metab Brain Dis. (2014) Dec;29(4):913-7.

Scott TR, Kronsten VT, Hughes RD, Shawcross DL. Pathophysiology of cerebral oedema in acute liver failure. *World Journal of Gastroenterology : WJG*. 2013;19(48):9240-9255.

Schmidt, A. P., Ávila, T. T., & Souza, D. O. (2005). Intracerebroventricular guanine-based purines protect against seizures induced by quinolinic acid in mice. Neurochem Res 30, 69−73.

Schmidt AP, Lara DR, Souza DO. Proposal of a guanine-based purinergic system in the mammalian central nervous system. Pharmacol Ther. (2007). Dec;116(3):401-16. Review.

Schmidt, A. P., & Souza, D. O.. The role of the guanine-based purinergic system in seizures and epilepsy. *Open Neurosci J*. (2010), *4*, 102-113.

Smith, D., Pernet, A., Hallett, W.A., Bingham, E., Marsden, P.K., Amiel, S.A., (2003). Lactate: a preferred fuel for human brain metabolism in vivo. J. Cereb. Blood Flow Metab. 23, 658–664.

Schurr, A., Lactate: the ultimate cerebral oxidative energy substrate? J. Cereb. Blood Flow Metab (2006.). 26, 142–152.

Stepanova M, Mishra A, Venkatesan C, Younossi ZM (2012) In- hospital mortality and economic burden associated with hepatic encephalopathy in the United States from 2005 to 2009. Clin Gastroenterol Hepatol 10(9):1034–1041.

Strauss E, da Costa MF. The importance of bacterial infections as precipating factors of chronic hepatic encephalopathy in cirrhosis. Hepatogastroenterology. (1998) May-Jun;45(21):900-4.

Strauss, G.I., Knudsen, G.M., Kondrup, J., Moller, K., Larsen, F.S., Cerebral metabolism of ammonia and amino acids in patients with fulminant hepatic failure. Gastroenterology (2001) 121, 1109–1119.

Strauss E, Tramote R, Silva EP, Caly WR, Honain NZ, Maffei RA, et al. Double-blind randomized clinical trial comparing neomycin and placebo in the treatment of exogenous hepatic encephalopathy. Hepato-gastroenterology 1992;39:542-545.

Sutter, R. & Kaplan, P. W. Clinical and electroencephalographic correlates of acute encephalopathy. Journal of clinical neurophysiology : official publication of the American Electroencephalographic Society 30, 443-453, (2013).

Swain M, Butterworth RF, Blei AT. Ammonia and related amino acids in the pathogenesis of brain edema in acute ischemic liver failure in rats. Hepatology. (1992) Mar;15(3):449-53. PubMed PMID: 1544626.

Traeger, H., Gabuzda, S., Ballou, A., Davidson, C. Blood ammonia concentration in liver disease and liver coma. Metabolism (1954) 3, 99–109.

Vilstrup H, Amodio P, Bajaj J, Cordoba J, Ferenci P, Mullen KD, Weissenborn K, Wong P. Hepatic encephalopathy in chronic liver disease: 2014 Practice Guideline by the American Association for the Study of Liver Diseases and the European Association for the Study of the Liver. Hepatology. 2014 Aug;60(2):715-35.

Vaquero J, Butterworth RF. Mechanisms of brain edema in acute liver failure and impact of novel therapeutic interventions. Neurol Res. 2007 Oct;29(7):683-90. doi: 10.1179/016164107X240099. Review.

Vinadé, E. R., Schmidt, A. P., Frizzo, M. E. S., Portela, L. V., Soares, F. A., Schwalm, F. D., et al. (2005). Effects of chronic administered guanosine on behavioral parameters and brain glutamate uptake in rats. J Neurosci Res 79, 248−253.

Vogels BA, Maas MA, Daalhuisen J, Quack G, Chamuleau RA, Memantine, a noncompetitive NMDA receptor antagonist improves hyperammonemia-induced encephalopathy and acute he- patic encephalopathy in rats. Hepatology (1997) 25(4):820–827. doi:10. 1002/hep.510250406